

1997

Polycyclic aromatic hydrocarbon (PAH) distributions within urban estuarine sediments

Siddhartha Mitra

College of William and Mary - Virginia Institute of Marine Science

Follow this and additional works at: <https://scholarworks.wm.edu/etd>



Part of the [Biogeochemistry Commons](#), [Environmental Sciences Commons](#), and the [Geochemistry Commons](#)

Recommended Citation

Mitra, Siddhartha, "Polycyclic aromatic hydrocarbon (PAH) distributions within urban estuarine sediments" (1997). *Dissertations, Theses, and Masters Projects*. Paper 1539616779.

<https://dx.doi.org/doi:10.25773/v5-74km-4h38>

This Dissertation is brought to you for free and open access by the Theses, Dissertations, & Master Projects at W&M ScholarWorks. It has been accepted for inclusion in Dissertations, Theses, and Masters Projects by an authorized administrator of W&M ScholarWorks. For more information, please contact scholarworks@wm.edu.

INFORMATION TO USERS

This manuscript has been reproduced from the microfilm master. UMI films the text directly from the original or copy submitted. Thus, some thesis and dissertation copies are in typewriter face, while others may be from any type of computer printer.

The quality of this reproduction is dependent upon the quality of the copy submitted. Broken or indistinct print, colored or poor quality illustrations and photographs, print bleedthrough, substandard margins, and improper alignment can adversely affect reproduction.

In the unlikely event that the author did not send UMI a complete manuscript and there are missing pages, these will be noted. Also, if unauthorized copyright material had to be removed, a note will indicate the deletion.

Oversize materials (e.g., maps, drawings, charts) are reproduced by sectioning the original, beginning at the upper left-hand corner and continuing from left to right in equal sections with small overlaps. Each original is also photographed in one exposure and is included in reduced form at the back of the book.

Photographs included in the original manuscript have been reproduced xerographically in this copy. Higher quality 6" x 9" black and white photographic prints are available for any photographs or illustrations appearing in this copy for an additional charge. Contact UMI directly to order.

UMI

**A Bell & Howell Information Company
300 North Zeeb Road, Ann Arbor MI 48106-1346 USA
313/761-4700 800/521-0600**

Polycyclic Aromatic Hydrocarbon (PAH) Distributions Within Urban Estuarine Sediments

**A Dissertation Presented to the Faculty of the School of Marine Science
The Virginia Institute of Marine Science
The College of William and Mary**

**In Partial Fulfillment of the
Requirements for the Degree of
Doctor of Philosophy**

by

Siddhartha Mitra

1997

UMI Number: 9815246

**UMI Microform 9815246
Copyright 1998, by UMI Company. All rights reserved.**

**This microform edition is protected against unauthorized
copying under Title 17, United States Code.**

UMI
300 North Zeeb Road
Ann Arbor, MI 48103


APPROVAL SHEET


This dissertation is submitted in partial fulfillment of the
requirements for the degree of

Doctor of Philosophy


Siddhartha Mitra

Approved December 1997


Rebecca Dickhut, Ph. D.
Committee Chairperson/Major Professor


James Bauer, Ph. D.


William MacIntyre, Ph. D.


Mark Patterson, Ph. D.


Linda Schaffner, Ph. D.



Bruce Brownawell Ph. D.
SUNY Stonybrook

TABLE OF CONTENTS

	<u>Page</u>
Acknowledgements	<i>i</i>
Dedication	<i>ii</i>
List of Tables	<i>iii</i>
List of Figures	<i>iv</i>
Abstract	<i>vi</i>
Chapter 1. Introduction	1
1.1 Introduction.....	1
1.2 Sorption theory.....	3
1.3 Hypotheses.....	10
1.4 Objectives.....	12
1.5 References.....	13
Chapter 2. Polycyclic aromatic hydrocarbon distribution coefficients in estuarine sediments: The role of PAH source and sediment geochemistry	17
2.1 Introduction.....	19
2.2 Factors hypothetically affecting PAH K'_{ocS}	21
2.3 Sediment heterogeneity.....	23
2.4 Site background.....	24
2.5 Methods.....	26
2.6 Results and Discussion.....	31
2.7 Conclusions.....	51
2.8 References.....	52
Chapter 3. Three phase modeling of polycyclic aromatic hydrocarbon association with pore water dissolved organic carbon	57
3.1 Introduction.....	59
3.2 Methods.....	63
3.3 Results and Discussion.....	66
3.4 Conclusions.....	72
3.5 References.....	76

	<u>Page</u>
Chapter 4. Polycyclic aromatic hydrocarbon deposition and geochemistry in Hudson River sediments.....	79
4.1 Introduction.....	81
4.2 Methods.....	82
4.3 Results.....	88
4.4 Discussion.....	102
4.5 Conclusions.....	107
4.6 References.....	108
Chapter 5. Summary.....	113
Appendices.....	116

ACKNOWLEDGMENTS

First and foremost, I must acknowledge my advisor Dr. Rebecca Dickhut for her outstanding mentorship, confidence in my abilities, financial support, and the often deserved "kick." I would also like to thank the rest of my committee members Dr. Jim Bauer, Dr. Bruce Brownawell, Dr. Bill MacIntyre, Dr. Mark Patterson, and Dr. Linda Schaffner. A special thanks to Dr. Linda Schaffner for her constant reminder to consider the "forest" while staring at the "tree" and to Dr. Bruce Brownawell for facilitating sampling the East River and Newark Bay. Many thanks to Dr. Catherine Chisholm-Brause and Dr. Elizabeth Canuel, not only for their advice over the years but also for use of their laboratory facilities.

Certainly second to none as the person who can do it all and keep smiling, my unfailing gratitude goes out to Libby MacDonald. Also, special thanks to Ginger Edgecombe for the hours and hours of dedication to processing my samples. Shannon Burcham and Linda Meneghini: I appreciate all of your answers to my endless questions. Special thanks to Linda Meneghini for all the snacks she has provided—you have no idea how much energy a Tootsie Roll can infuse at 2 am when there is just one more sample to process. To the students on the third floor of Chesapeake Bay Hall, North Wing: I want to thank you for all of your help over the last few years and for your assistance in keeping us in organic geochemistry a "fine-tuned-silicone-lubricated-machine".

There are some additional people who deserve special recognition - friends who helped sample at least once: Pat Calautti, Tim Dellapena, Kimani Kimbrough, Krisa Murray, Michelle Thompson, Andy Zimmerman - I thank you and hope you enjoyed your stint in urban oceanography; my roommate and friend of 6 years and thus, quite possibly the most tolerant person I have ever met: Aswini Volety; my lab cohorts and often partners in crime-working away during the wee hours: Becky Countway, Kurt Gustafson, Kimani Kimbrough, Kewen Liu, Jennifer Putnam, and Padma T. Venkatraman; and, some of the most unconditionally supportive and thought-provoking friends over the years: Tim Dellapena, Kitty Gallagher, Jennie Gundersen, Laurence Libelo, Laurent Mezin, and, Michelle Thompson.

Last but most certainly not least, I would also like to thank my family for their love, encouragement, and support; Stephen Bennett, Jan Cordes, Martha Nizinski, Laura Rose, and Flavia Rutkosky for our conversations, and often engaging the chicken-wing eating, guitar playing side of my brain; and, to Britt Anderson for her friendship, patience, and understanding over the last few months. There is no doubt that all of the people mentioned above have contributed to my development as a student and human being.

***In loving memory of my grandfather,
Barun Kumar Mitter***

LIST OF TABLES

<u>Table</u>		<u>Page</u>
Table 2.1	Factors hypothetically affecting PAH apparent field distribution coefficients.....	22
Table 2.2	Elizabeth River sediment ²¹⁰ Pb activity.....	50
Table 3.1	Elizabeth River - curve fit coefficients for Equation 3-3.....	70
Table 3.2	Elizabeth River - variables used in three phase partitioning model	74
Table 4.1	East River and Newark Bay - PAH recoveries in sediment and pore water samples.....	86

LIST OF FIGURES

Figure	Page
Chapter 1. Overall Introduction	
1.1 Selected PAH structures.....	2
1.2 Hypothetical sediment aggregate.....	7
Chapter 2. Polycyclic aromatic hydrocarbon distribution coefficients in estuarine sediments: The role of PAH source and sediment geochemistry	
2.1 Map of Elizabeth River and sampling sites.....	25
2.2 Elizabeth River sediment grain size distributions.....	32
2.3 Elizabeth River sediment X-radiograph positives.....	34
2.4 Elizabeth River geochemical profiles of sediment cores.....	36
2.5 Elizabeth River particle surface area.....	37
2.6 Elizabeth River (July 1994) K'_{OC} vs. K_{OW} for selected PAHs.....	39
2.7 Elizabeth River - observed sediment/pore water K'_{OCs}	40
2.8 Elizabeth River - pore water PAH concentrations.....	41
2.9 Elizabeth River - sediment PAH concentrations.....	42
2.10 Elizabeth River - % OC versus particle surface area.....	45
2.11 Elizabeth River - Site 2; K'_{OCs} versus particulate C/N ratio.....	47
2.12 Elizabeth River - PAH isomer concentration ratios in sediments.....	49
Chapter 3. Three phase modeling of polycyclic aromatic hydrocarbon association with pore water dissolved organic carbon	
3.1 Map of Elizabeth River and sampling sites.....	64
3.2 Elizabeth River (July 1994) K'_{OC} vs. K_{OW} for selected PAHs.....	67
3.3 Elizabeth River (September 1995) K'_{OC} vs. K_{OW} for selected PAHs.....	68
3.4 Elizabeth River - measured and predicted PAH K'_{OC} as a function of K_{OW}	73
3.5 Elizabeth River - Modeled pore water PAH K_{DOC}	75
Chapter 4. Polycyclic aromatic hydrocarbon deposition and geochemistry in Hudson River sediments	
4.1 Map of East River and Newark Bay sampling sites in the Hudson River...	83
4.2 East River and Newark Bay - ^{210}Pb profiles.....	89
4.3 East River and Newark Bay - Sediment grain size distributions.....	91
4.4 East River and Newark Bay - sediment x-radiograph positives.....	92
4.5 East River and Newark Bay - sediment PAH concentrations.....	94
4.6 East River and Newark Bay - pore water DOC concentrations.....	96

<u>Figures (continued)</u>		<u>Page</u>
4.7	Newark Bay - PAH K'_{oc} s.....	97
4.8	Newark Bay - Actual and modeled PAH K'_{oc} s versus K_{ow} as a function of pore water DOC concentrations.....	98
4.9	East River and Newark Bay - depth profiles of PAH source indicators...	100
4.10	East River and Newark Bay - sedimentary geochemical variables.....	101

ABSTRACT

Sediments and pore waters from two urban estuaries ranging in sediment mixing energy were studied to evaluate the potential release of contaminants from particles during sediment diagenesis. Two sites in Elizabeth River, VA and two tributaries in the Hudson River Watershed were sampled for polycyclic aromatic hydrocarbons (PAHs)- a suite of compounds comprised of known and suspected carcinogens. To test the hypothesis that in estuarine sediments, compositional variables of sedimentary organic matter are of primary importance in redistributing and mobilizing particle-associated PAHs deposited to the sediment bed, sediment age (inferred by ^{210}Pb and ^{137}Cs activity), total organic carbon content, carbon to nitrogen (C/N) ratios, and particle surface area were also sampled at these sites. These results reveal that both sediment geochemistry and depositional environment are significant factors controlling PAH distributions in urban estuarine sediments.

In the Elizabeth River, ^{210}Pb activity was uniform and low (~1 dpm/g) while ^{137}Cs activity was not detectable, implying that both sites have been non-depositional for the past 70 y or are comprised of old dredge spoil. Pore water concentrations of PAHs were similar at both sites in Elizabeth River despite significantly higher sediment PAH concentrations at one site across the channel from a creosote wood treatment facility (Site 2). Organic carbon normalized sediment/pore water distribution coefficients for PAHs (K'_{OCs}) were significantly higher at Site 2 compared to Site 1. Taken together, these results would indicate a different type of particle-PAH association at each site independent of the amount of total sediment organic carbon. At Site 1 K'_{OCs} decreased with sediment depth by 2-3 orders of magnitude, far in excess of the 0.5 log unit maximum range in K'_{OC} suggested in the literature. Decreasing down-core K'_{OCs} at Site 1 in the Elizabeth River are hypothesized to be a function of the coincident down-core decrease in particulate organic matter accessible for PAH binding at this site. At Site 2 in the Elizabeth River, high and uniform K'_{OCs} with depth are hypothesized to result from particles coated with organics which sequester PAHs within the particle matrix.

Depth profiles of ^{210}Pb activities were uniform and generally ranged from 4 -6.5 dpm/g in East River, NY sediments and 1 - 4.4 dpm/g in Newark Bay, NJ sediments. Deposition rates in the East River and Newark Bay were estimated using ^{137}Cs and were calculated to be ~27 cm/y and ~ 2 cm/y, respectively. Sediment PAH concentrations were significantly higher in the East River than Newark Bay; a fact coincident with the higher amounts of organic carbon and particle surface area in East River sediments. However, low molecular weight PAHs were not detectable in East River sediments and PAHs were not detectable in East River pore waters. Coupled with the sediment accumulation history at this site, and sediment geochemistry, the East River seems to be a site of intense physical mixing where PAHs are not able to equilibrate between sediments and pore waters. In contrast, PAHs in Newark Bay sediments are able to attain equilibrium due to lower intensity of physical mixing.

PAH-dissolved organic carbon (DOC) binding accounts for observed two phase disequilibria between sediments and pore waters for the more hydrophobic PAHs. However,

binding to pore water DOC accounts for no more than an order of magnitude decrease in K'_{oc} with depth in sediments. In Newark Bay sediments, which are subject to lower energy mixing events, the results of a three-phase model indicated K'_{oc} s were controlled by pore water DOC concentrations. In high energy areas such as the East River, pore water PAHs possibly bound to DOC are continuously mobilized out of the seabed.

These results suggest that PAH distributions in areas that are subject to high energy physical disturbances, may be controlled by the physical energy affecting the system rather than compositional aspects of particulate or pore water dissolved organic matter. In contrast, aspects of sediment geochemistry such as the occlusion of particulate organic carbon for PAH binding, particle porosity, and amount of pore water DOC seem more likely to affect PAH distributions in areas which the physical forces "allow" preservation of sedimentary structure.

Chapter 1. Overall Introduction

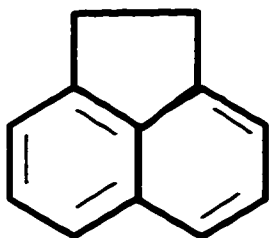
1-1. Introduction

Polycyclic aromatic hydrocarbons (PAHs) have been studied extensively due to their potential harmful effects on organisms and persistence in the environment (Neff, 1979; NRC, 1983). Large quantities of PAHs are released into the environment as a result of incomplete combustion of fossil fuels and other anthropogenic events such as oil spills (LaFlamme and Hites, 1978). PAHs may also be formed naturally in recent sediments by diagenetic and anthropogenic processes (Wakeham and Farrington, 1980). PAHs vary in structure from 2 to 6 ring aromatic compounds (Figure 1-1), with associated variations in their physical-chemical properties (Lee *et al.*, 1981). Toxic effects of PAHs generally result from activation and transformation along an organism's metabolic pathway, often to mutagenic intermediates (Gelboin, 1980; Vollhardt, 1987).

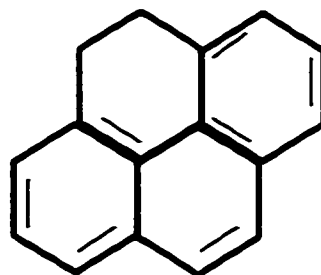
PAH behavior in the environment has been demonstrated to vary as a result of each compound's differing hydrophobicity as represented by the compounds' octanol-water partition coefficient (K_{ow}) (e.g. Karickhoff *et al.*, 1979; Schwarzenbach, *et al.*, 1993). In aqueous systems, the association of PAHs with organic matter is thermodynamically favorable (Schwarzenbach *et al.*, 1993). Consequently, marine and freshwater sediments which contain large pools of organic matter, both particulate and interstitially dissolved, can represent the primary repository for PAHs.

PAHs in sediments exist in three phases: sorbed to particulate organic matter (POM), and sorbed to dissolved organic matter (DOM), or freely dissolved. PAH-organic matter associations strongly influence the bioavailability of these compounds, in turn determining their ecological risk (e.g. DiToro *et al.*, 1991). As the aqueous solubility of a hydrophobic organic contaminant

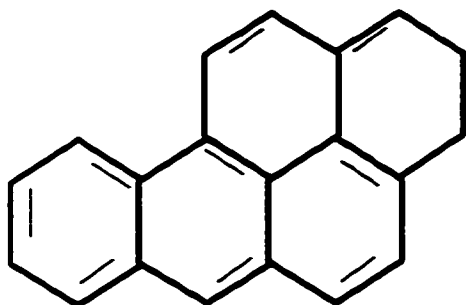
Figure 1-1. Selected polycyclic aromatic hydrocarbon (PAH) structures and molecular weights.



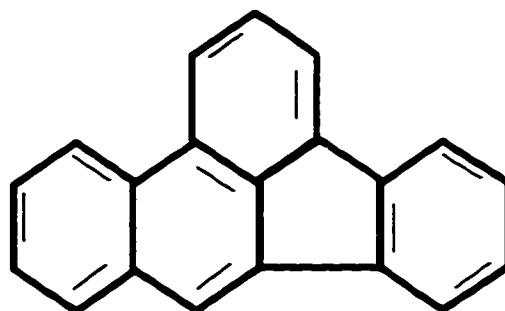
Acenaphthene (M. Wt. = 154)



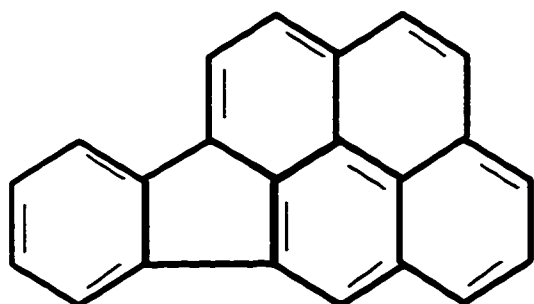
Pyrene (M. Wt. = 202)



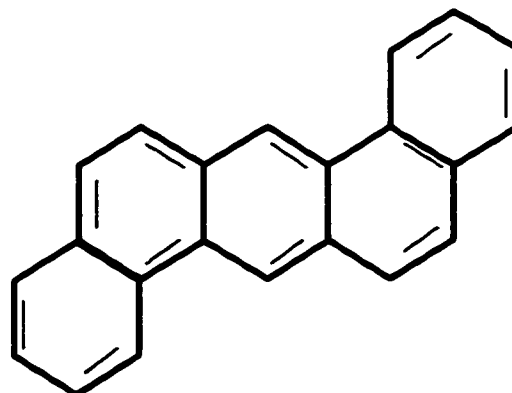
Benzo[a]pyrene (M. Wt. = 252)



Benzo[b]fluoranthene (M. Wt. = 252)



Indeno[1,2,3-c,d]pyrene (M. Wt. = 276)



Dibenz[a,h]anthracene (M. Wt. = 278)

(HOC) such as a PAH is inversely related to its surface area (Hermann, 1972), larger PAHs tend to be less water soluble, more lipophilic, and associate to a greater degree with hydrophobic moieties such as organic matter. Nonetheless, the specific compositional aspects of organic matter which control its association with PAHs, are not well defined (e.g. Schwarzenbach *et al.*, 1993).

1-2. Sorption Theory

Sorption of PAHs to particles can entail adsorption of the PAH to the particle surface and/or partitioning into the particle's matrix (*i.e.*, absorption). PAHs will adsorb to the surface sites of a particle until saturation. As PAHs sorb to all available surface sites of a particle, additional sorption can continue to occur at slower rates by multilayer sorption of the PAHs and partitioning into the particle's matrix (Karickhoff, 1980), or possibly intra-aggregate diffusion through pore spaces if the particle is an aggregate (Wu and Gschwend, 1986).

In a simple two phase system, the equilibrium distribution of a chemical between the particle phase and the surrounding aqueous media can be expressed as:

$$C_p = K_D * C_w \quad (1-1)$$

where C_p is the concentration of the chemical associated with the particle phase (mg/kg dry weight particles), C_w is the freely dissolved concentration of the chemical (mg/L), and K_D is the particulate-water equilibrium distribution coefficient for the chemical (L/kg). Thermodynamically, this equilibrium distribution can be defined as the condition under which chemical fugacities or

"escaping tendencies" in the sorbed and freely dissolved phases are equal. For given particle sizes, K_D for PAHs has been implied to be directly related to organic carbon content of the sorbent (Lambert *et al.*, 1965; Karickhoff *et al.*, 1979) with higher fractions of organic carbon in sediments leading to greater binding by the particles. This relationship modifies equation (1-1) to the following:

$$C_p = f_{oc} * K_{oc} * C_w \quad (1-2)$$

where f_{oc} is the fraction organic carbon for a given particle size, and K_{oc} is the particulate organic carbon normalized equilibrium distribution coefficient (L/kg). In natural systems, this term is referred to as the *apparent* organic-carbon normalized distribution coefficient (K'_{oc}).

The affinity of a PAH for organic matter is directly related to the compound's K_{ow} (Karickhoff *et al.*, 1979). K_{oc} for a given sorbate can be related empirically to its K_{ow} in the following manner:

$$\log_{10} K_{oc} = \alpha \log_{10} K_{ow} + \beta \quad (1-3)$$

where α and β are curve fitted coefficients (Karickhoff, 1984). Theoretically, α should equal one and β zero, if PAHs partition to sediment organic carbon in exactly the same manner and degree as their distribution between n-octanol and water. However, resultant curves diverge from theoretical expectations (*e.g.* Karickhoff *et al.*, 1979). Specifically, the degree of sorption is often observed to be less than predicted for PAHs with high K_{ow} s, presumably due to factors which

kinetically hinder thermodynamic equilibrium in natural systems (Karickhoff, 1984), or experimental artifacts such as: incomplete separation of dissolved and colloidal phases of organic matter (Gschwend and Wu, 1985); volatilization of dissolved HOCs, or sorption to container surfaces (Schrap and Opperhuizen, 1992). Further, for chemicals with low K_{OW} values, or for sediments with < 0.1% organic carbon, experimental K_{OC} s are greater than expected supposedly due to non-hydrophobic contributions (*i.e.* adsorption to mineral surfaces) allowing for additional sorption (*e.g.* Karickhoff, 1984). Thus, a general form of equation (1-3) cannot be used to predict PAH distributions to particulate matter *a priori*.

Equation (1-2) assumes that a PAH will associate identically with all types organic carbon. However, for numerous PAHs, the POM-associated concentrations predicted by equation (1-2) do not agree with the measured concentrations despite normalization to the amount of organic carbon (*e.g.* Garbarini and Lion, 1986; Weber *et al.*, 1992). Specifically, K_{OC} and K_{DOM} values for the same PAH are observed to vary by as much as a factor of ten for different sediment/soil types (Weber, *et al.*, 1983; Garbarini and Lion, 1986; Gauthier, *et al.*, 1987; Gratwohl, 1990; Weber *et al.*, 1992). McGroddy and Farrington (1995) have observed K'_{OC} s to be ~ 2 orders of magnitude higher than predicted by equilibrium partitioning for PAHs in Boston Harbor sediments. Eadie *et al.* (1990) reported measured distribution coefficients for two PAHs to be four times higher than those predicted by equation (1-2). Such discrepancies in aqueous systems have been attributed to the varying nature (*i.e.* molecular composition) of the sedimentary or soil organic matter or the dissolved organic matter (*e.g.* Gauthier, *et al.*, 1987; Smets and Rittman, 1990; Rutherford *et al.*, 1992).

PAH and DOM Binding

In addition to distributing between particles and the surrounding aqueous media, PAHs can also associate with DOM. This operationally defined fraction constitutes a significant portion of the organic matter in interstitial water (Burgess *et al.*, 1996), and must be considered in the distribution of PAHs in sediments (Di Toro *et al.*, 1991). The expression for a PAH's affinity for DOM is analogous to equation (1-2):

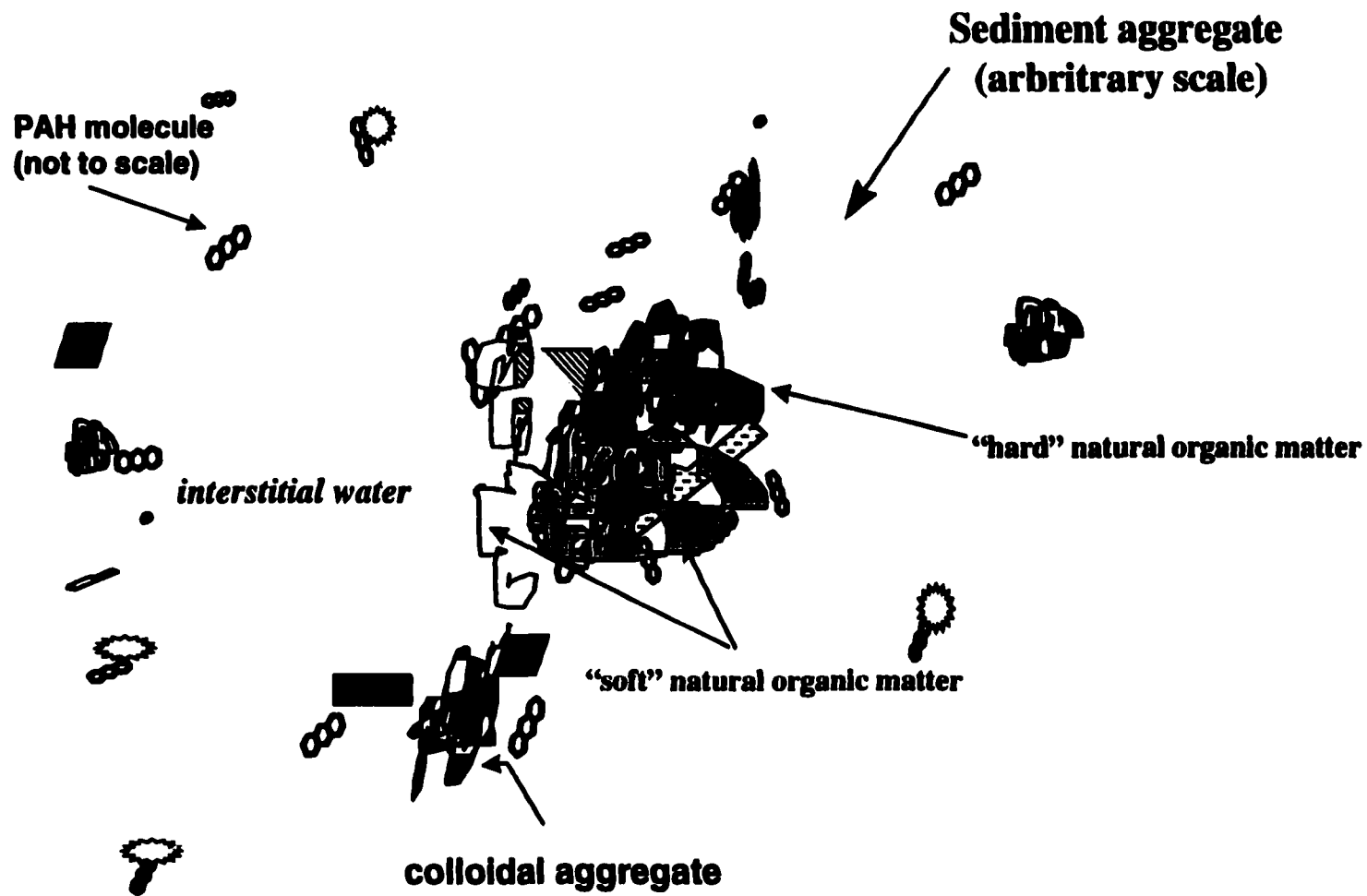
$$C_{\text{DOM}} = m_{\text{DOM}} * K_{\text{DOM}} * C_w \quad (1-4)$$

where C_{DOM} is the concentration of PAH associated with DOM (mg/L), m_{DOM} is the DOM concentration (kg/L), and K_{DOM} is the DOM normalized equilibrium distribution coefficient for a PAH (L/kg). Inconsistencies have also been noted in the affinity of PAHs for DOM, again being attributed to the qualitative nature of the organic matter (Morehead *et al.*, 1986; Gauthier *et al.*, 1987). McCarthy *et al.* (1989) suggest that PAH binding to DOM depends on the existence of an open structure in the DOM as well as its hydrophobicity. These results suggest that any approach to predicting bioavailable concentrations of organic matter-bound PAHs must take into account the composition of the POM and DOM.

PAH and POM Binding

One possible reason for such discrepancies between predicted and actual distributions of HOCs is the notion that different regions of a soil or sediment matrix may contain different types and amounts of surfaces and soil organic matter (Figure 1-2). Weber *et al.* (1992) have addressed

Figure 1-2. Hypothetical sediment aggregate in the seabed. Organic matter associated with the aggregate is expected to be extremely heterogenous and variable in age and degree of condensation.



this concept with their Distributed Reactivity Model (DRM) suggesting that environmental solids are intrinsically heterogeneous and that sorption processes in environmental systems are comprised of a spectrum of reaction mechanisms. Each organic and inorganic component of this soil/sediment heterogeneity has its own energy and sorptive properties. Thus the overall sorption isotherm for a natural solid is the sum of the sorption isotherms for each active component (Weber and Huang, 1996). Gratwohl (1990) has suggested that low sorption of nonionic compounds to natural organic matter in soils and sediments is proportional to high amounts of oxygen-containing functional groups. Young and Weber (1995) and Xing and Pignatello (1997) further propose natural organic matter is diagenetically transformed from loose amorphous ("soft") natural organic matter to older more aromatic ("hard") organic matter consisting of condensed polymers with increasing micro- and nanometer sized holes. Differences in HOC sorption across different soils/sediments are attributed to heterogeneity of sorption energies of these sub-particle microenvironments differing in their affinity for HOCs. Thus "older" organic matter is said to have a higher sorption capacity and contribute to a greater extent to sorption isotherm non-linearity relative to "younger" organic matter.

One such condensed aromatic particle matrix which has been suggested to be responsible for high K'_{OCs} , is pyrogenic soot carbon; a highly porous particle matrix comprised of condensed aromatic carbon (Gustafsson et al., 1997). Specific densities of soot range from 1.8-2.1 g/cm³, similar to that of pure graphite and specific surface areas are ~100 m²/g (Gustafsson and Gschwend, 1997). As soot originates from pyrogenic processes, it is hypothesized to contribute significantly to PAH loading in urban estuaries. Moreover, the bioaccumulation potential of PAHs associated with highly porous particle matrices such as soot carbon is expected to deviate

greatly from that predicted by equilibrium partitioning of PAHs between sediments and pore waters.

PAH Distributions in Sediments

PAH distributions within sediments have been studied in numerous environments (Karickhoff *et al.* 1979; Means *et al.* 1980; Wakeham and Farrington 1980; McGroddy and Farrington, 1995). Because anoxic degradation of PAHs occurs at negligible rates relative to their oxic degradation (Capone and Bauer, 1992), PAH distributions are expected to vary as a function of changing organic matter concentration and composition which occur during sediment burial and diagenesis. Changes in PAH sediment distribution are also expected to be a function of the contaminants physicochemical properties, with relatively soluble compounds preferentially partitioning into pore water and diffusing out of the sediment column.

The factors responsible for changing distributions of PAHs in estuarine sediments have not been extensively evaluated. In the Chesapeake bay and its tributaries, various researchers have predominantly characterized surface sediment concentrations of PAHs, PCBs, polychlorinated terphenyls (PCTs), and kepone (Huggett *et al.* 1980; Bieri *et al.* 1986; Hale *et al.* 1990). However, it is anticipated that trends in the sediment distributions of PAHs are a function of the natural organic matter composition, the sedimentological regime (*i.e.* the extent of mixing and accumulation rates) (Olsen *et al.*, 1982), and the PAHs' physicochemical properties.

Parameters such as molecular weight of the HOC, available surface area, lipid composition, and aromatic content of the organic matter have been proposed to influence HOC distribution coefficients (Beller and Simoneit, 1986; Gauthier *et al.*, 1987; McCarthy *et al.*, 1989).

For example, Beller and Simoneit (1986) demonstrated that over 90% of total sedimentary PCBs and petroleum hydrocarbons were recovered in the free lipid portion of their extracts. Likewise, Gauthier *et al.*, (1987) demonstrated a strong correlation between pyrene distribution coefficients and the degree of aromaticity in 14 different humic materials as determined by three separate analytical methods. Thus, to better understand bioavailability and fate of particle-associated PAHs, it is necessary to identify the most significant geochemical factors affecting PAH distribution and transport within sediments.

1-3. Hypotheses

Overall Hypothesis:

The fundamental hypothesis of this research is that in estuarine sediments, compositional variables of sedimentary organic matter are of primary importance in redistributing and mobilizing particle-associated PAHs deposited to the sediment bed.

Working Hypothesis #1

PAH distributions will change with depth in sediments from the Elizabeth and Hudson River estuaries, and will correlate with specific compositional changes in organic matter which occur with burial.

Sediment characteristics such as organic matter concentration and composition change with depth in the sediments due to microbial mineralization (Henrichs, 1993). Specifically, characteristics of the sediments such as the carbon to nitrogen (C/N) ratio, degree of aromaticity, total organic carbon, and particle surface area, may also display trends with depth in sediments. It is proposed that changes in distribution of PAHs buried in estuarine sediments occur as a result of decreased affinity of PAHs for geochronologically "older" POM and DOM, as well as by

decreasing amounts of compositionally "attractive" organic matter available for association. A decreased affinity of PAHs for sedimentary organic matter is hypothesized to be coincident with a) decreasing hydrophobicity of sedimentary POM and DOM, and/or b) decreasing accessibility of the POM and DOM for PAH sorption.

Working Hypothesis # 2 :

The role of pore water DOC in associating with PAHs leading to two phase disequilibria can be estimated with a three phase equilibrium model.

Specifically , it is proposed that the amount of pore water dissolved organic carbon and its binding affinity for PAHs can account for observed disequilibria in sediment/pore water K'_{ocS} .

Working Hypothesis # 3 :

Existing relationships between PAH distributions and organic matter composition are, in general, predictive and can be used to model PAH distributions in other sedimentary environments.

If specific variables of sediment composition influence PAH distributions in sediments, these same compositional variables may be used to predict PAH distributions in other sites similar in sedimentation regime. That is, sediment parameters found to control the sediment-pore water distributions of PAHs in the Elizabeth River are hypothesized to control sediment-pore water distributions of PAHs in the Hudson River. This hypothesis was tested directly by comparing data from these two estuarine environments.

1-4. Objectives

Objective 1

Determine and correlate *in situ* PAH distribution coefficients with compositional variables of associated organic matter as a function of depth in sediments from an urban estuary.

Specifically, PAH distribution coefficients were measured as a function of depth in the sediment bed in the Elizabeth River and related to amount and compositional aspects of particulate and dissolved organic carbon (e.g. total organic carbon, C/N ratio, sedimentary soot carbon and particle surface area). Compositional variables of sedimentary organic matter having the most significant effect on PAH distribution coefficients were identified.

Objective 2

Propose and evaluate a three-phase model for the observed PAH distributions in estuarine sediments.

Theoretical PAH-pore water DOC binding coefficients were calculated. Subsequently, the role of pore water DOC as a third PAH-binding phase was compared to that of sediment geochemistry, in affecting down-core trends in PAH K'_{oc} s.

Objective 3

Measure and correlate PAH distributions between sediments and pore waters in the lower Hudson River with compositional variables of the sediments to determine if common geochemical factors affect PAH distributions in urban estuaries.

The compositional variables of sedimentary organic matter which were found to affect PAH distribution coefficients in Elizabeth River sediments were also measured in Hudson River

sediments. PAH distributions between sediments and pore waters in the Hudson River were compared to these geochemical variables to determine to what extent PAH distributions in urban estuarine sediments are affected by similar variables pertaining to sediment geochemistry.

1-5. References

- Beller, H.R. and Simoneit, B. R. T 1986. Polychlorinated biphenyls and hydrocarbons: Distributions among bound and unbound lipid fractions of estuarine sediments. In Mary Sohn, [ed.]. Organic Marine Geochemistry, American Chemical Society Publication, Washington, D.C.
- Bieri, R. H., Hein, C., Huggett, R. J., Shou, P., Sloane, H., Smith, C., and Su, C. W. 1986. Polycyclic aromatic hydrocarbons in surface sediments from the Elizabeth River subestuary. *J. Environ. Anal. Chem.*, 26, 97-113.
- Burgess, R. M. , McKinney, R. A., Brown, W. A., Quinn, J. G. 1996a. Isolation of marine sediment colloids and associated polychlorinated biphenyls: an evaluation of ultrafiltration and reverse-phase chromatography. *Environ. Sci. Technol.*, 30, 1923-1932.
- Capone, D. and Bauer, J.E. Microbial processes in coastal pollution. 1992. Environmental Microbiology, Wiley-Liss Publishers. pp. 191-237.
- Di Toro, D. M., Zarba, C. S., Hansen, D. J., Berry, W. J., Swartz, R. C., Cowan, C., Pavlou, S. P., Allen, H. E., Thomas, N. A., and Paquin, P. R.. 1991. Technical basis for establishing sediment quality criteria for nonionic organic chemicals using equilibrium partitioning. *Environ. Toxicol. & Chem.*, 10, 1541-1583.
- Eadie, B., Morehead, N. R. and Landrum, P. F. 1990. Three-phase partitioning of hydrophobic organic compounds in Great Lakes waters. *Chemosphere*, 20, 161-178.
- Garbarini, D. R. and Lion, L. 1986. influence of the nature of soil organics on the sorption of toluene and trichloroethylene. *Environ. Sci. Technol.*, 20, 1263-1269.
- Gauthier, T. D., Seitz, W. R., and Grant, C. L. 1987. Effect of structural and compositional variations of dissolved humic materials on pyrene K_{OC} values. *Environ. Sci. Technol.*, 21, 243-247.
- Gelboin, H. 1980. Benzo(a)pyrene metabolism, activation, and carcinogenesis: Role and regulation of mixed-function oxidases and related enzymes, pp. 1107-1166. In Physiological Reviews - Vol. 60.

Gratwohl, P. 1990. Influence of organic matter from soils and sediments from various origins on the sorption of some chlorinated aliphatic hydrocarbons: implications on K_{OC} correlations. *Environ. Sci. Technol.*, 24, 1687-1693.

Gschwend, P.; Wu, S. C. 1985. On the constancy of sediment-water partition coefficients of hydrophobic organic pollutants. *Environ. Sci. Technol.*, 19, 90-96.

Gustafsson, O., Haghseta, F., Chan, C., Macfarlane, J., and Gschwend, P. M. 1997. Quantification of the dilute sedimentary soot phase: Implications for PAH speciation and bioavailability. *Environ. Sci. Technol.*, 31, 203-209.

Gustafsson, O. and Gschwend, P. M. 1997. Soot as a strong partition medium for polycyclic aromatic hydrocarbons in aquatic systems. In Eganhouse, R. P., [ed.]. Molecular Markers in Environmental Geochemistry, ACS Symposium Series 671, American Chemical Society, Washington, DC.

Hale, R. C., Greaves, J., Gallagher, K., and Vadas, G. G. 1990. Novel chlorinated terphenyls in sediments and shellfish of an estuarine environment. *Environ. Sci. Technol.*, 24, 1727-1731.

Hermann, R.B. 1972. Theory of hydrophobic bonding-II. The correlation of hydrocarbon solubility in water with solvent cavity surface area. *Phys. Chem.*, 19, 2754-2759.

Huggett, R. J., Bender, M. E., and Unger, M. A. 1980. Polycyclic aromatic hydrocarbons in the Elizabeth River, Virginia, pp. 327-341. In R. A. Baker, [ed.]. Contaminants and Sediments, Ann Arbor Science, Ann Arbor, MI.

Karickhoff, S. W. 1984. Organic pollutant sorption in aquatic systems. *J. Hydraul. Eng.*, 110, 707-735.

Karickhoff, S. W. 1980. Sorption kinetics of hydrophobic pollutants in natural sediments, pp.193-206. In R.A. Baker, [ed.]. Contaminants and Sediments, Ann Arbor Science, Ann Arbor, MI.

Karickhoff, S. W., Brown, D. S., and Scott, T. A. 1979. Sorption of hydrophobic pollutants on natural sediments. *Water Res.*, 13, 241-248.

LaFlamme and Hites, R. 1978. The global distribution of polycyclic aromatic hydrocarbons in recent sediments. *Geochim. Cosmochim. Acta*, 42, 289-303.

Lambert, S. M., Porter, P.E., and Schieferstein, R. H.. 1965. *Weeds*, 13, 185-190.

Lee, M. L., Novotny, M. V., and K. D. Bartle. 1981. Analytical Chemistry of Polycyclic Aromatic Compounds. Academic Press, New York, NY.

- McCarthy, J. F. 1989. Bioavailability and toxicity of metals and hydrophobic organic contaminants, pp. 263-277. In I.H. Suffett and P. MacCarthy [eds.]. Aquatic Humic Substances - Influences on Fate and Treatment of Pollutants. Advances in Chemistry Series, # 219. American Chemical society, Washington D.C.
- McGroddy, S., and Farrington, J. 1995. Sediment porewater partitioning of PAHs in three cores from Boston Harbor, MA. *Environ. Sci. Technol.*, 29, 1542-1550.
- Means, J. C., Wood, S. G., Hassett, J. J. and Banwah, W. L. 1980. Sorption of polynuclear aromatic hydrocarbons by sediments and soils. *Environ. Sci. Technol.*, 14, 1524-1528.
- Morehead, N. R., Eadie, B. J., and Lake. B. 1986. The sorption of PAH onto dissolved organic matter in Lake Michigan waters. *Chemosphere*, 115, no.4, pp.403-412.
- National Research Council. 1983. Polycyclic Aromatic Hydrocarbons: Evaluation of Sources and Effects. National Academy Press, Washington DC.
- Neff, J. M. 1979. Polycyclic aromatic hydrocarbons in the aquatic environment: sources, fates and biological effects. London, Applied science Publishers.
- Olsen, C. R., Cutshall, N. H., and Larsen, I. L. 1982. Pollutant-particle associations and dynamics in coastal marine environments: a review. *Mar. Chem.*, 11, 501-533.
- Rutheford, D. W., C. T. Chiou, and Kile D. E.. 1992. Influence of soil organic matter composition on the partition of organic compounds. *Environ. Sci. Technol.*, 26, 336-340.
- Schrap, S. M. and Opperhuizen, A. 1992. On the contradictions between experimental sorption data and the sorption partitioning model. *Chemosphere*, 24, 1259-1282.
- Schwarzenbach, R., Gschwend, P.M., and Imboden, D. M. 1993. Environmental Organic Chemistry. John Wiley and Sons, Inc., NY.
- Smets, B. F. and Rittman, B. E. . 1990. Sorption equilibria for trichloroethene on algae. *Water Res.*, 24, 355-360.
- Vollhardt, K. P. C. 1987. Organic Chemistry. W. H. Freeman and Co., New York, NY.
- Wakeham, S. G. and Farrington, J. W. 1980. Hydrocarbons in contemporary aquatic sediments. In Contaminants and Sediments - v. 1, Baker, R. A. [ed.] Ann Arbor Science.
- Weber, W. J. and Huang, W. 1996. A Distributed Reactivity Model for sorption by soils and sediments. 4. Intraparticle heterogeneity and phase-distribution relationships under non-equilibrium conditions. *Environ. Sci. Technol.*, 30, 881-888.

Weber W. J., McGinley, P. M., Katz, L. E. 1992. A distributed reactivity model for sorption by soils and sediments. 1. Conceptual basis and equilibrium assessments. *Environ. Sci. Technol.*, 26, 1955-1962.

Weber, W. J., Voice, T. C., Pirbazari, M., Hunt, G. E., Ulanoff, D. M. 1983. Sorption of hydrophobic organic contaminants by sediments, soils and suspended solids-II: Sorbent evaluation studies. *Water Res.*, 17, 1443-1452.

Wu, S. C. and Gschwend, P. M. 1986. Sorption kinetics of hydrophobic organic compounds to natural sediments and soils. *Environ. Sci. Technol.*, 20, 717-725.

Xing, B and Pignatello, J. J. 1997. Dual-mode sorption of low-polarity compounds in glassy poly(vinyl chloride) and soil organic matter. *Environ. Sci. Technol.*, 31, 792-799.

Young, T. M. and Weber, W. J. 1995. A distributed reactivity model for sorption by soils and sediments. 3. Effects of diagenetic processes on sorption energetics. *Environ. Sci. Technol.*, 29, 92-97.

Chapter 2. Polycyclic aromatic hydrocarbon (PAH) distribution coefficients in estuarine sediments: The role of PAH source and sediment geochemistry.

Abstract

Sediments and pore waters from two sites in the urbanized Elizabeth River, Virginia were sampled for levels of polycyclic aromatic hydrocarbons (PAHs). Pore water PAH concentrations were similar between Sites 1 & 2, despite sediment PAH concentrations being much greater at Site 2. Organic-carbon normalized distribution coefficients (K'_{OCs}) for all PAHs were significantly higher at Site 2 compared to Site 1, but decreased substantially with depth in the sediments at Site 1. Dilute sedimentary soot carbon and other geochemical factors potentially affecting PAH distribution coefficients in these sediments, including their age, grain size, particle surface area both before and after organic digestion, and organic carbon / nitrogen ratios were also analyzed. Different factors were determined to control particle surface area at each site offering the most insight to explaining observed PAH K'_{OCs} . At Site 1, increased mineral surface area correlates with decreasing downcore PAH K'_{OCs} , overall lower K'_{OCs} , and sediment PAH concentrations compared to Site 2. This suggests that sediment organic matter becomes increasingly inaccessible with depth at Site 1. At Site 2, large and invariant K'_{OCs} may result from sediments coated with organic matter sequestering PAHs within the particle matrix. PAH isomer concentration ratios, indicators of differential PAH sources, mirrored trends in PAH distribution coefficients. Our results indicate there is significant heterogeneity in PAH distribution coefficients in estuarine sediments, which may be attributed to PAH source(s) and sediment geochemistry.

2-1. Introduction

Major changes in both the concentration and composition of natural organic matter occur in the upper layers of aquatic sediments (Henrichs, 1993). Mineralization of the various components of this organic matter proceed at widely different rates (Westrich and Berner, 1984; Henrichs and Doyle, 1986; Burdige, 1991; Henrichs, 1993). The majority of these biogeochemical changes result from oxidation of labile sedimentary organic matter to reduced inorganics (Berner, 1980). In aquatic systems, the majority of hydrophobic organic contaminants (HOCs) are associated with this natural organic matter predominantly in sediments (e.g. Wakeham and Farrington, 1980; Hites *et al.*, 1980; Prahl and Carpenter, 1983). HOC associations and cycling with natural organic matter therefore influence their fate, transport, and bioavailability in aquatic environments.

In a two-phase aqueous system at equilibrium, the concentration of a chemical in the freely dissolved phase (C_w , mg/l) relative to that in a sorbed phase (C_s , mg/kg), is described by a linear equation:

$$K_D = C_s/C_w \quad (2-1)$$

where K_D (l/kg) is the sediment/pore water distribution coefficient. The actual distribution of a chemical in nature between its dissolved and particulate phases, can depend on several factors such as the composition of the sorbent, hydrophobicity of the sorbate (K_{ow}), and sorption kinetics (e.g. Karickhoff, 1984 ; Schwarzenbach *et al.*, 1993). Since HOCs have a strong affinity for organic carbon, one influential factor affecting their K_D (for sorbents comprised of at least 1%

organic carbon), is the fraction of organic carbon (f_{OC}) in the sorbent (Karickhoff *et al.*, 1979; Means *et al.*, 1980; Brown and Flagg, 1981). Normalization to the amount of organic carbon modifies equation (2-1) to:

$$K_{OC} = K_D / f_{OC} \quad (2-2)$$

where K_{OC} is the organic carbon-normalized two-phase distribution coefficient. Sedimentary organic matter thus acts as a “solvent” for HOCs for which uptake is controlled by the amount of organic carbon associated with the mineral matrix (Karickhoff *et al.*, 1979; Brown and Flagg, 1981; Karickhoff, 1984). To that end, normalizing HOC distribution coefficients to f_{OC} is presumed to account for observed differences in their partitioning to different solids (Karickhoff, 1984). In most cases, this normalization step is said to predict a specific HOC’s association with sedimentary and soil organic matter to within a factor of two (Schwarzenbach *et al.*, 1993).

One important group of HOCs in estuarine and coastal environments is polycyclic aromatic hydrocarbons (PAHs), which include known carcinogenic compounds such as benzo[a]pyrene (Gelboin, 1980; Denissenko, *et al.*, 1996). PAHs are widely distributed in the aquatic environment (Neff, 1979; NRC, 1983), and can be generated by anthropogenic or natural processes such as pyrolysis and combustion or *in situ* rapid transformation of biogenic precursors during sediment diagenesis (Blumer, 1976; Wakeham and Farrington, 1980). Estuarine sediments that contain large pools of organic matter, both particulate and interstitially dissolved, can be a significant repository for PAHs (Prah and Carpenter, 1983). Thus compositional changes in organic matter, which occur during deposition and burial of sediments, are

hypothesized to alter PAH associations with both particulate and dissolved organic matter. The objective of this research was to identify specific compositional and physical changes of particulate and dissolved organic matter (that occur in the sediment column during burial) responsible for controlling PAH K'_{oc} s.

2-2. Factors Hypothetically Affecting PAH Field Distribution Coefficients (K'_{oc} s)

Several factors specific to both the sediments and pore waters can cause PAH K'_{oc} s to appear higher or lower than their values predicted by compound K_{ow} s (Table 2-1). Since K'_{oc} is the ratio of PAHs in the particulate phase to the dissolved phase normalized to the amount of particulate organic carbon, any process depleting PAHs in pore waters would result in higher than predicted K'_{oc} s. For example, microbial respiration and oxidation of pore water PAHs would deplete PAHs in pore waters. In a similar manner, pore water and associated PAHs may be irrigated faster than the rate at which sediment-sorbed PAHs desorb and reequilibrate. In both of these cases, K'_{oc} s would appear higher than predicted. In contrast, increased PAH-pore water dissolved organic carbon (DOC) binding would result in overall decrease in two phase K'_{oc} s.

Factors specific to the particulate phase may also affect PAH K'_{oc} s. For example, K'_{oc} s would be higher than predicted by K_{ow} for PAHs entrapped or slow to desorb from within the particle matrix into surrounding pore water. As suggested by Young and Weber, 1995, organic matter subject to a greater degree of diagenetic alteration may entrap PAHs within the micropores of the particle matrix (see Chapter 1). Alternatively, soot carbon, a highly porous and condensed aromatic matrix (Gustafsson and Gschwend, 1997) may also sequester PAHs. An organic coating around PAH enriched sediment particles may serve to constrain PAH desorption into pore water;

Table 2-1. Factors affecting PAH apparent field distribution coefficients (K'_{oc})

	K'_{oc}
<i>Processes affecting dissolved phase PAHs</i>	
Increased microbial respiration or oxidation of pore water PAHs	↑
Increasing concentrations of pore water dissolved organic carbon	↓
Advection or mobilization of dissolved phase PAHs	↑
<i>Processes affecting particulate phase PAHs</i>	
Slow desorption (e.g. soot particles)	↑
Increasing amounts of organic matter not suitable for PAH binding	↑↓
Entrapment of PAHs in particle matrix	↑

hence, elevated K'_{oc} s. In these scenarios mentioned above, there is an inherent assumption particles are enriched in PAHs relative to surrounding pore water. In contrast, PAHs may sorb onto/into the particle matrix from a dissolved phase. In such a case, particles consisting of porous dissolved organic matter, organic matter-coated particles, or particulate organic matter of low PAH binding capacity (e.g. cellulose) depleted in PAHs, may be kinetically limited in their ability to sorb PAHs; hence lower K'_{oc} s than predicted.

2-3. Sediment Heterogeneity

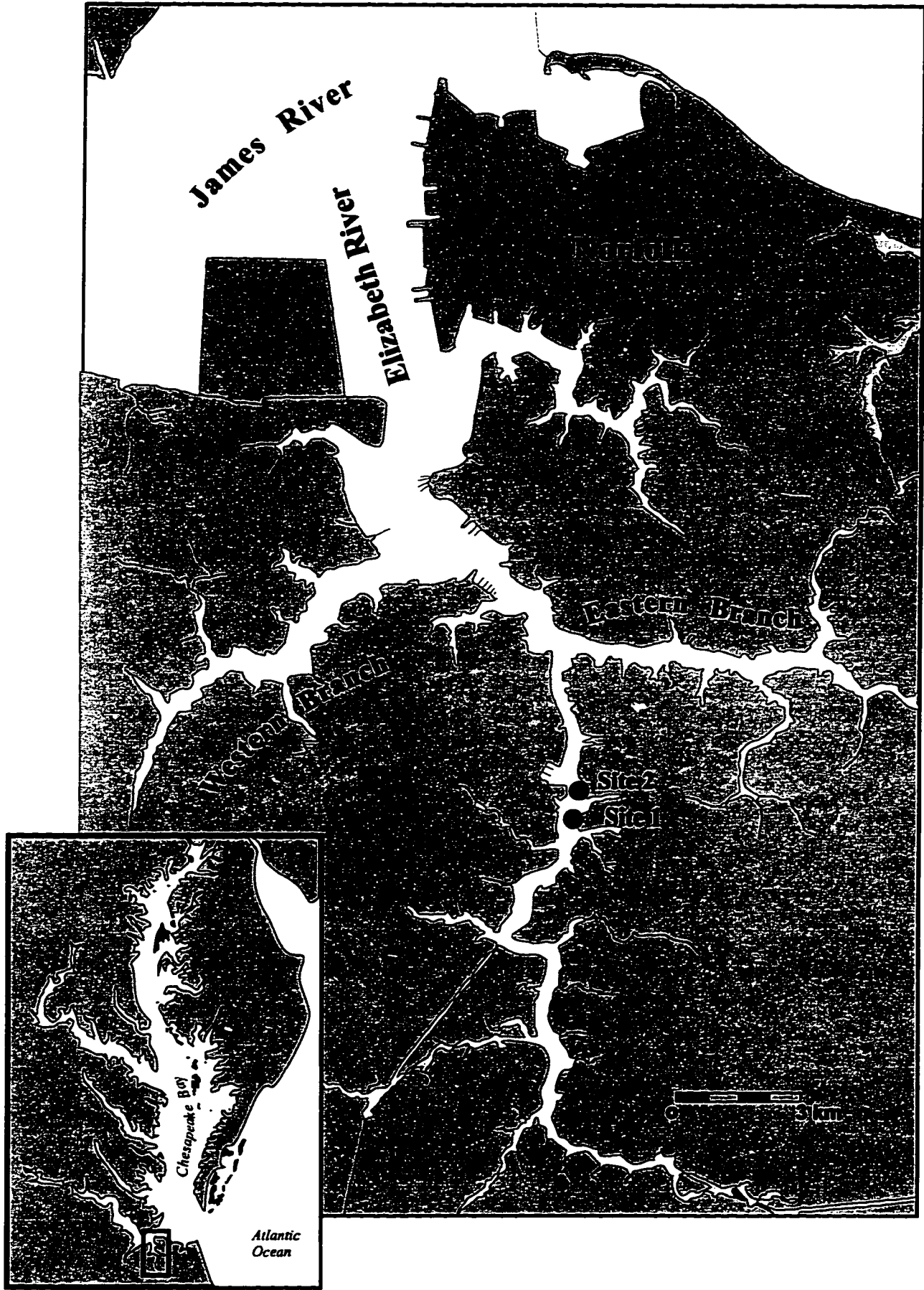
Sources of organic matter and associated pollutants as well as benthic biogeochemical processes in estuarine sediments can vary spatially and temporally (Olsen *et al.*, 1982; Nichols and Biggs, 1985; Olsen *et al.*, 1993). For example, the seabed of the lower Chesapeake Bay region exhibits a wide range of energy conditions, bottom lithology types and biological characteristics (Wright *et al.*, 1987). Estuarine sediments also exhibit a wide range of particle types from single clay minerals to groups of porous flocs (Nichols and Biggs, 1985). Thus, the scale of spatial heterogeneity can extend across adjacent areas in the same estuary or across microzones within the same "aggregate" (Figure 1-2). Large scale spatial heterogeneity precludes the use of few sediment cores to accurately extrapolate observations throughout an estuary. Similarly, empirical interpretations of sorption data may be confounded by aggregate-scale heterogeneity (Weber *et al.*, 1992). Results presented below represent select individual cores from sediments in the Elizabeth River, Virginia, East River, New York, and Newark Bay, New Jersey. Admittedly, without additional sampling and statistical interpretation of data, factors thought to be responsible for PAH K'_{oc} s and geochemical profiles in sediments may not be common across estuaries or

numerous particles. Nonetheless, this study presents a first approximation at assessing the role of several geochemical factors (sedimentary C/N ratio, soot carbon, particle surface area) thought to control observed trends in down-core distributions of sediment-associated PAHs within each select core.

2-4. Site Background

The Southern Branch of the Elizabeth River (Figure 2-1), an urban tributary of lower Chesapeake Bay, Virginia has been historically subject to severe anthropogenic inputs of pollutants such as PAHs (Lu, 1982). Although three wood-preserving facilities known to use creosote (a coal tar distillate enriched in PAHs) have historically existed along the Southern Branch, sediments are contaminated with hydrocarbons from both carbonized coal and petroleum products (Merrill and Wade, 1985). In some areas of the Southern Branch, concentrations of PAHs exceed thousands of parts per million (Huggett *et al.*, 1984). In such narrow urban waterways, resuspension of particle-associated and dissolved PAHs may occur due to natural processes such as tides and storms or by anthropogenic processes such as dredging and shipping traffic. As PAHs distribute between POC and DOC, urban harbors and estuaries can often serve as a secondary source of elevated levels of PAHs into the water column from both the particulate and dissolved phases. Although several researchers have reported the levels of PAHs in surface sediments of urban estuaries (e.g. Huggett *et al.*, 1984; Merrill and Wade, 1985; Adams, 1996), this work focuses on the geochemical factors of particles within urban sediments which affect PAH distributions between sediments and pore waters.

Figure 2-1. Map of the Elizabeth River and sampling sites. Both sites were in the southern branch of the Elizabeth River and situated within 1 km of each other along the eastern flank of the main channel. The main channel has historically been subjected to considerable dredging to support shipping traffic. An abandoned creosote wood-treatment facility is situated across the main channel from Site 2.



2-5. Methods

Sediment sampling

July 1994

Preliminary sampling of sediments in the southern branch of the Elizabeth River was conducted in July of 1994 using a Grey-O'hara box core (Grey-O'hara, College Station, TX) (26.5 cm x 26.5 cm x 60 cm). Sediments were subsampled using (60 cm x 7.5 cm i.d. x 0.6 cm wall thickness) polyvinyl chloride tubing, which was sealed to maintain anoxic conditions. Site 1 (36°48.00 N, 76°17.39' W) was ~100 m southwest of a public boat launch in ~1.5 m of water. Site 2 (36°48.68 N, 76°17.41' W) was located in about 1 m of water and situated across the main channel from a former wood treatment facility, historically responsible for creosote spills to the area. Upon returning to the lab, sediments were extruded at 2 cm depth intervals and samples were analyzed for PAHs and particulate organic carbon as described below. Due to a 24 % vertical core compression and the pore water content, only 22 cm of sediment were available to be processed at this time.

September 1995

In this subsequent sampling expedition, sediment cores were taken from the same sites as noted above, but were collected using both a spade box coring device (30 cm x 21 cm x 60 cm) and a kasten corer (12.7 cm x 12.7 cm x 3 m) (Kuehl et al., 1985). Two box cores and one kasten core were collected at each site. Due to logistical constraints in resolving all analytical parameters at a 1 cm depth interval and the number of analytical parameters involved (e.g. particle and pore water PAHs, TOC, surface area), only data from one box core at each site will be presented. Box cores were subsampled with galvanized aluminum tubing (15 cm dia. x 61 cm x

0.1 cm). The subsampled cores were then sealed, wrapped in two plastic bags, and placed upright in a large garbage pail with ambient seawater for transport back to the lab. A 28% core compression occurred while returning to the lab. Note, minimizing core compression by maintaining a vacuum in the overlying headspace while subsampling is only way to account for core compression. However, onset of rapid phase PAH equilibration is thought to occur immediately.

Within 72 h, the subcores were extruded at 1 cm depth intervals. For each depth interval, the 0.5 cm outer edge was discarded to minimize cross-contamination and ~15 ml of sediment was transferred to a plastic centrifuge tube for measurement of water content. These sediments were dried at 60° C for several days until their weights stabilized for at least 48 h. Remaining sediment from each depth interval was centrifuged in pre-ashed (400° C for 4 h) pint sized glass jars at 1500 g for 25 min. Overlying water was pipetted off and vacuum filtered through a 1µm nominal pore size Gelman Sciences Type A/E glass fiber filter (combusted 4h @ 450° C) to separate particulate and pore water fractions. Thus, the pore water filtrates contained both freely dissolved and dissolved organic carbon (DOC)-bound PAHs.

Filtered pore water was collected in pre-ashed 50 ml glass centrifuge tubes. A majority of the filtered pore water from each depth interval was extracted with hexane (4 x 20 ml after addition of surrogate standards) and analyzed for PAHs as described below. If a sufficient volume of pore water was available, 5 to 10 ml was subsampled into pre-ashed vials for measurement of DOC. The headspace of each DOC sample vial was purged with N₂ prior to freezing (-80 ° C). DOC concentrations and associated PAH binding coefficients are presented in Chapter 3. Sediment was transferred to pre-ashed vials and frozen (-80° C) prior to analysis for

PAHs.

PAH Analyses: sediments and pore water

Sediment samples (~ 5 g wet wt) were transferred to pre-ashed 50 ml glass tubes, to which a surrogate standard mixture containing deuterated PAHs (d_1 -naphthalene, d_{10} -anthracene, d_{12} -benz[a]anthracene, d_{12} -benzo[a]pyrene, d_{12} -benzo[g,h,i]perylene) was added. Sediments were extracted with acetone (1 x 20 ml) and methylene chloride (DCM) (4 x 20 mls) for all samples except Site 2 (Sept. 1995), which were extracted with DCM only (4 x 20 mls), by sonicating 1 h in a ultrasonic bath and shaking for 2 min. The extracts were filtered through pre-cleaned Pasteur pipettes filled with solvent rinsed glass wool and pre-cleaned (Soxhlet extracted with DCM for 48 h) anhydrous Na_2SO_4 , rotoevaporated and solvent exchanged with hexane. The hexane extracts (sediments and pore water) were then cleaned-up by solid-liquid chromatography on silica to remove organic polymers, aliphatic, and polar compounds (Dickhut and Gustafson, 1995). Subsequently, the extracts were concentrated and an internal/recovery standard containing d_{10} -acenaphthene, d_{12} -phenanthrene, d_{12} -chrysene, and d_{12} -perylene was added. PAHs were quantified relative to deuterated surrogate PAHs by gas chromatography/mass spectrometry using selected ion monitoring. Recoveries ranged from 64.4 ± 12.3 % for naphthalene to 97.0 ± 16.8 % for less volatile PAHs.

Radioisotope geochronology, x-radiographs, and grain size

Sediment samples for analysis of ^{137}Cs and 7Be activities were taken from the kasten core at 4 cm depth intervals. Sediments were homogenized and packed into 70 ml plastic petri dishes, which were then sealed using electrical tape. Radioisotope activity was measured over 24 h using

a semi-planar intrinsic Ge detector in conjunction with a multichannel analyzer. Net count rates were converted to activities using efficiency factors specific to each gamma-ray energy level. Sample geometry was identical for all petri dishes. Determination of ^{210}Pb content in sediments was made by measuring the concentration of its granddaughter ^{210}Po (Nittrouer *et al.*, 1979). Briefly, dried and ground sediments were spiked with a ^{209}Po standard of known activity and acid leached (HNO_3 and HCl). The leachate was plated onto silver planchets and activity measured on an alpha detector.

To assess faunal activity in sediments, a 6 cm x 2 cm x 40 cm acrylic liner was vertically imbedded into the box core from each site for X-radiography. Each acrylic liner was placed flush on Kodak AA Industrex X-ray film and photographed using a Dinex 120-F X-ray unit set at 3 mA and 60 kV. Exposure time varied between 45-120 seconds depending on sediment density and grain size.

Grain size analysis was done on selected samples by soaking samples in 10% Calgon detergent, and wet sieving to separate coarse grains (62.5 μm) from fine grains (<62.5 μm), clays and silts. The fine fraction was analyzed using a Micromeritics Sedigraph 5100 Automated particle size analyzer.

Particulate organic carbon, nitrogen, soot carbon and dissolved organic carbon

Particulate organic carbon (OC), nitrogen, and soot carbon were quantified using a CHNS-O (Fisons, EA 1108 - Beverly, MA) analyzer. Soot carbon has been operationally defined as the residual carbon remaining after combusting acidified sediment at 375°C for 24 h (Gustafsson *et al.*, 1997). Pre-weighed samples of sediment and soot were each acidified with 6

N HCl and dried to remove inorganic carbon. Each sample was then placed in the analyzer and flash heated to 1020°C to convert organic matter to CO₂, NO_x, and H₂O (Verado *et al.*, 1990).

Particle surface area

Measurement of the volume of N₂ adsorbed onto a solid at various partial pressures of nitrogen are well correlated with intraparticle surface area (Gregg and Sing, 1982). Sediments were freeze-dried for 24 h and then gently separated for surface area analysis. Freeze-dried sediments were heated at 200°C under N₂ flow for ~ 60 min to remove any residual water. Sediment surface area was determined by adsorbing N₂ at liquid nitrogen temperatures using a Micromeritics Gemini III - 2375 Surface Area Analyzer. This technique for determining surface area is referred to as the Brunnauer, Emmett, and Teller (BET) method (Gregg and Sing, 1982). To better elucidate the role of organic matter sorption on particle surface area, organic matter in these sediments was digested using a peroxide / sodium pyrophosphate procedure (Mayer, 1994). For selected sediment samples, organic matter was removed by overnight incubation in 10 ml of 30% hydrogen peroxide + 40 ml of 0.1 M sodium pyrophosphate. Solutions were heated to ~ 80°C and peroxide added in 5 ml aliquots until bubbling ceased. At this point, residual mineral grains were washed in 10% acetone in water (to remove salt), centrifuged, and freeze-dried prior to surface area analysis.

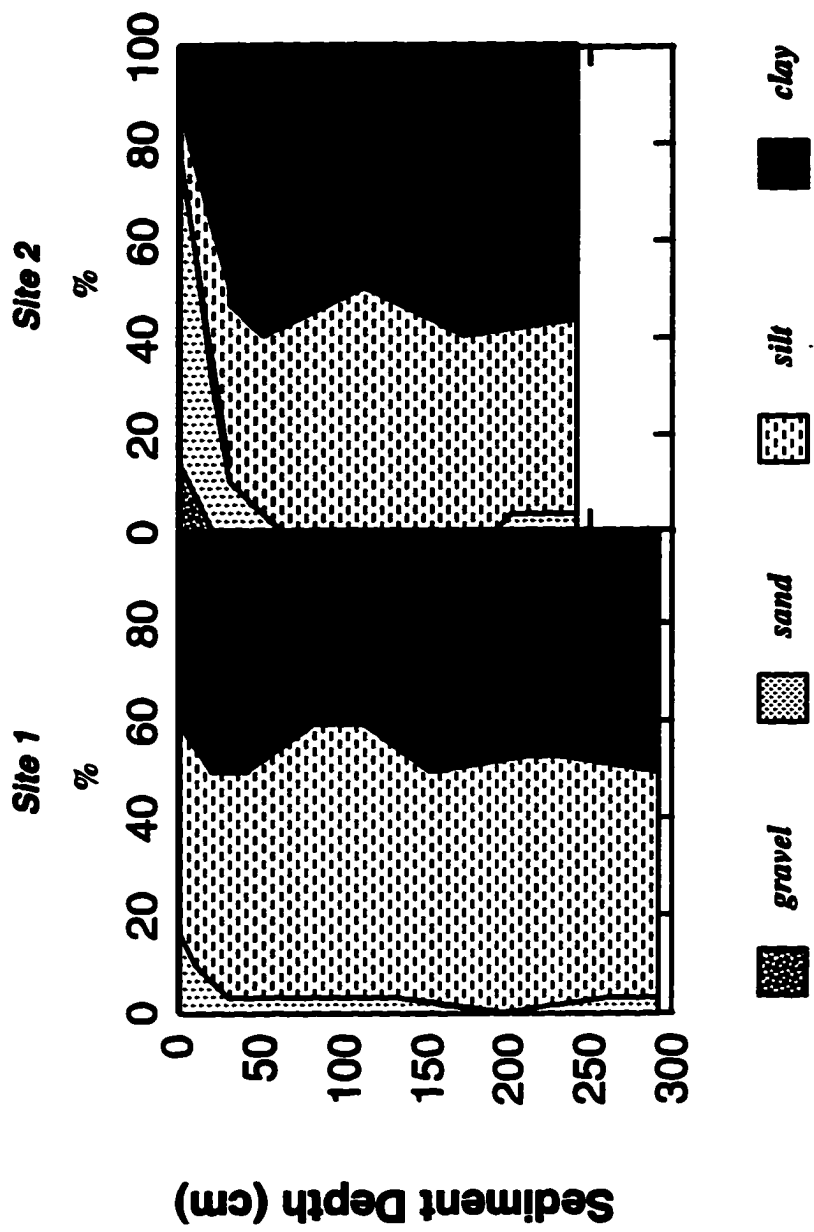
2-6. Results and discussion

Geochronology and sediment characteristics

Kasten Core - Grain size and isotope profiles

Textural analyses revealed significant differences between the sampling sites in the upper 0.5 m of the seabed, particularly in terms of silt and sand content (Figure 2-2). Woody debris and shell hash contribute to the relatively high abundance of sand at Site 2, as well as to the presence of gravel in the upper seabed. Below about a meter depth in the seabed, both sites display low (< 2%) sand abundances and unequal amounts of silt and clay. Radiochemical analyses of sediments from Sites 1 and 2 show low, relatively uniform ^{210}Pb ($t_{1/2} = 22.3$ y) activities throughout the depth (~ 2.5 m) of each kasten core (Table 2-2). The observed activity levels (~1 dpm/g) are consistent with that expected from decay of ^{226}Ra contained in the sediments. This suggests that no excess ^{210}Pb is present at either site. Further, measurements of ^7Be ($t_{1/2} = 53.3$ d) and ^{137}Cs ($t_{1/2} = 30.1$ y) revealed no detectable activity in either core. Taken together, these observations suggest the absence of recent sediment accumulation at either site. As the global introduction of significant ^{137}Cs fallout from atmospheric weapons testing began in 1954, we can conclude that no net accumulation of "new" sediment has occurred at either site since that time. Given the absence of significant excess ^{210}Pb , it also appears likely the period of non-accumulation extends back even further, perhaps the past 60-80 years. Although this interpretation is consistent with radiochemical observations, the position of the sites with respect to a main shipping channel that undergoes periodic dredging suggests another possible explanation. Dumping of dredge spoils along channel flanks has been a common practice in the Elizabeth River as well as other areas (Nichols, pers. comm.). The possibility exists that older sediment excavated through dredging,

Figure 2-2. Grain size distribution profiles (% by weight) from kasten cores collected at each site in the Elizabeth River (see Fig. 1). Greater amounts of woody debris and shell hash at Site 2 are evidenced by relatively higher weights of particles in gravel and sand fractions in the upper layers of sediment.



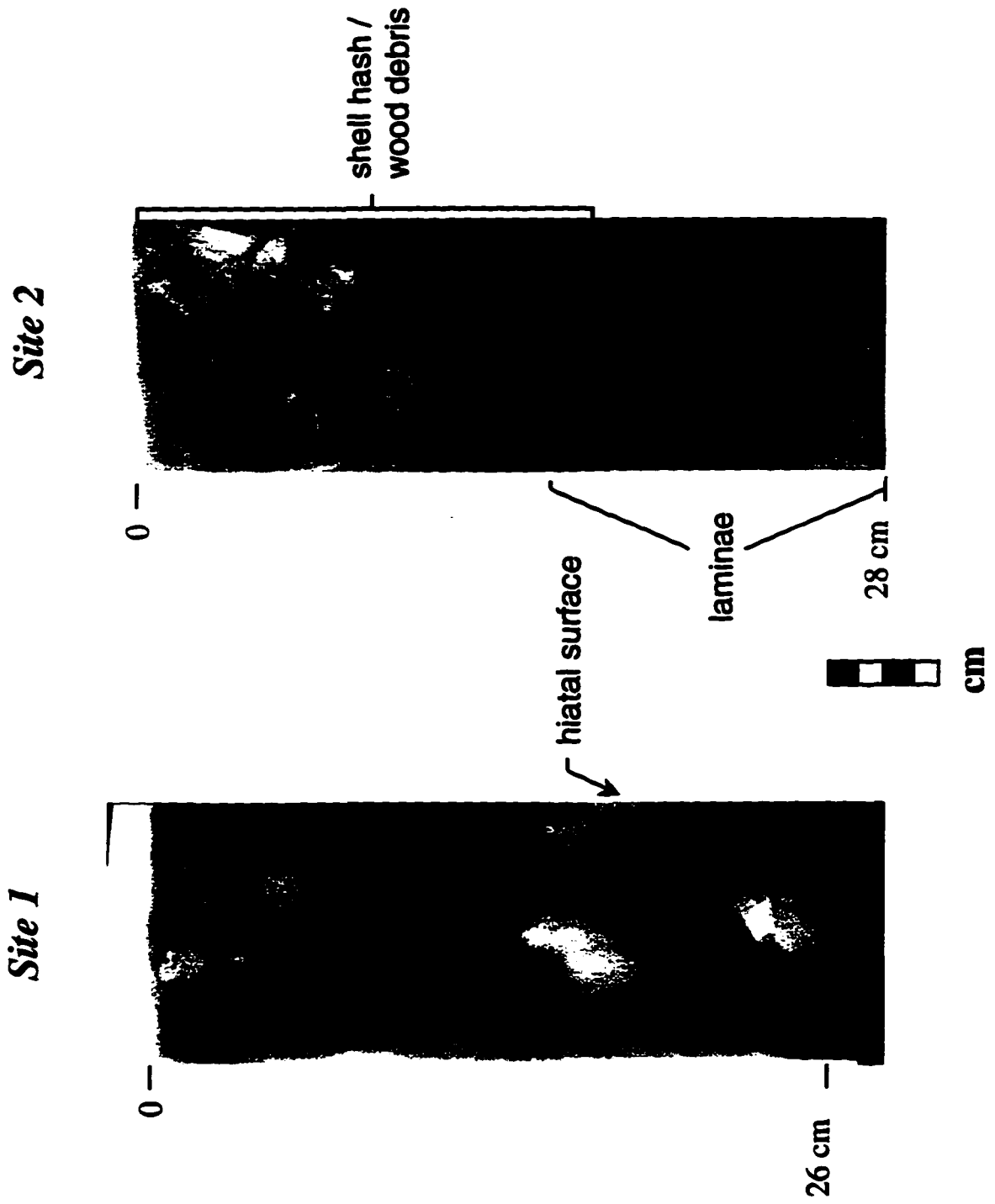
which has not been in contact with the water column in the past 60-80 years, has been dumped at Sites 1 and 2. Such rapid dumping of older sediment would likely preclude scavenging of significant amounts of ^{210}Pb or ^{137}Cs , thus confounding the interpretation of sediment geochronology based on the radioisotope profiles.

With sediments comprised of old dredge spoil or situated in a non-depositional zone, PAHs may have been introduced several decades by natural or non-industrial combustion sources (e.g. forest fires, domestic heating). Alternatively, concentrated dissolved sources of PAHs may have been rapidly scavenged by particles during deposition or resuspension.

Box core - X-radiographic and geochemical profiles

X-radiographic observations provide evidence that the depositional histories of Sites 1 and 2 were distinctly different, despite their relatively close proximity and similar water depths (Figure 2-3). The Site 1 core displays a mottled structure throughout, suggesting that relatively intense reworking by benthic macrofauna characterized this depositional environment. A possible hiatal (scour) surface is observed at ~15-20 cm depth (Figure 2-3), which indicates an erosional event followed by the probable resumption of former depositional conditions. The amount of "missing time" represented by this hiatus could not be determined as the short-lived tracers used in this study (i.e. ^{210}Pb and ^{137}Cs) were absent both above and below the scour surface. In contrast, Site 2 is characterized by coarse shell/wood hash in the upper ~15 cm, with physically laminated muds below. The presence of physical laminations suggests that the associated depositional environment was characterized either by absence of macrofauna, or by very rapid accumulation that would preclude the development of biogenic structures (i.e. mottling). The relatively coarse

Figure 2-3. Box core sediment X-radiograph positives of Site 1 and Site 2 indicating different historical deposition environments for each site despite their close proximity. Site 1 radiograph shows mottled sediments throughout the core with the exception of a scour surface at ~ 15-20 cm depth representative of an erosional event. At Site 2, the radiograph depicts the presence of coarse shell hash and woody debris in the top 15 cm of the core followed by the presence of physically laminated muds below.



shell/wood hash at the surface of this core likely represents a storm (lag) layer where coarse material carried as bed load during an energetic event was deposited at the site.

Depth profiles of sediment %OC and C/N ratio indicate more heterogenous sources of particulate organic matter at Site 2 relative to Site 1 (Figure 2-4). Specifically, depth profiles of both %OC and C/N ratio vary at Site 2 to a greater extent than at Site 1. In addition, the C/N ratio markedly decreases with depth at Site 2, consistent with the sediment grain size distributions at this site. Wood and other terrestrial organic matter tends to be higher in C/N ratios relative to marine plants and organisms (Meyers, 1994 and references therein). Deposition of this terrestrial-derived organic matter as runoff or in-situ woody debris at the surface of Site 2 likely controls the observed nonuniform sediment C/N profiles.

At both sites, total sediment surface area tends to increase with depth (Figure 2-5). Calculations indicate that surface area changes with depth are independent of bulk changes in grain size. Thus, increasing surface area may either be a function of increasing porosity of mineral grains, greater sorption of porous organic matter with depth, or relatively greater amounts of a smooth organic coating on the surface sediments relative to those deeper in the core. The difference in surface area before and after organic digestion (Figure 2-5), is greater for sediments at Site 2 compared to those at Site 1. Nonetheless, organic-free surface areas are ~40% lower than those measured before digestion near the surface (0-11 cm) of *both* cores. This suggests the presence of some porous organic matter in each core rather than a smooth organic coating. Greater amounts of a porous organic coating with depth are likely responsible for the increasing total sediment surface area with depth at Site 2, as evidenced by the contrast between total and organic-free surface area (Figure 2-5). In contrast, increasing porosity of the mineral

Figure 2-4. Geochemical profiles for Elizabeth River sediment cores (see Fig. 1). Site 1 (filled symbols); Site 2 (open symbols). Percent organic carbon and C/N ratios support the notion that sources of particulate organic matter have been more heterogenous at Site 2 relative to Site 1. Similar amounts of soot carbon at both sites indicates variations in soot carbon are not responsible for observed PAH distributions at these sites. The presence of woody debris or inputs of terrestrial organic matter gradually decreasing in amount with depth at Site 2 is evidenced by decreasing C/N ratios. Although not on the same depth scales, the more pronounced decrease in water content with depth at Site 2 in the top few cm of sediment support the grain size profiles in Figure 2-2.

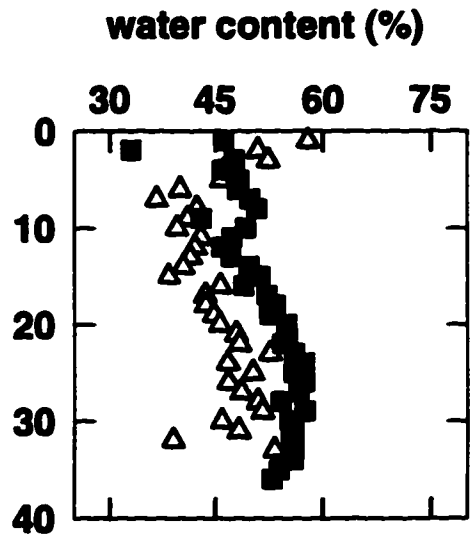
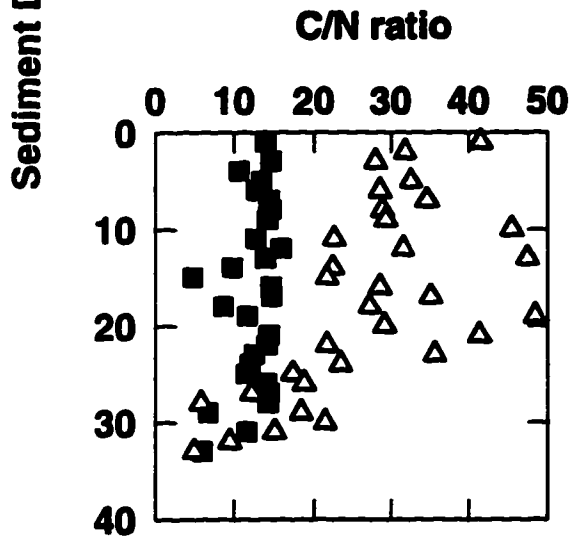
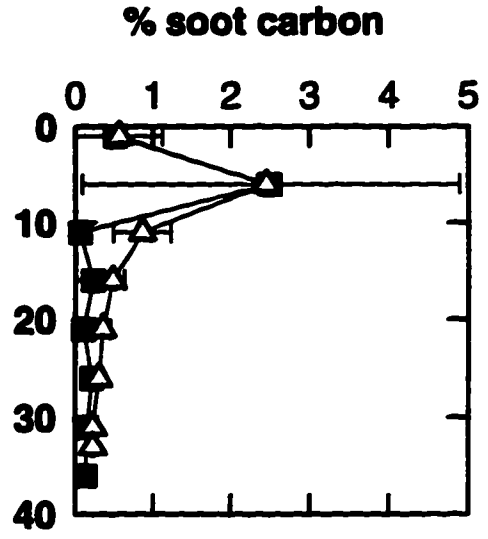
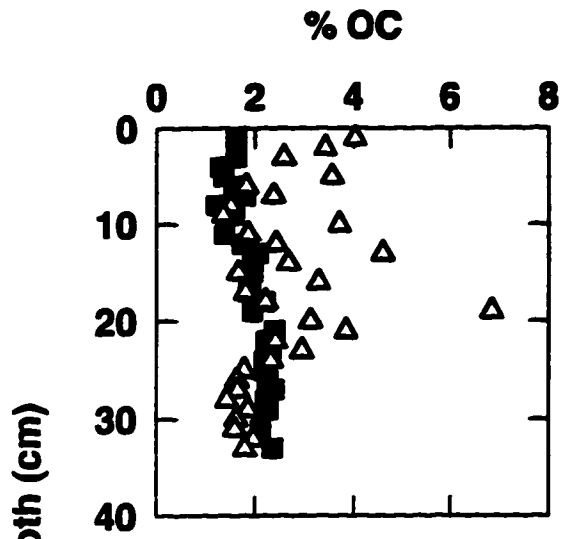
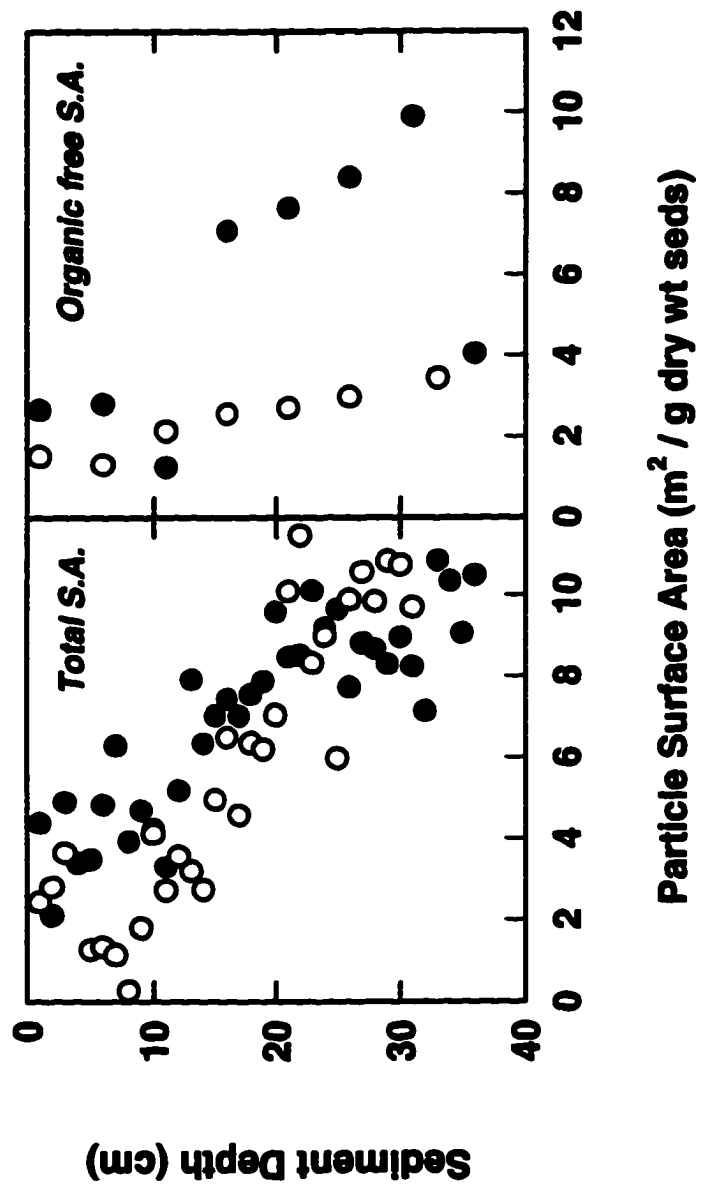


Figure 2-5. Particle surface area of Elizabeth River sediments before (total surface area) and after digestion of organics (organic-free surface area): Site 1 (filled symbols); Site 2 (open symbols). Total surface area increases with depth at both sites (independent of grain size). Organic-free surface area varies from total surface area at Site 2 more so than at Site 1. Trends in total surface area at Site 1 are likely a function of increasing porosity within each respective grain size class (see Figure 2-2) with depth, whereas at Site 2, increasing total surface area with depth is a function of greater sorption of porous organic matter with depth.



grains with depth at Site 1 likely controls the trend in sediment surface area in this core since both the mineral and total surface area profiles are similar.

PAH Concentrations and Distribution Coefficients

Data collected in July 1994 indicated that PAH sediment/pore water distribution coefficients decreased with depth in the cores despite normalization to the amount of particulate organic carbon at each depth interval (Figure 2-6). Additional sediment cores were collected at the same sites in the Elizabeth River in the subsequent year to further investigate these findings. In the sediment cores collected during Sept. 1995, K'_{oc} s for PAHs were also observed to decrease as much as three orders of magnitude with depth at Site 1, but not at Site 2 (Figure 2-7). The lack of a decrease in K'_{oc} with depth at Site 2 compared to our earlier observations (Figure 2-6) likely indicates that our collection of sediment cores in Sept. 1995 was not in precisely the same location as in July 1994. This indicates there is large spatial heterogeneity in sediment deposition in this perturbed estuarine environment as discussed further below. The role of DOC in affecting the observed distributions of PAHs in a two phase sediment/pore water system is discussed in Chapter 3, whereas the role of particle geochemistry in affecting PAH K'_{oc} s is discussed below.

In the Sept. 1995 cores, pore water PAH concentrations were similar between Site 1 and Site 2 (Figure 2-8) although particle-associated PAH concentrations were substantially higher at Site 2 (Figure 2-9). This reflects differential PAH-sediment binding at each site; despite normalizing to the amount of sediment organic carbon, substantially higher K'_{oc} s for PAHs were observed at Site 2 compared to Site 1 (Figure 2-7). In addition, sediment-associated PAH

Figure 2-6. Relationship between K'_{OC} and K_{OW} for selected PAHs in Elizabeth River sediments sampled at Site 2 in July 1994 (○: 2-4 cm; □: 18-20 cm). The curvature indicates that PAH distributions between sediments and pore waters at this site were not at equilibrium between these two phases (i.e. particle-associated and freely dissolved). The overall lower log K'_{OC} values at 18-20 cm compared to 2-4 cm implies that accounting for differences in particulate organic carbon with depth does not explain differences in observed sediment/pore water distributions of PAHs.

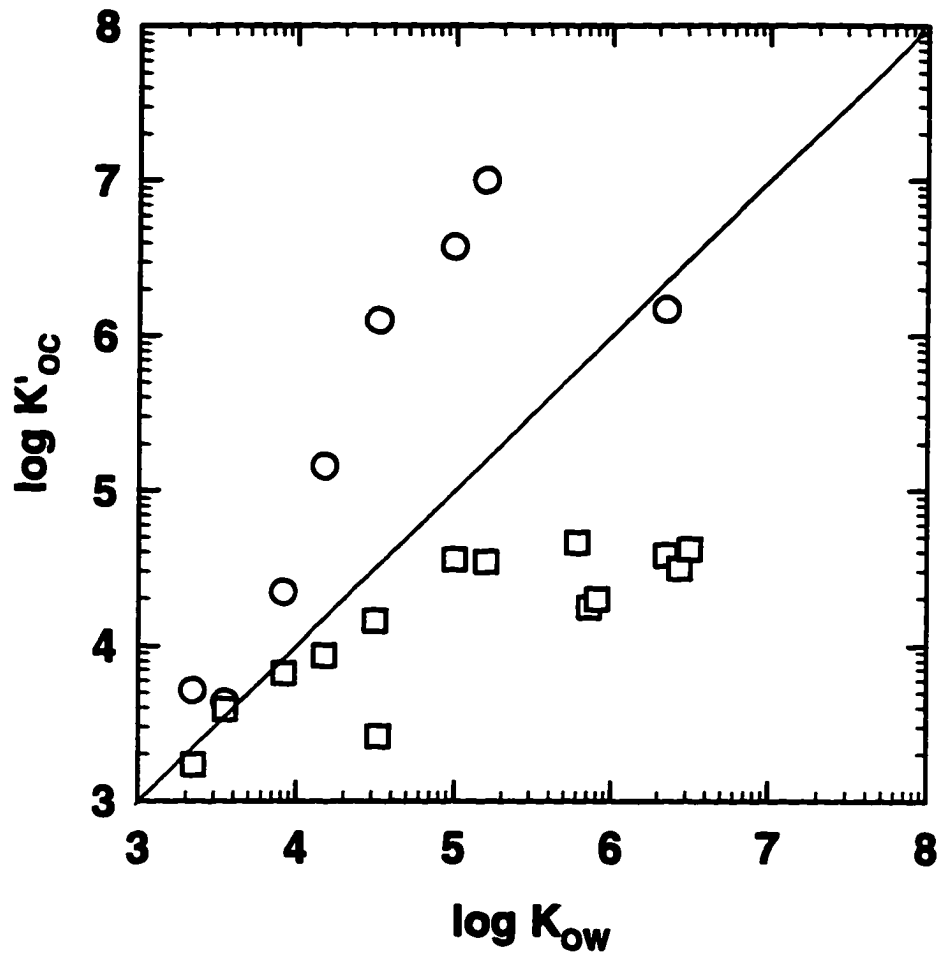


Figure 2-7. Observed organic carbon-normalized sediment/pore water distribution coefficients of selected PAHs in Elizabeth River sediments collected in Sept. 1995. Site 1 (filled symbols); Site 2 (open symbols). Selected PAHs were chosen to represent a range of molecular weights (*ace* - acenaphthene; *pyr* - pyrene; *b[a]p* - benzo[a]pyrene; *b[b]f* - benzo[b]fluoranthene; *i[1,2,3-cd]p* - indeno[1,2,3-cd]pyrene; *d[a,h]a* - dibenz[a,h]anthracene). Log K'_{oc} s decrease by as much as three orders of magnitude with depth in sediments at Site 1. In contrast, uniform log K'_{oc} profiles with depth are evident at Site 2.

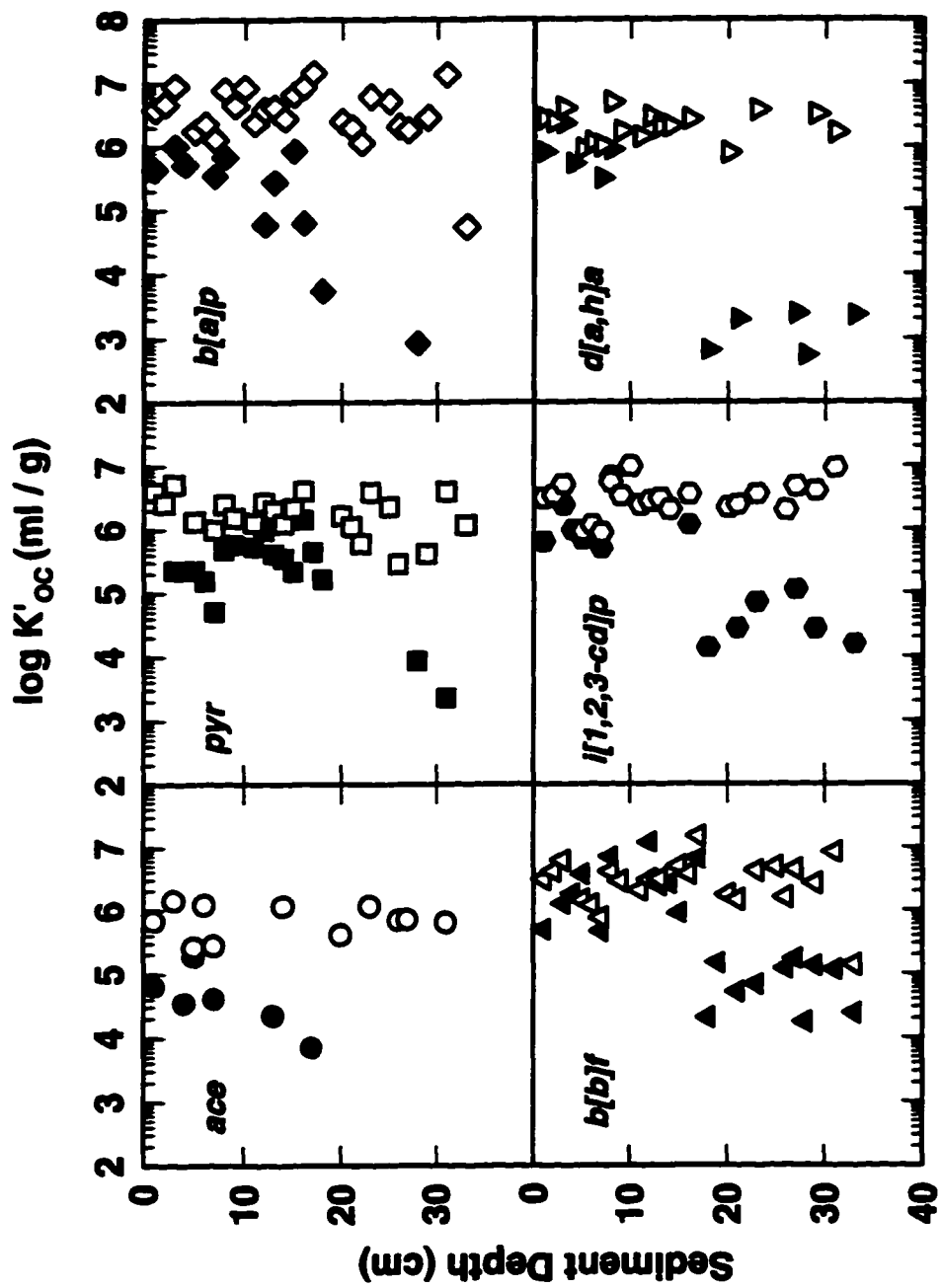


Figure 2-8. Depth profiles of PAH concentrations in Elizabeth River pore waters. Site 1 (filled symbols); Site 2 (open symbols). Selected PAHs were chosen to represent a range of molecular weights (see Figure 2-7 for definitions of abbreviations). Similar pore water PAH concentrations are evident between both sites for the range of compounds chosen.

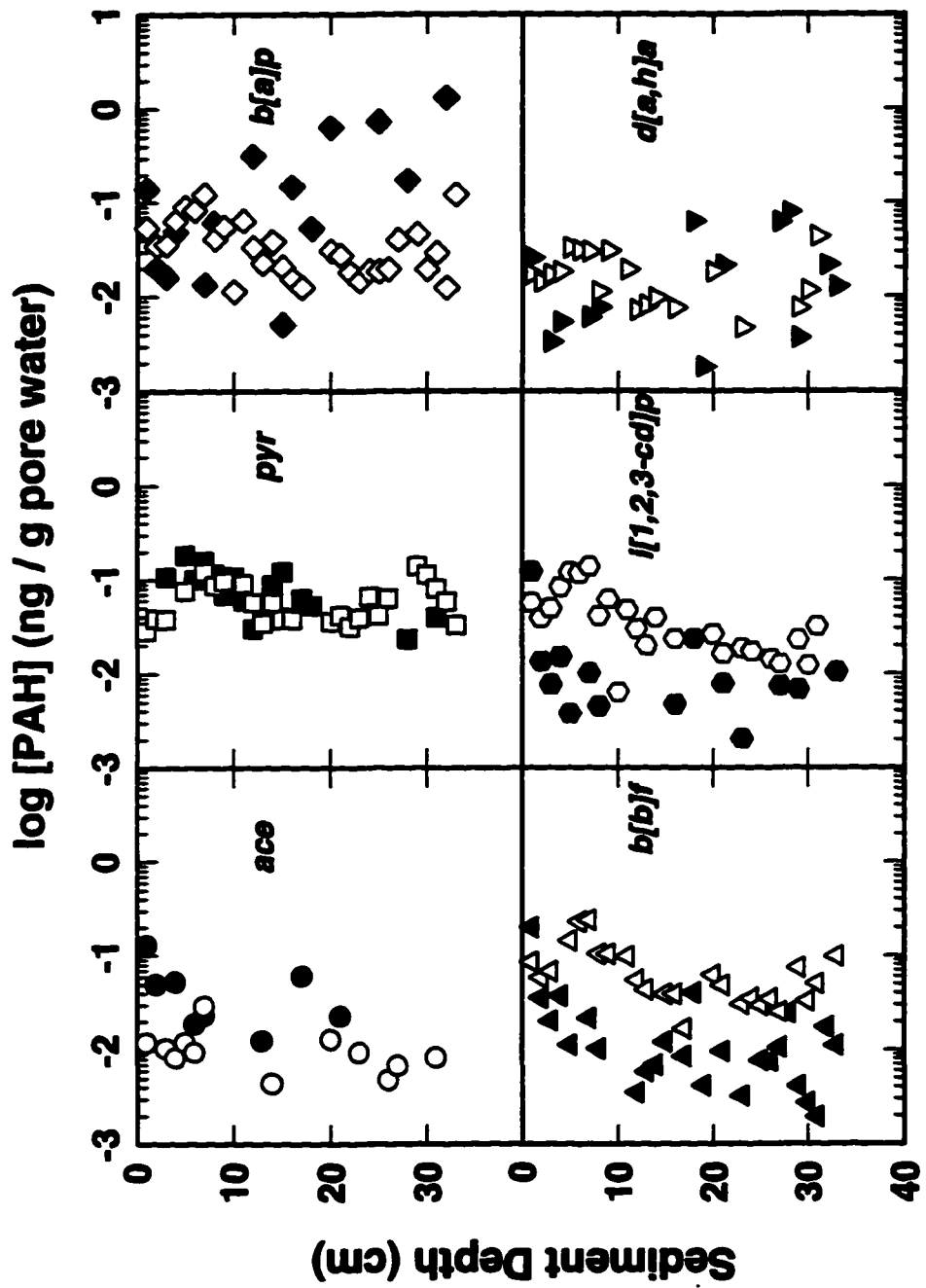
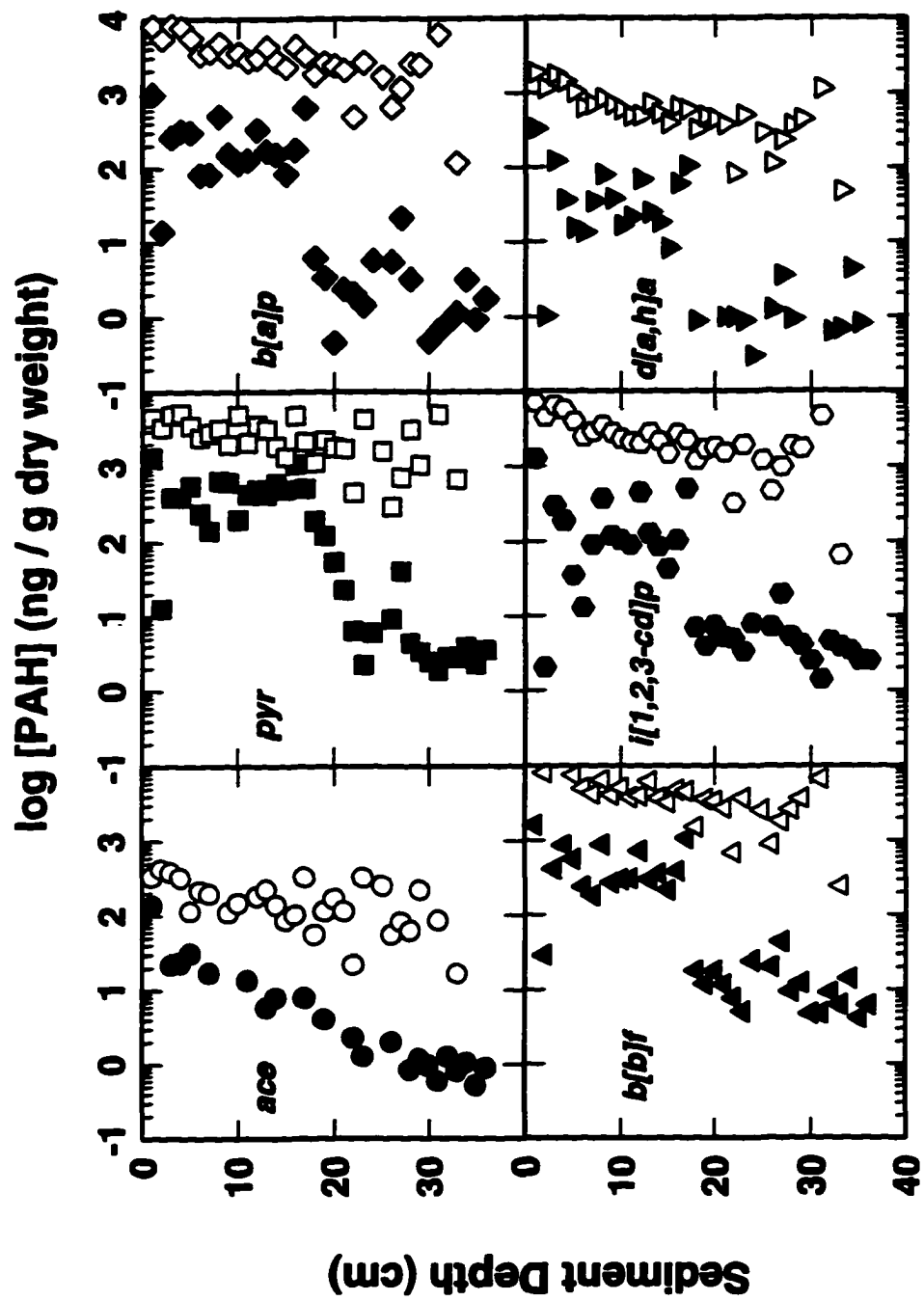


Figure 2-9. Depth profiles of PAH concentrations in Elizabeth River sediments. Site 1 (filled symbols); Site 2 (open symbols). Selected PAHs were chosen to represent a range of molecular weights (see Figure 2-7 for definitions of abbreviations). Higher sediment concentrations at Site 2 relative to Site 1 are possibly a result of the greater amounts of creosote treated woody debris at Site 2.



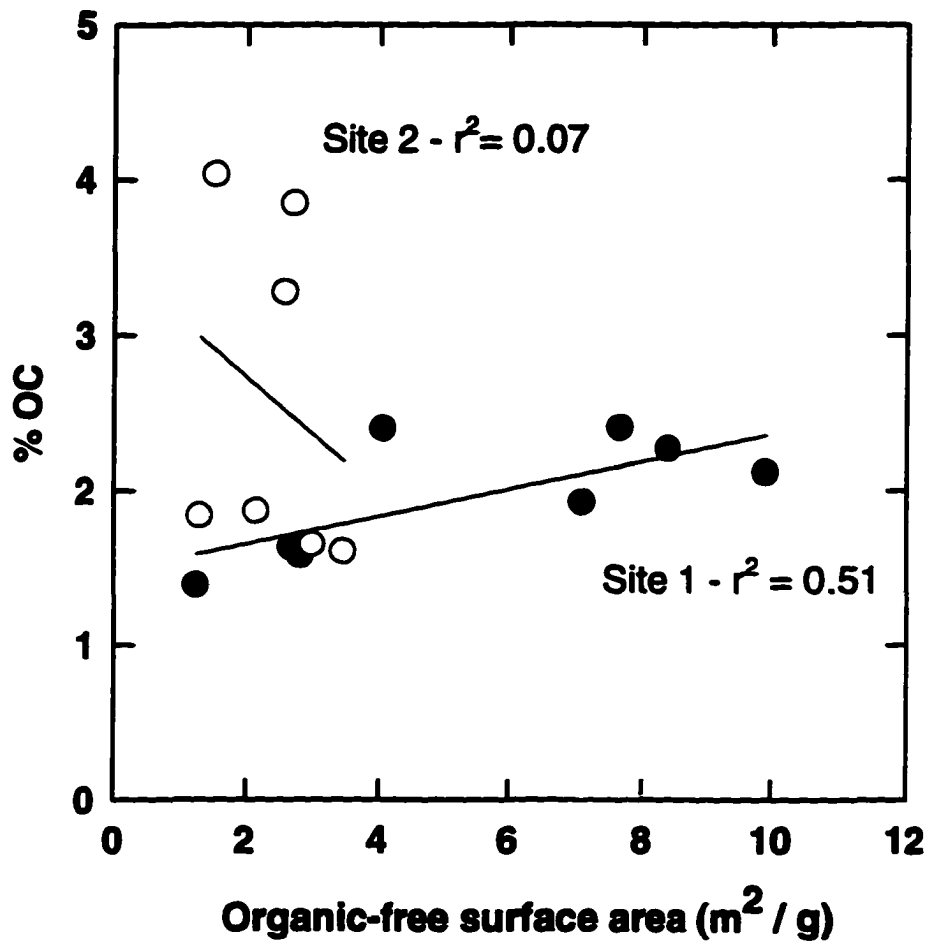
concentrations decrease with depth at both sites, but more so at Site 1 compared with Site 2 (Figure 2-9). The decreased sediment-associated PAH concentrations with depth could be due to increased PAH inputs to the Elizabeth River estuary with time or diffusion of a single (e.g. non-aqueous phase liquid) source of these contaminants downward from the sediment surface. As demonstrated below, the PAHs at Site 1 are not derived from a single source. Secondly, although it is likely that PAH inputs to the Elizabeth River have increased with time, this does not explain the observed K'_{oc} profiles for PAHs. As stated earlier, normalization to the amount of sedimentary organic carbon is expected to account for variability in K'_{oc} s for a PAH to within a factor of two. A three phase model was used to calculate the role of pore water DOC on PAH binding. The results of the model indicate PAH-DOC binding contributes to a maximum one order of magnitude change in down-core K'_{oc} s (Chapter 3). Thus, both the decreasing sediment-associated PAH concentrations and K'_{oc} s with depth are interpreted in terms of the properties of the particles, which are also associated with the age of the sediment.

Although there are distinct differences in OC content and C/N ratio between sites (Figure 2-4), trends in these data do not mirror PAH concentrations or distribution coefficients at each site. For example, the C/N ratio of sediments at Site 1 varies little with depth (Figure 2-4), but the PAH distribution coefficients (Figure 2-7) and particle-associated concentrations (Figure 2-9) at the same site vary approximately three orders of magnitude. Likewise, sedimentary soot concentrations, used to explain high sediment/pore water PAH distribution coefficients in Boston Harbor (Gustafsson *et al.*, 1997), are consistent between sites (Figure 2-4), in contrast to PAH distribution coefficients and concentrations. Thus, sedimentary soot does not explain observed differences in PAH distributions between sediments and pore waters at these sites. Finally, total

surface area of the sediment particles increases in a similar manner with depth at both sites (Figure 2-5) in contrast to $\log K'_{oc}$ and sediment-associated PAH concentrations, but the organic-free surface area of the sediment particles in each of the cores collected in Sept. 1995 (Figure 2-5) reflects trends in measured particle-associated PAH concentrations (Figure 2-9) and $\log K'_{oc}$ values (Figure 2-7).

As noted above, at Site 1 the increase in total particle surface area with depth is likely due to increased down-core mineral porosity, with some organic matter sorption to the sediments in the top portion of the core. The organic carbon content of the sediments at this site increases with mineral surface area (Figure 2-10). It is difficult to reconcile this fact with the decreasing sediment-associated PAH concentrations and K_{oc} s with depth at this site. We propose that the accessible particulate organic matter for PAH partitioning decreases downcore at Site 1. This decrease in accessible particulate organic matter with depth is evident from the surface area data before and after digestion of organic matter associated with these particles. In the top ~11 cm of the core, digestion of organic matter results in an ~ 40 - 60% decrease in surface area, whereas between 16-31 cm depth, digestion of organic matter results in only a 0 - 10% decrease in surface area. This suggests the presence of a porous dissolved organic matter coating on sediments in the top 11 cm at Site 1 but not deeper in the core. Since the organic carbon content of the sediments at this site increases in the sediment column in proportion to particle surface area (Figure 2-10), it is evident that there is particulate organic matter deeper in the core at this site is inaccessible for partitioning of PAHs (e.g. hard organic matter - Figure 1-2). Such occlusion of particulate organic matter for digestion can result from the presence of iron oxides or humified organic residues (Sequi and Aringhieri, 1977). Distribution of PAHs between particulate organic matter

Figure 2-10. Percent organic carbon in sediments versus organic-free surface area. Site 1 (filled symbols); Site 2 (open symbols). Organic carbon in sediments at Site 1 increases with mineral surface area. In contrast, very little inter-dependance exists between the amount of particulate organic carbon and organic-free surface area in sediments at Site 2.



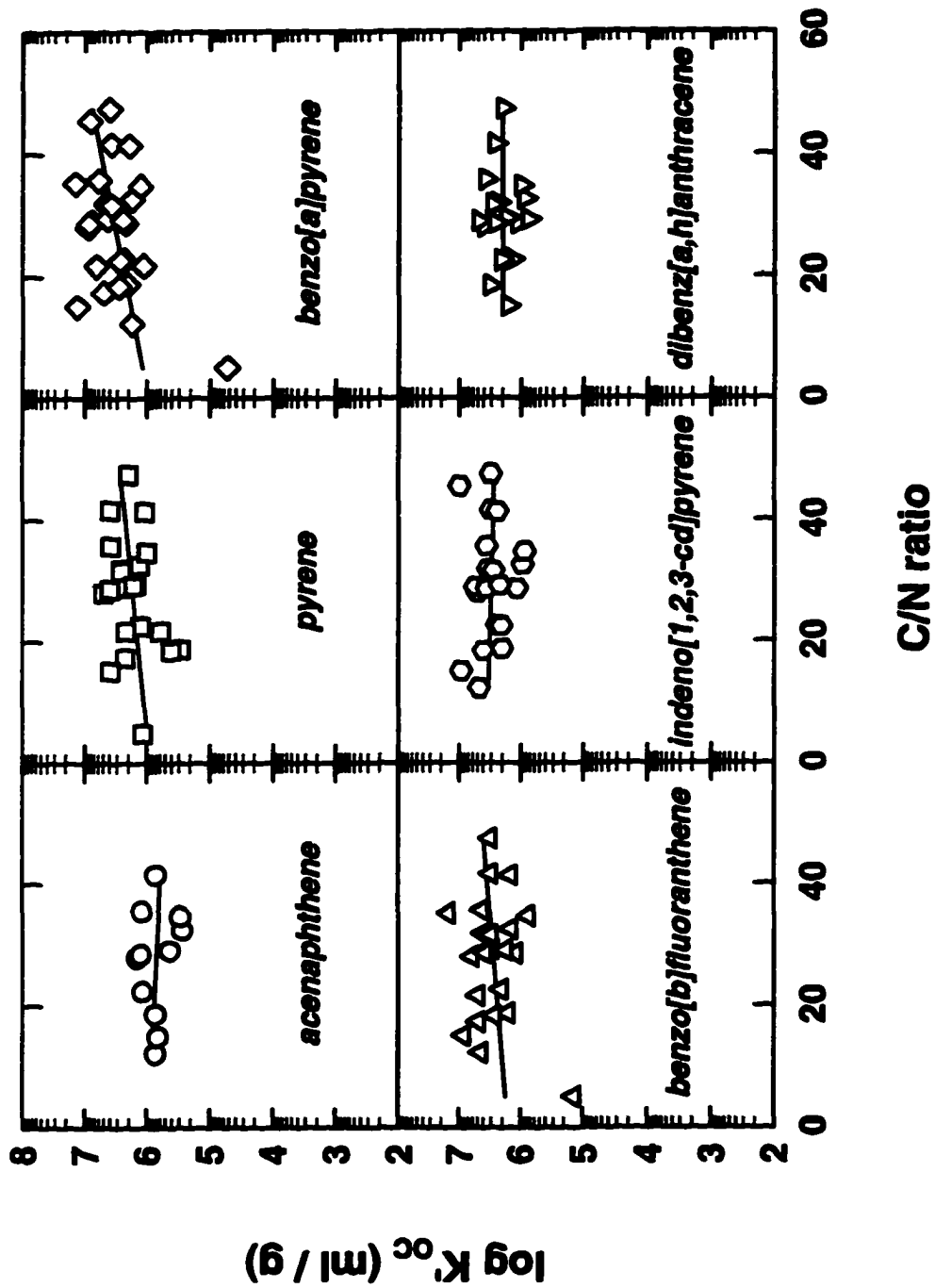
in sediments and pore water deep in the sediments at this site is therefore inhibited. PAHs may be at equilibrium with respect to partitioning to available surfaces; however, the inaccessibility of the particulate organic matter deep in the core implies that this distribution is between mineral surfaces and pore water. Thus, distribution coefficients are low at Site 1, since mineral surfaces are a less desirable matrix for hydrophobic contaminants (Schwarzenbach et al., 1993).

Moreover, organic carbon-normalization does not account for down core changes in PAH distribution coefficients.

At Site 2, core profiles of particle-associated PAH concentrations and their respective K'_{oc} values also may be explained by particle surface areas, which at this site are dictated by the sorption of porous organic matter to the sediment surface. The relationships between PAH K'_{ocs} and C/N ratios of the particulate matter at this site (Figure 2-11) indicate that the particles at this site may consist of terrestrial runoff or possibly in-situ woody debris (e.g. pilings) coated with porous dissolved organic matter which entraps PAHs within the particle matrix. Wood pilings are pressure treated and thus infused with creosote (usually a concentrated mixture of PAHs and other petroleum hydrocarbons) to minimize fouling and degradation. One may speculate that remnants of such pilings may be responsible for PAH distributions at this site. Wood debris and/or other particles originating from terrestrial runoff coated with natural organic matter will act to sequester PAHs within the particle matrix such that they will not partition to pore waters during sediment burial and diagenesis. In this case, K'_{ocs} will remain high (i.e. PAHs stay on the particles) throughout depth in the sediment as observed at Site 2 (Figure 2-7).

The notion of a single predominant source of PAHs that are bound within the particle matrix at Site 2 can be inferred from the uniform PAH isomer ratio profiles at this site with depth

Figure 2-11. Organic-carbon normalized PAH distribution coefficients (K'_{ocS}) in sediments at Site 2 in the Elizabeth River as a function of sediment C/N ratios.



in the core (Figure 2-12). Concentration ratios of structurally similar PAHs associated with sediments may vary between sites or with time, due to differences in PAH source material composition, transport pathways, and potentially, geochemical reactivity between isomers. Thus, variable ratios of PAH isomers should be a tracer of PAH transformation during transport from their origin to deposition and burial, or simply reflect differences in PAH sources between sites or which occur with time (Sporstol *et al.*, 1983; Colombo *et al.*, 1989; Zeng and Vista, 1997). The PAH isomers that were selected for these analyses were: phenanthrene/anthracene, fluoranthene/pyrene, and benzo(e)pyrene/benzo(a)pyrene (Figure 2-12). In each case, the compound in the denominator is the more photoreactive isomer (Mackay, 1992; Liu, 1996). Note the similarity in isomer ratios between both sites in the top 15 cm of the sediments followed by considerable variation in ratios of all three groups of compounds with depth at Site 1. Additionally, the most reactive isomers are consistently depleted with depth below 15 cm at Site 1.

Coupled with information provided by X-radiographs (Figure 2-3), and ^{210}Pb geochronology (Table 2-2), it would appear that at Site 1, particulate organic matter and associated PAHs have been deposited at this site in a bimodal manner over the last 60-80 y. PAHs deposited below the hiatal layer are depleted in reactive isomers indicating significant geochemical loss of extractable PAHs presumably via degradation during transport and deposition. Near the top 10-15 cm of the core, PAH sources at Site 1 appear to be similar to those at Site 2 or alternatively, PAHs may be sequestered within the particle matrix by an organic coating at both sites. At Site 2, ratios of PAH isomers are fairly uniform with depth, indicating continued historical inputs from similar PAH sources and little photochemical degradation of

Figure 2-12. PAH isomer concentration ratios with depth in sediments as indicators of source(s) and geochemical reactivity of PAHs: phenanthrene/anthracene (top frame); fluoranthene/pyrene (middle frame); benzo[e]pyrene/benzo[a]pyrene (bottom frame). Site 1 (filled symbols); Site 2 (open symbols). The compound in the denominator in each case is the more reactive PAH isomer. At Site 1, PAH isomer concentration ratios are fairly uniform to a depth of ~ 15 cm indicating similar PAH sources, transport pathways, and transformation mechanisms before and after burial possibly the result of particles being surrounded by an organic coating. Below this depth, ratios increase, indicating differential transformation between the isomers presumably prior to deposition or a consistent change in PAH source(s) with time. The onset of this departure from uniform isomer ratios at this site below ~ 15 cm depth corresponds to the hiatal layer in the sediments seen in Figure 3. At Site 2, the relatively uniform isomer concentration ratios imply a consistent source of PAHs throughout time and no preferential degradation of reactive isomers.

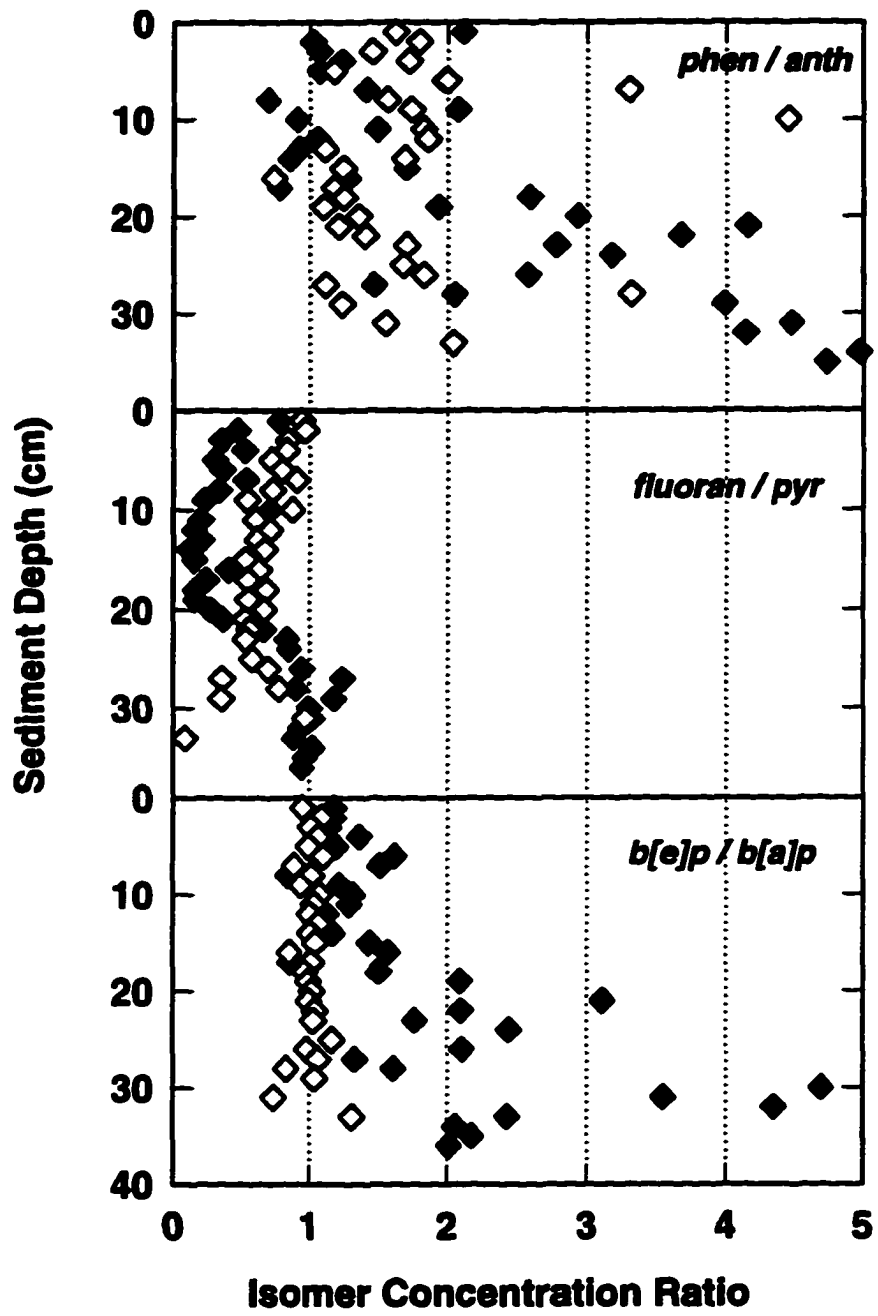


Table 2-2. Total ²¹⁰Pb Activity (dpm/g dry wt.) in sediment cores from the Elizabeth River.

Depth In Sediment (cm)	Site 1	Site 2
0-4	0.692	0.997
8-12	0.771	0.819
16-20	0.767	0.792
24-28	0.856	0.767
32-36	0.767	0.812
40-44	0.844	0.872
48-52	0.835	0.769
78-82	0.937	0.838
108-112	1.005	0.814
138-142	1.118	0.853
168-172	1.143	0.844
198-202	1.145	0.874
238-242	1.165	0.972
258-262	1.139	N/A

reactive isomers prior to burial at this site. The lack of preferential depletion of the reactive isomers could be explained by PAH sequestration within the particle matrix rendering them unavailable for transformation both prior and subsequent to burial at this site.

2-7. Conclusions

Sediments and pore waters of the Elizabeth River estuary were sampled for PAHs and selected geochemical variables. Both sites sampled have been in a non-depositional environment for the past ~ 60-80 y. At Site 1, PAH distributions between sediments and pore waters (K'_{ocS}) varied by several orders of magnitude from the surface to bottom of a core. This phenomena was also observed in previously collected cores from these sites. In contrast, in a core from Site 2, PAH K'_{ocS} were fairly uniform with depth, but larger than their respective K_{owS} (see Chapter 3). Although dilute sedimentary soot has been invoked as an explanation for anomalously high PAH K'_{ocS} relative to their K_{owS} (Gustafsson, *et al.*, 1997), these results indicate that neither sedimentary soot nor specific geochemical variables of sediments (*e.g.* grain size), are directly responsible for observed PAH concentrations and distribution coefficients in the Elizabeth River. Rather, particle surface area of sediments before and after digestion of organics indicate that at Site 1, large down core decreases in PAH K'_{ocS} may be the result of decreased accessibility of the particulate organic matter with depth in the sediment column. Moreover, at Site 2, we speculate that organic matter coating of terrestrial runoff or in-situ wood debris serves to sequester PAHs within the particle matrix. Thus, photochemical degradation of PAHs prior to deposition, as well as possible microbial access and subsequent degradation of PAHs are minimized, resulting in elevated PAH K'_{ocS} relative to their K_{owS} in this core.

Our results coupled with those of Gustafsson *et al.*, (1997) indicate that there are cases where PAH distributions between sediments and pore waters in harbor sediments will not be accurately described by normalizing distribution coefficients to the amount of particulate organic carbon. Large vertical and horizontal heterogeneity in sediment/pore water PAH K'_{oc} s over short spatial scales is apparent in the urban Elizabeth River. Our data indicate that such wide-ranging K'_{oc} s may result from PAH inaccessibility to the entire pool of organic carbon within the particle matrix. Moreover, for PAHs as a suite of compounds, source(s) to sediments play a significant role in determining their distribution, bioavailability, and biogeochemical cycling. PAHs entrapped within particle matrices by substances such as creosote, and in the case of PAHs bound with soot (Gustafsson *et al.*, 1997), yielding high K'_{oc} s and little distribution of PAHs to pore waters. However, where PAHs have become associated with sediments from other presumably diffuse sources (e.g. oil spills, atmospheric gas exchange), these carcinogenic compounds may be readily associated with pore water during sediment diagenesis rendering them available for exchange to overlying water and organisms.

2-8. References

- Adams, D. 1996. Abstract. Society of Toxicology and Chemistry National Meeting. Washington D. C.
- Berner, R. A. 1980. Early diagenesis: A theoretical approach. Princeton University Press, Princeton, NJ, 241 pp.
- Blumer, M. 1976. Polycyclic aromatic compounds in nature. *Scientific American*, 234, 34-45.
- Brown, D. S. and Flagg, E.W. 1981. Empirical prediction of organic pollutant sorption in natural sediments. *J. Environ. Qual.*, 10, 382.

- Burdige, D. 1991. The kinetics of organic matter mineralization in anoxic marine sediments. *J. Mar. Res.*, 49, 727-761.
- Colombo, J. C., Pelletier, E., Brochu, C., Khalil, M. 1989. Determination of hydrocarbon sources using *n*-alkane and polyaromatic hydrocarbon distribution indexes. Case Study: Rio de La Plata Estuary, Argentina. *Environ. Sci. Technol.*, 23, 888-894.
- Denisenko, M. F., Pao, A., Tang, M., Pfeifer, G. P. Preferential formation of benzo[a]pyrene adducts at lung cancer mutational hotspots in P53. *Science*, 274, 430-432.
- Dickhut, R.M and Gustafson, K. E. 1995. Atmospheric inputs of selected polycyclic aromatic hydrocarbons and polychlorinated biphenyls to southern Chesapeake Bay. *Mar. Pollut. Bull.*, 30, 385-396.
- Gelboin, H. 1980. Benzo[a]pyrene metabolism, activation, and carcinogenesis: Role and regulation of mixed function oxidases and related enzymes. In Physiological Reviews - v. 60.
- Gregg, S. J. and Sing, K. S. W. 1982. Adsorption, surface area, and porosity. Academic Press.
- Gustafsson, O., Haghseta, F., Chan, C., MacFarlane, J., Gschwend, P. M., 1997. Quantification of the dilute sedimentary "soot-phase": Implications for PAH speciation and bioavailability. *Environ. Sci. Technol.* 31, 203-209.
- Gustafsson, O. and Gschwend, P. M. 1997. Soot as a strong partition medium for polycyclic aromatic hydrocarbons in aquatic systems. In Eganhouse, R. P., [ed.]. Molecular Markers in Environmental Geochemistry, ACS Symposium Series 671, American Chemical Society, Washington, DC.
- Henrichs, S. M. 1993. Early diagenesis of organic matter: the dynamics (rates) of cycling of organic compounds. In: Engel, M.H. and Macko, S.A. [eds]. Organic geochemistry: principles and applications, pp. 101-114.
- Henrichs, S. M. and Doyle, 1986. Decomposition of ¹⁴C labeled organic substances in marine sediments. *Limnol. Oceanogr.*, 31, 765-778.
- Hites, R. A., LaFlamme, R. F., Windsor, J. G., Farrington, J. W., and Denser, W. G. 1980. Polycyclic aromatic hydrocarbons in an anoxic sediment core from the Pettaquamscutt River (Rhode Island, U.S.A). *Geochim. Cosmochim. Acta*, 44, 873-878.
- Huggett, R. J., Bender, M. E., and Unger, M. A. 1984. Polynuclear aromatic hydrocarbons in the Elizabeth River, Virginia. In: Dickson, K. L., Maki, A. W., Brungs, W. A. [eds.] Fate and Effects of Sediment-Bound Chemicals in Aquatic Systems. Proceedings of the Sixth Pellston Workshop. Pergamon Press, New York, NY.

- Karickhoff, S. W. 1984. Organic pollutant sorption in aquatic systems. *J. Hydraul. Eng.*, 110, 707-735.
- Karickhoff, S. W.; Brown, D.S.; Scott, T. A., 1979. Sorption of hydrophobic pollutants on natural sediments. *Water Res.*, 13, 241
- Kuehl, S. A., Nittrouer, C. A, DeMaster, D. J., Curtin, T. B. 1985. A long, square-barrel gravity corer for sedimentological and geochemical investigation of fine-grained sediments. *Mar. Geo.*, 62, 365-370.
- Liu, K. 1996. Fate and transport processes for polycyclic aromatic hydrocarbons in the surface microlayer of southern Chesapeake Bay. PhD Dissertation. Virginia Institute of Marine Science
- Lu, M. Z. 1982. Organic compound levels in a sediment core from the Elizabeth River of Virginia. M. S. Thesis. College of William and Mary, Williamsburg, VA.
- Mackay, D., Shiu, W. Y., Ma, K.C. 1992. Illustrated handbook of physical-chemical properties and environmental fate for organic chemicals-v. 2: polynuclear aromatic hydrocarbons, polychlorinated dioxins, and dibenzofurans. Lewis Publishers, Ann Arbor, MI.
- Mayer, L. M. 1994. Surface area control of organic carbon accumulation in continental shelf sediments. *Geochim. Cosmochim. Acta*, 58, 1271-1284.
- Means, J. C., Wood, S. G., Hassett, J. J., Banwart, W. L. 1980. Sorption of polycyclic aromatic hydrocarbons by sediments and soils. *Environ. Sci. Technol.*, 14, 1524-1528.
- Merrill, E. G., and Wade, T. L. 1985. Carbonized coal products as a source of aromatic hydrocarbons to sediments from a highly industrialized estuary. *Environ. Sci. Technol.*, 19, 597-603.
- Meyer, P. 1994. Preservation of elemental and isotopic source identification of sedimentary organic matter. *Chemical Geology*, 11, 289-302.
- National Research Council. 1983. Polycyclic aromatic hydrocarbons: evaluation of sources and effects. National Academy Press, Washington DC.
- Neff, J. M. 1979. Polycyclic aromatic hydrocarbons in the aquatic environment: sources, fates and biological effects. London, Applied science Publishers.
- Nichols, M. M. 1996. Personal communication.
- Nichols, M. M. and Biggs, R. B. 1985. Estuaries. In: Davis, R. A. [ed.]. Coastal Sedimentary Environments. Springer-Verlag, New York, New York.

- Nittrouer, C.A., Sternberg, R. W., Carpenter, R., Bennett, J. T. 1979. The use of ^{210}Pb geochronology as a sedimentological tool: application to the Washington Continental Shelf. *Mar. Geo.*, 31, 297-316.
- Olsen, C. R., Larsen, I. L., Mulholland, P. J., VonDamm, K. L., Grebmeier, J. M., Schaffner, L. C., Diaz, R. J., Nichols, M. M. 1993. The concept of an equilibrium surface applied to particle sources and contaminant distributions in estuarine sediments. *Estuaries*, 16, 683-696.
- Olsen, C. R., Cutshall, N. H., Larsen, I. L. 1982. Pollutant-particle associations and dynamics in coastal marine environments: A review. *Mar. Chem.*, 11, 501-533.
- Prahl, F. G. and Carpenter, R. 1983. Polycyclic aromatic hydrocarbon (PAH)-phase associations in Washington Coastal Sediments. *Geochim. Cosmochim. Acta*, 47, 1013-1023.
- Schrap, S. M. and Opperhuizen, A. 1992. On the contradictions between experimental sorption data and the sorption partitioning model. *Chemosphere*, 24, 1259-1282.
- Schwarzenbach, R., Gschwend, P. M., Imboden, D. M. 1993. Environmental organic chemistry. John Wiley and Sons, Inc., New York, NY, p. 262-328.
- Sequi, P., and Aringhieri, R. 1977. Destruction of Organic Matter by Hydrogen Peroxide in the Presence of Pyrophosphate and Its Effect on Soil Specific Surface Area. *Soil Sci. Soc. Am. J.*, 41, 340-342.
- Sporstol, S., Gjos, N., Lichtenthaler, R. G., Gustavsen, K. O., Urdal, K., Orelid, F., and Skel, J. 1983. Source identification of aromatic hydrocarbons in sediments using GC/MS. *Environ. Sci. Technol.*, 17, 282-286.
- Sugimura, Y and Suzuki, Y. 1988. A high-temperature catalytic oxidation method for the determination of non-volatile dissolved organic carbon in seawater. *Mar. Chem.*, 24, 105-131.
- Verado, D. J., Froelich, P. N., McIntyre, A. 1990. Determination of organic carbon and nitrogen in marine sediments using the Carlo Erba NA-1500 Analyzer. *Deep-Sea Research*, 37, 157-165.
- Wakeham, S. G. and Farrington, J. W. 1980. Hydrocarbons in contemporary aquatic sediments. In Contaminants and Sediments - v. 1, Baker, R. A. [ed.] Ann Arbor Science.
- Westrich, J. T. and Berner, R. A. 1984. The role of sedimentary organic matter in bacterial sulfate reduction: The G model tested. *Limnol. Oceanogr.*, 29, 236-249.
- Wright, L. D., Prior, D. B., Hobbs, C. H., Byrne, R. J., Boon, J. D., Schaffner, L. C., and Green, M. O. 1987. Spatial variability of bottom types in the lower Chesapeake Bay and Adjoining Estuaries and Inner Shelf. *Estuar. Coast. & Shelf Sci.* 24, 765-784.

Young, T. M. and Weber, W. J. 1995. A distributed reactivity model for sorption by soils and sediments. 3. Effects of diagenetic processes on sorption energetics. *Environ. Sci. Technol.*, 29, 92-97.

Zeng, E. Y., and Vista, C. L. 1997. Organic pollutants in the coastal environment off San Diego, California. 1. Source identification and assessment by compositional indices of polycyclic aromatic hydrocarbons. *Environ. Toxicol. Chem.*, 16, 179-188.

**Chapter 3. Three Phase Modeling of Polycyclic Aromatic Hydrocarbon (PAH) Association
with Pore Water Dissolved Organic Carbon**

Abstract

Log-log plots of observed organic carbon-normalized sediment-pore water distribution coefficients (K'_{OCs}) for several polycyclic aromatic hydrocarbons (PAHs) at two sites in the Elizabeth River, Virginia versus their octanol-water partition coefficients (K_{OWs}) show large deviations from linearity. K'_{OCs} of these PAHs decreased by up to 3 orders of magnitude with depth as well. The vertical profiles of PAH K'_{OCs} were found to predominantly result from sediment geochemistry (i.e. the accessibility of sedimentary organic carbon for PAH binding). To determine to what extent pore water dissolved organic carbon, including colloidal organic carbon, was responsible for the PAH K'_{OCs} deviating from linearity, a three phase model was used to estimate dissolved organic carbon binding coefficients (K_{DOC}). Partitioning of PAHs to DOC (i.e. K_{DOC}) is estimated to account for no more than one order of magnitude of the observed decrease in K'_{OC} with depth. The results of this study are consistent with a three-phase partitioning model for PAHs between sediment organic matter, pore water DOC, and freely dissolved PAH.

3-1. Introduction

Hydrophobic organic contaminants (HOCs) in sediments exist in three phases: sorbed to particulate organic matter, sorbed to colloidal or dissolved organic matter, or unbound and freely dissolved. Traditionally the distinction between each of these phases has been operationally defined (Libes, 1992). Moreover, the concentration of a HOC in a sorbed phase relative to that in the unbound, freely dissolved phase is described by a distribution coefficient (K_D). Distribution coefficients can help to elucidate a HOC's potential bioavailability and relative mobility in benthic systems.

In a two phase aqueous system at equilibrium, the concentration of a chemical in the freely dissolved phase (C_w , mg/l) relative to that in a sorbed phase (C_s , mg/kg), can be ideally depicted by a linear equation:

$$K_D = C_s/C_w \quad (3-1)$$

indicating that the concentration of the HOC sorbed to the solid phase is proportional to the freely dissolved concentration. Thermodynamically, this equilibrium distribution describes the condition under which chemical fugacities or "escaping tendencies" in the sorbed and freely dissolved phases, are equal.

The actual distribution of a chemical in nature between its dissolved and particulate phases, can be dependent on several factors (*e.g.* chemical composition of sorbate and sorbent, and sorption kinetics) (Schwarzenbach *et al.* 1993). For HOCs, one influential factor affecting K_D (for sorbents comprised of at least 1% organic carbon), is the fraction of organic matter in the

sorbent (Karickhoff *et al.*, 1979; Means, *et al.*, 1980). In aqueous systems, HOCs have a strong affinity for carbon and other natural organic matter because they offer relatively non-polar, thermodynamically favorable environments (Karickhoff, 1984) . The fraction of particulate organic carbon (f_{OC}) in soils and sediments is often measured and used to explain the variance in sorption for a given compound to different solids (Karickhoff *et al.*, 1979). Normalization to the amount of organic carbon modifies equation (3-1) to:

$$K_{OC} = K_D / f_{OC} \quad (3-2)$$

where K_{OC} is the organic carbon-normalized two-phase distribution coefficient. Thus it is assumed that sedimentary organic matter acts as a “solvent” for HOCs and that their uptake is proportional to the amount of organic carbon associated with the mineral matrix (Karickhoff *et al.*, 1979). In this manner, normalization of a HOC’s distribution coefficient to the amount of organic carbon should account for its variability within a factor of two or 0.3 log units (Schwarzenbach *et al.*, 1993).

Because the aqueous solubility of a HOC is inversely related to its molecular surface area (Hermann, 1972), larger HOCs tend to be less water soluble, more lipophilic, and associate to a greater degree with hydrophobic moieties such as organic matter. Thus, K_{OC} is directly related to the compounds’ hydrophobicity (Karickhoff, 1984) by the following linear relationship:

$$\log K_{OC} = a * \log K_{OW} + b \quad (3-3)$$

where K_{ow} is the octanol-water partition coefficient of the chemical. Theoretically, a should equal one and b , zero, if HOCs partition to sediment organic matter in exactly the same manner as n-octanol; however, experimental curves diverge from theoretical expectations (Karickhoff, 1984). Values of b may vary due to differences in HOC affinity for various types of organic carbon (Schwarzenbach *et al.*, 1993). In addition, observed K_{oc} s are often less than predicted for HOCs with high K_{ow} s. Presumably this is due to factors that kinetically hinder thermodynamic equilibrium in natural systems (Karickhoff, 1984; Swackhamer and Skoglund, 1993), or experimental artifacts such as incomplete separation of dissolved and colloidal phases of organic matter (Gschwend and Wu, 1985), or volatilization of dissolved HOCs or sorption to container surfaces (Schrap and Opperhuizen, 1992). K_{oc} s can also be greater than expected due to kinetic limitations on desorption (e.g. Connaughton *et al.*, 1993). Thus, a general form of equation (3-3) cannot be used to predict HOC distributions to particulate matter *a priori*.

In natural systems, where organic carbon normalization does not account for observed differences in equilibrium distribution coefficients, a third sorbing organic phase, or colloidal phase has been suggested to control HOC partitioning (Morel and Gschwend, 1987). Colloids are particularly important because of their high specific surface area (Hiemenz, 1986), and hence their potential adsorptive capacity for HOCs in water. In estuarine sediments where colloidal organic carbon in pore waters can contribute as much as 10% to 90% of the measured dissolved organic carbon (Burgess *et al.*, 1996a), HOC partitioning to pore water colloids is potentially an important process affecting the contaminant distribution and bioavailability (McCarthy and Jimenez 1985; Landrum *et al.*, 1987; McCarthy, 1989; DiToro *et al.*, 1991; Martin *et al.*, 1995; Burgess *et al.*, 1996b).

Three phase partitioning of HOCs between particles, colloids, and the freely dissolved phase is described by the following (Morel and Gschwend, 1987):

$$K'_D = K_{OC} * f_{OC} / (1 + K_{COL} * C_{COC}) \quad (3-4)$$

where K'_D is the *observed* or apparent distribution coefficient for a HOC in a three phase system in which colloid-associated HOCs are operationally defined as dissolved, K_{COL} is the colloid binding coefficient (l/mg colloidal organic carbon), and C_{COC} is the concentration of colloidal organic matter (mg colloidal organic carbon/l). From eq 4, it is obvious that as C_{COC} or K_{COL} increases, K'_D decreases. Moreover, the affinity of a particular HOC for colloids is dependent in part upon the hydrophobicity of the compound as well as the source of the dissolved or colloidal organic matter (Di Toro *et al.*, 1991). Thus, the magnitude of K_{DOC} in addition to the DOC concentration determine the extent to which DOC complexation takes place.

The objectives of this paper were a) to determine if observed disequilibria in two phase organic carbon normalized distribution coefficients (K'_{OCs}) of polycyclic aromatic hydrocarbons (PAHs) in the urban Elizabeth River estuary are consistent with the hypothesis of DOC binding, and b) determine to what extent pore water dissolved and colloidal organic carbon contribute to observed decreases in K'_{OCs} with depth in the sediments.

3-2. Methods

Sediment sampling

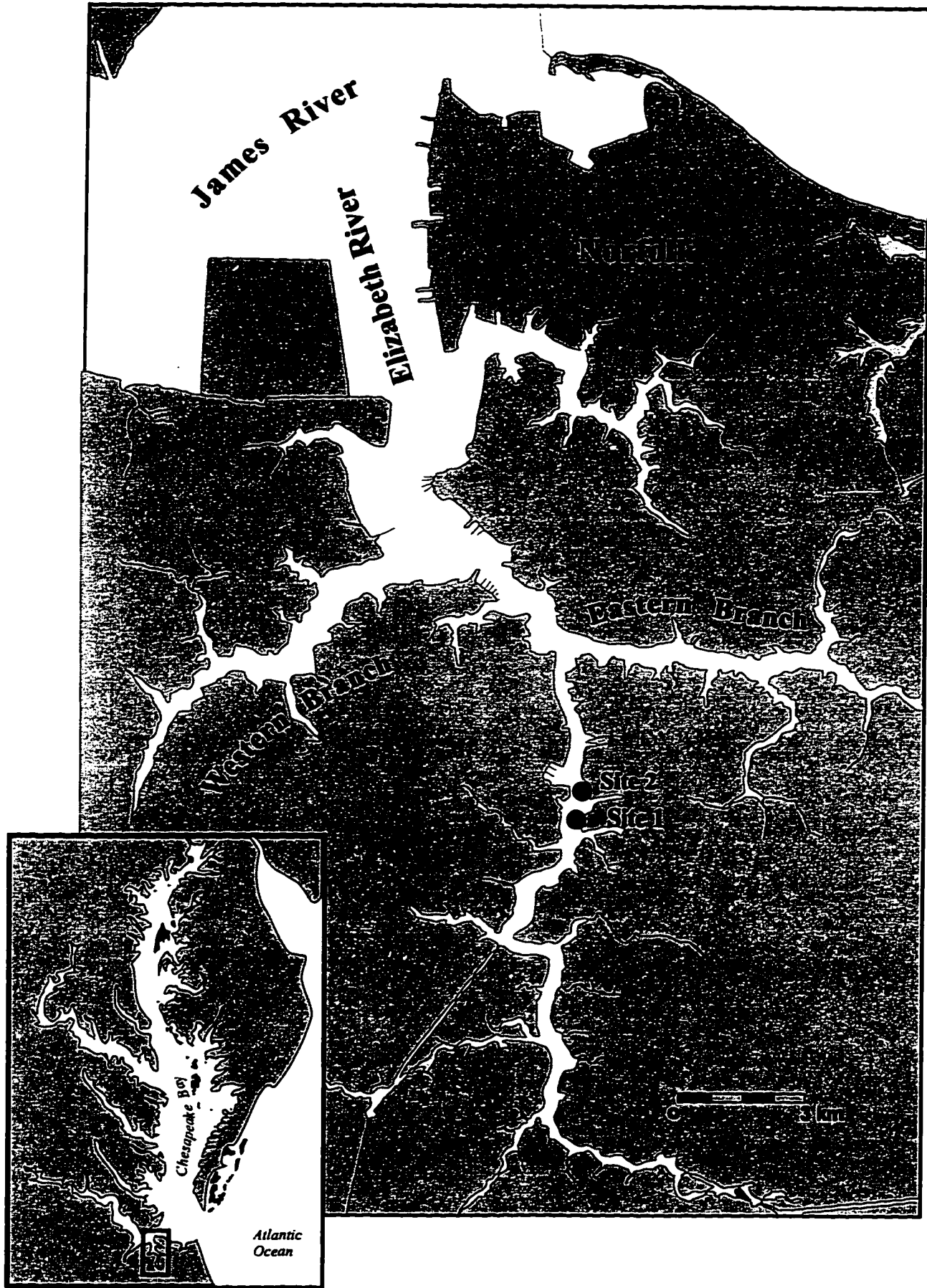
Sediment cores were taken from selected sites in the Southern Branch of the Elizabeth River estuary, an urban tributary of the lower Chesapeake Bay (Figure 3-1). Preliminary sampling of sediments was conducted in July of 1994 using a box core (26.5 cm x 26.5 cm x 60 cm). Sediments were subsampled using (60 cm x 7.5 cm i.d. x 0.6 cm wall thickness) polyvinyl chloride tubing, which was sealed to maintain anoxic conditions. Site 1 (36°48.00 N, 76°17.39' W) was ~100 m southwest of a public boat launch in ~1.5 m of water. Site 2 (36°48.68 N, 76°17.41' W) was located in about 1 m of water and situated across the main channel from a former wood treatment facility, historically responsible for creosote spills to the area. Upon returning to the lab, sediments were extruded at 2 cm depth intervals and processed as described below. Due to 24 % vertical core compression and the high pore water content, only 22 cm of sediment were available to be processed at this time upon return to the lab. Samples were analyzed for particulate organic carbon (POC) and pore water and sediment-associated PAHs as described below. No DOC samples were collected from these cores.

In a subsequent visit to each site in September 1995, additional box cores were collected from each site. Within 72 h, these subcores were extruded at 1cm depth intervals. Samples were collected for POC, DOC, and PAH analyses as described in Chapter 2.

Separation of Particulate and Dissolved Phases

For each depth interval, the 0.5 cm outer edge was discarded to minimize cross-contamination and sediment from each depth interval was centrifuged in pre-ashed (400 °C for 4 h) pint sized glass jars at 1500 g for 25 min. Overlying water was pipetted off and vacuum

Figure 3-1. Map of Elizabeth River and sampling sites.



filtered through a 1µm nominal pore size (Gelman Type A/E) glass fiber filter (combusted for 4h @ 450° C) to separate particulate and pore water fractions. Thus, the pore water filtrates contained both freely dissolved and DOC-bound PAHs.

PAH and organic carbon analysis

Filtered pore water from each depth interval was extracted with hexane (4 x 20 ml after addition of surrogate standards) and analyzed for PAHs as described below. Sediment samples (~ 5 g wet wt) were transferred to pre-ashed 50 ml tubes, to which a surrogate standard mixture containing 5 deuterated PAHs (~1 ug PAH / g hexane) was added. Sediments were extracted with acetone (1 x 20 ml) and methylene chloride (DCM) (4 x 20 ml) for all samples except Site 2 (Sept. 1995), which were extracted with DCM only (4 x 20 ml), by sonicating 1 h in an ultrasonic waterbath and shaking for 2 min. The extracts were filtered through pre-cleaned Pasteur pipettes filled with solvent rinsed glass wool and pre-cleaned (Soxhlet extracted with DCM - 48 h) anhydrous Na₂SO₄, rotoevaporated and solvent exchanged with hexane. The sample extract was then further purified by solid-liquid chromatography on silica to remove organic polymers, aliphatic, and polar compounds (Dickhut and Gustafson, 1995). Subsequently, the extracts were concentrated and an internal/recovery standard containing additional deuterated PAHs was added. PAHs were quantified by gas chromatography/mass spectrometry using selected ion monitoring relative to deuterated surrogate PAHs. Recoveries ranged from 64.4 ± 12.3 % for naphthalene to 97.0 ± 16.8 % for less volatile PAHs.

Particulate organic carbon was quantified using a CHNS-O analyzer. Briefly, pre-weighed sediment samples were acidified with 6 N HCl and allowed to evaporate to dryness to remove

inorganic carbon. The sample was then placed in the analyzer and flash heated to 1020°C to convert organic carbon to CO₂ (Verado *et al.*, 1990). Pore water samples for measurement of DOC were stored in pre-ashed vials and the headspace of each sample vial purged with N₂(g) prior to freezing (-80 ° C). Dissolved organic carbon was subsequently measured using a Shimadzu TOC 5000 total organic carbon analyzer. Analysis was done by high temperature oxidation of pore water samples after acidification with 1-3 drops of 6 N HCl per 10 mls of sample (Sugimura and Suzuki, 1988).

3-3. Results and Discussion

Preliminary results for sediments collected in July of 1994 at Site 2 in the Elizabeth River indicated that PAH distribution coefficients in these cores decreased with sediment depth despite normalizing to organic carbon (Figure 3-2). The decrease in log K'_{OC} with depth seen at Site 2 can be noted by the spread of the data points between the selected depth intervals. Further, PAH log K'_{OC}s deviated from linearity when plotted against each PAH's log K_{OW} (Figure 3-2), indicating that sediment pore water distributions of PAHs were not at two phase equilibrium between sediments and freely dissolved in pore water.

In September 1995, PAH K'_{OC}s measured at Site 1 exhibited more than a two order of magnitude decrease with depth and also deviated from linearity when compared with each PAH's K_{OW} (Figure 3-3). Investigations into the sediment geochemistry at this site revealed that the decreasing log K'_{OC}s at Site 1 are a function of greater amounts of inaccessible organic matter precluding PAH binding with depth (Chapter 2). K'_{OC}s fall consistently above the 1:1 line when plotted against K_{OW} at Site 2 for the 1995 sample. Several possible reasons may result in high

Figure 3-2. Relationship between K'_{oc} and K_{ow} for selected PAHs in Elizabeth River sediment sampled at Site 2 in July 1994: (○: 0-2 cm; □: 18-20 cm).

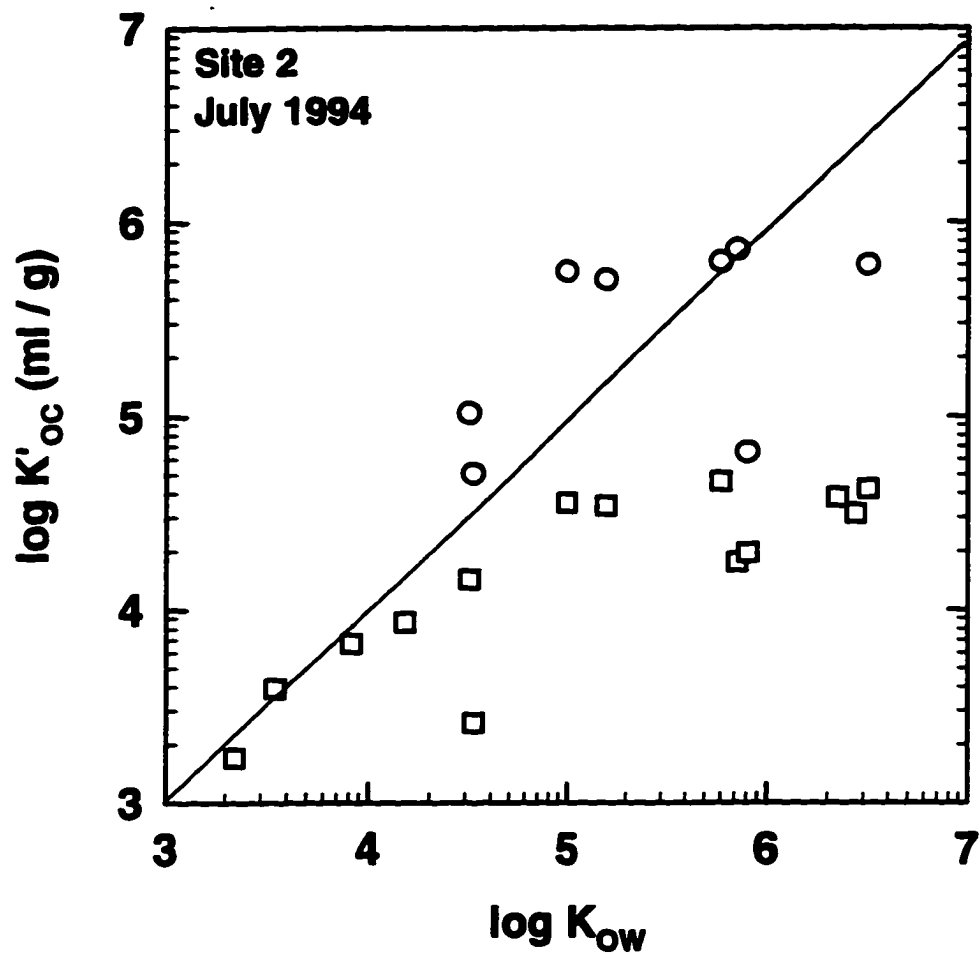
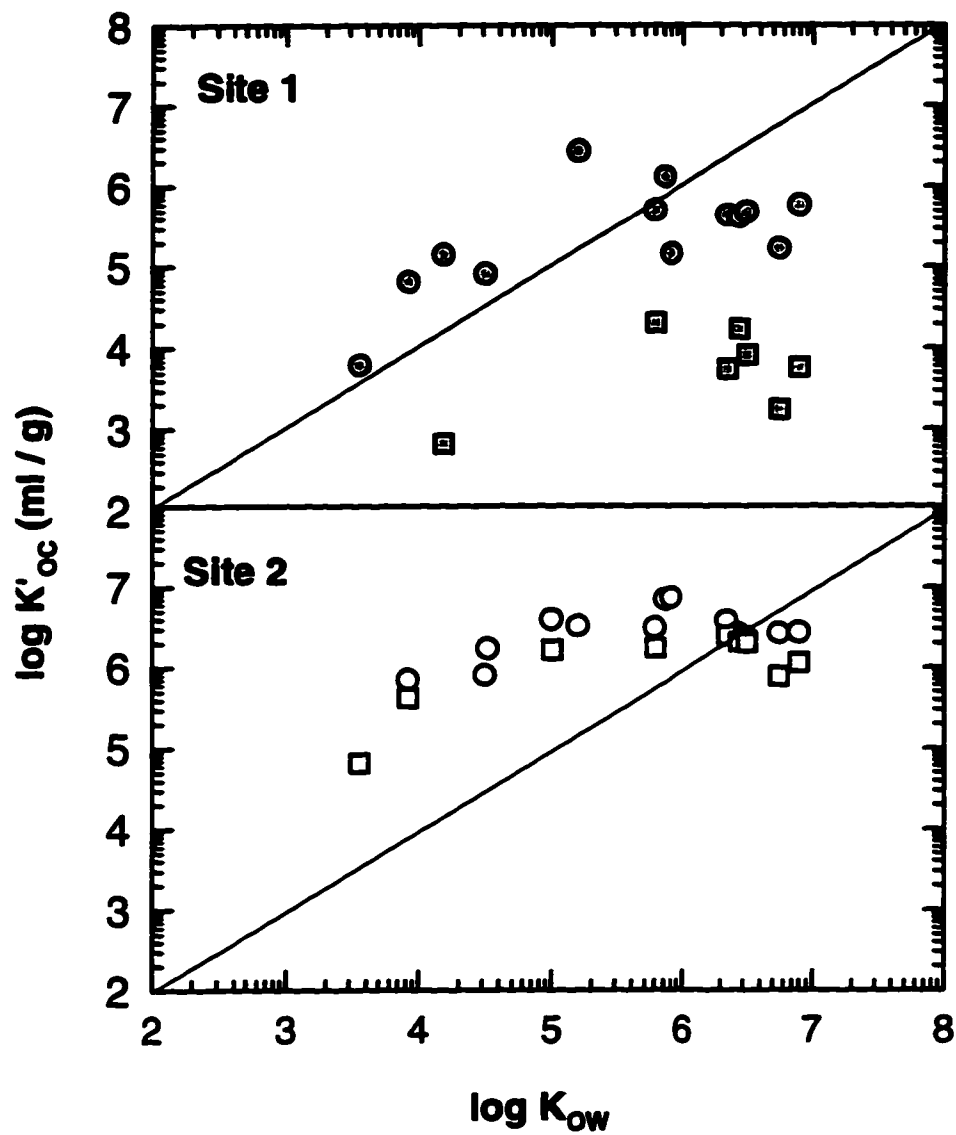


Fig 2

Figure 3-3. Relationship between K'_{oc} and K_{ow} for selected PAHs in Elizabeth River sediment sampled in September 1995: Site 1- gray symbols (●: 0-1 cm; ■: 17-18 cm); Site 2 - open symbols (○: 0-1 cm; □: 19-20 cm).



PAH K'_{oc} s in relation to their K_{ow} (Chapter 2). Sediment-associated PAHs in this core are likely sequestered within the particle matrix. The differences in measured K'_{oc} s at Site 2 between 1994 and 1995 (Figure 3-2 vs. Figure 3-3) likely reflects spatial heterogeneity in this perturbed estuarine environment. These observations prompted us to investigate to what extent binding to DOC is responsible for observed disequilibria in K'_{oc} vs. K_{ow} by generating modeled PAH-DOC binding coefficients.

Modeling of PAH-DOC binding

Since values of $\log K'_{oc}$ for PAHs in Elizabeth River sediments do not increase linearly with $\log K_{ow}$ above a $\log K_{ow}$ of ~ 5 (Figures 3-2 & 3-3), this chapter addresses the issue of a third phase for PAH binding in pore water is influencing the PAH distributions, as proposed by other reserachers (Oliver, 1987; Socha and Carpenter, 1987; DiToro *et al.*, 1991). Assuming that relatively hydrophilic PAHs bind minimally to DOC (Eadie *et al.*, 1990; DiToro *et al.*, 1991), equation 3-3 was fit to the K'_{oc} data for compounds with $\log K_{ow} < 6$ to solved for the coefficient b , which describes the relative affinity of the PAHs for sedimentary organic matter compred to n-octanol. Thus, assuming thermodynamic equilibrium ($a = 1$) is valid for PAHs with $\log K_{ow} < 6$, values of b (the y intercept of equation 3-3), were determined from linear regressions of $\log K'_{oc}$ vs. $\log K_{ow}$ for each depth interval (Table 3-1) for the 1995 data set. The relative standard error for these estimates ranged from 7% to 53% and averaged 21%, indicating the validity of the assumptions.

The bimodal distribution in down-core values of b at Site 1 (Table 3-1) are a measure of the difference in PAH accessibility to sedimentary organic matter at this site; that is, the higher

Table 3-1. Curve Fit Coefficients for eq 3 fitted to K'_{oc} data for PAHs with $\log K_{ow} < 6$.

Depth Interval (cm)	max log K_{ow} used for fit	Site 1	Site 2
		$b \pm SE_b$	$b \pm SE_b$
0-1	5.2 ¹	0.7461 ± 0.1858	1.588 ± 0.1086
4-5	5.78 ²	0.8006 ± 0.2100	
5-6	5.2		1.644 ± 0.1882
6-7	5.2		1.230 ± 0.0900
7-8	5.78	0.7838 ± 0.1398	
8-9	5.2		1.401 ± 0.2125
12-13	5.78	0.7034 ± 0.1867	
14-15	5.2		1.472 ± 0.3317
	5.78	0.2141 ± 0.0579	
16-17	5.78	0.6521 ± 0.2956	
19-20	5.2		1.396 ± 0.1548
24-25	5.2		1.508 ± 0.1606
26-27	5.2		1.270 ± 0.6682
27-28	5.78	-1.403 ± 0.1391	
30-31	5.2		2.030 ± 0.1901
	5.78	-1.135 ± 0.4182	
31-32	5.78	-1.212 ± 0.2083	

1- fluoranthene; 2 - benzo(b)fluoranthene

values of b in the top portion of the core are proportional to more accessible sedimentary organic matter for PAH binding, and vice versa for negative values of b . Values of b at Site 2 are higher than those at Site 1 and hence illustrate the greater affinity of PAHs for sediment organic carbon at Site 2 compared to Site 1. To determine PAH binding coefficients to DOC, non-linear curve fitting of the log transformed version of equation 3-4 :

$$\log K'_D = \log [K_{OC} * f_{OC}] - \log (1 + \lambda * K_{OW} * DOC) \quad (3-5)$$

was used, substituting $\lambda * K_{OW}$ for K_{COL} , and the concentration of dissolved organic carbon (DOC in mg carbon/l) for C_{COL} . Theoretical or "expected" values of K_{OC} were calculated by multiplying corresponding K_{OW} s by 10^b (equation 3-3, Table 3-1). In equation 3-5, λ , which describes the relative affinity of PAHs for DOC, is the only unknown; all other variables were either measured (K'_D , f_{OC} , DOC, K_{OW}) or estimated (*i.e.* K_{OC}). Values of λ determined from equation 3-5 (Table 3-2) had relative standard errors ranging from 20% to 75% ($\bar{x} = 36\%$), again supporting the validity of the model assumptions.

Our three phase model was applied to July 1994 sediment/pore water PAH partitioning data in order to verify its general applicability. Calculated values of K_{DOC} as well as known values of K'_D , f_{OC} , K_{OC} , were applied to equation 3-5, to solve for pore water DOC concentrations. Calculated DOC concentrations ranged from 2.5 - 55 mg/L at Site 1 and 4.8 - 34.6 mg/L at Site 2. All DOC concentrations *derived* from the 1994 PAH partitioning data, with the exception of 55 mg/L (Std Err. = 155 %) were within the range of pore water DOC concentrations at Site 1 and Site 2 from our September 1995 samples, further validating our three phase model.

3-4. Conclusions

The three phase partitioning model, along with the assumptions that $\log K_{OC}$ and $\log K_{DOC}$ are linearly related to $\log K_{OW}$, describe the observed distribution coefficients well (Figure 3-4). Consequently, partitioning of PAHs to DOC appears to account for the lower than expected values of K'_{OC} for the high K_{OW} compounds (*i.e.* the curvature in Figures 3-2 & 3-3). Note however, that λ varies only by a factor of ~2-3 at both sites and at different depths (Table 3-2), indicating K_{DOC} varies by less than one order of magnitude with depth (Figure 3-5). Thus, DOC binding of pore water PAHs can account for no more than a one order of magnitude decrease in K'_{OC} with depth in the sediment. Three phase partitioning to pore water DOC does account for less-than-predicted values of K'_{OC} for high molecular weight PAHs. However, binding to pore water DOC only explains a fraction of the observed decreases in K'_{OC} with depth in sediments from the urban Elizabeth River estuary. Results presented in Chapter 2 indicate that sediment geochemistry, including availability of particulate organic matter for PAH binding, is responsible for the trends in observed PAH distribution coefficients with depth in these urban estuarine sediments.

Figure 3-4. Measured (symbols) and predicted (lines) $\log K'_{oc}$ values for PAHs in Elizabeth River sediments assuming DOC binding of PAHs with $\log K_{ow} > 6$.

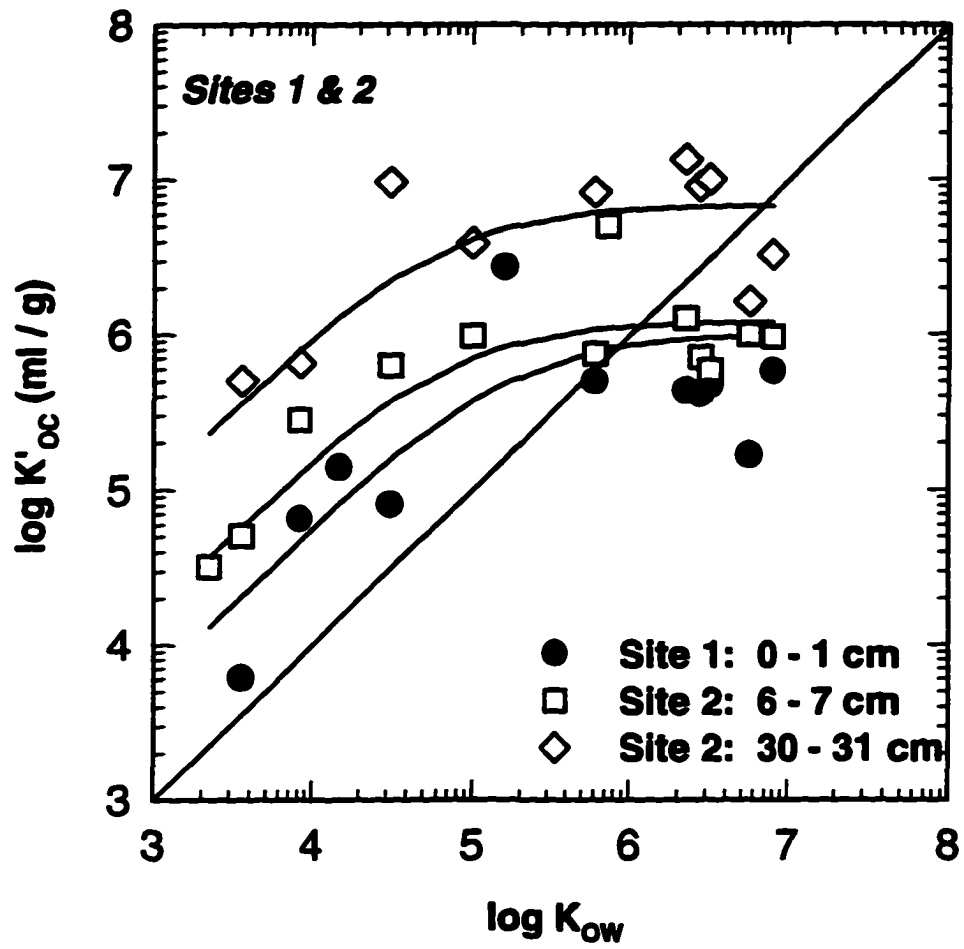
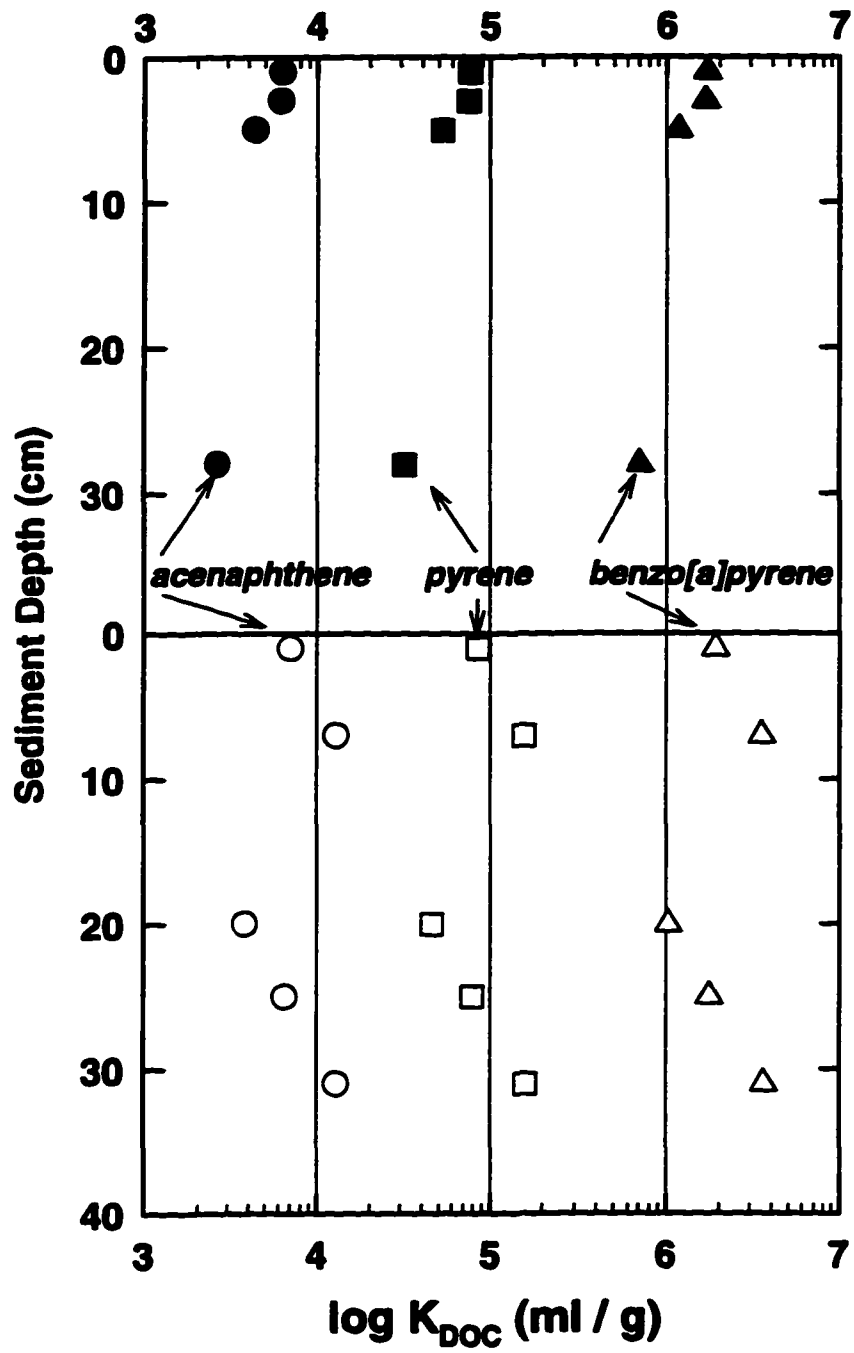


Table 3-2. Variables used in Three Phase Partitioning Model (eq 5) and Curve Fit Results

Depth (cm)	Site 1			Site 2		
	f_{oc}	DOC (mg/L)	$\lambda * 10^{-7} \pm SE_{\lambda} * 10^{-7}$	f_{oc}	DOC	$\lambda * 10^{-7} \pm SE_{\lambda} * 10^{-7}$
0-1	0.0163	13.9	7.63 ± 2.91	0.0403	7.39	8.54 ± 2.1
2-3*	0.0163	9.93	7.47 ± 2.06			
4-5	0.0137	9.89	5.29 ± 3.95			
6-7				0.0237	8.97	15.7 ± 3.8
19-20				0.0311	31.5	4.6 ± 0.94
24-25				0.0179	10.32	7.9 ± 1.6
27-28	0.0222	21.6	3.17 ± 1.85			
30-31				0.0187	9.82	16.1 ± 5.2

* b interpolated between 0-1 cm and 4-5 cm

Figure 3-5. Modeled pore water DOC binding coefficients, K_{DOC} ($\lambda * K_{ow}$): Site 1 (filled symbols); Site 2 (open symbols).



3-5. References

- Achman, D.R., Brownawell, B.J., Zhang, L. 1996. Exchange of polychlorinated biphenyls between sediment and water in the Hudson River Estuary. *Estuaries*, 19, 950-965.
- Brown, D. S., Flagg, E.W. 1981. Empirical Prediction of Organic Pollutant Sorption in Natural Sediments. *J. Environ. Qual.*, 10, 382-386.
- Burgess, R. M. , McKinney, R. A., Brown, W. A. 1996b. Enrichment of marine sedimentary colloids with PCBs: Trends resulting from PCB solubility and chlorination. *Environ. Sci. Technol.*, 30, 2556-2566.
- Burgess, R. M. , McKinney, R. A., Brown, W. A., Quinn, J. G. 1996a. Isolation of marine sediment colloids and associated polychlorinated biphenyls: an evaluation of ultrafiltration and reverse-phase chromatography. *Environ. Sci. Technol.*, 30, 1923-1932.
- Connaughton, D. F., Stedinger, J. R., Lion, L. W., Shuler, M. L. 1993. Description of time-varying desorption kinetics: release of naphthalene from contaminated soils. *Environ. Sci. Technol.*, 27, 2397-2403.
- Dai, M., Martin, J-M., Cauwet, G. 1995. The significant role of colloids in the transport and transformation of organic carbon and associated trace metals (Cd, Cu, and Ni) in the Rhone Delta, France. *Mar. Chem.*, 51, 159-175.
- Dickhut, R.M., Gustafson, K. E. 1995. Atmospheric inputs of selected polycyclic aromatic hydrocarbons and polychlorinated biphenyls to southern Chesapeake Bay. *Mar. Pollut. Bull.*, 30, 385-390.
- Di Toro, D. M.; Zarba, D. S.; Hansen, D. J.; Berry, W.J.; Swartz, R. C.; Cowan, C. E.; Pavlou, S. P.; Allen, H. E.; Thomas, N. A.; Paquin, P. R. 1991. Technical basis for establishing sediment quality criteria for nonionic organic chemicals using equilibrium partitioning. *Environ. Toxicol. & Chem.*, 10, 1541-1583.
- Eadie, B. J.; Morehead, N. R.; Landrum, P. F. 1990. Three-phase partitioning of hydrophobic organic compounds in great lakes waters. *Chemosphere*, 20, 161-178.
- Gschwend, P.; Wu. S. C. 1985. On the constancy of sediment-water partition coefficients of hydrophobic organic pollutants. *Environ. Sci. Technol.*, 19, 90-96.
- Hermann, R.B. 1972. Theory of hydrophobic bonding-II. The correlation of hydrocarbon solubility in water with solvent cavity surface area. *Phys. Chem.*, 19, 2754-2759.

- Hiemenz, P. C.; *Principles of Colloid and Surface Chemistry*. 1986. 2nd ed. Marcel Dekker, Inc., New York, 815pp.
- Karickhoff, S. W. 1984. Organic pollutant sorption in aquatic systems. *J. Hydraul. Eng.*, 110, 707-735.
- Karickhoff, S. W., Brown, D.S., Scott, T. A. 1979. Sorption of hydrophobic pollutants on natural sediments. *Water Res.*, 13, 241-248.
- Landrum, P. F.; Nihart, S. R.; Eadie, B. J.; Herche, L. R. 1987. Reduction in bioavailability of organic contaminants to the amphipod, *Pontoporeia hoyi*, by dissolved organic mater of sediment interstitial waters. *Environ. Toxicol. & Chem.*, 6, 11-20.
- Libes, S. M. *Marine Biogeochemistry*. John Wiley and Sons: New York, 1992, p. 30.
- Martin, J. M., Dai, M. H., Cauwet, G. 1995. Significance of colloids in the biogeochemical cycling of organic carbon and trace metals in a coastal environment - an example of the Venice Lagoon (Italy). *Limnol. Oceanogr.*, 40, 119-131.
- McCarthy, J. F. 1989. Bioavailability and toxicity of metals and hydrophobic organic contaminants. In: *Aquatic Humic Substances - Influences on Fate and Transport of Pollutants*; MacCarthy, P and Suffett, I. H. Eds. Advances in Chemistry Series #219, ACS Publishing, Washington D.C., p.263.
- McCarthy, J. F., Jimenez, B. D. 1985. Reduction in bioavailability to bluegills of PAHs bound to dissolved humic materials. *Environ. Toxicol. & Chem.*, 4, 511-521.
- Means, J. C.; Wood, S. G.; Hassett, J. J.; Banwart, W. L. 1980. Sorption of polynuclear aromatic hydrocarbons by sediments and soils. *Environ. Sci. Technol.*, 14, 1524-1528.
- Morel, F. M. M., Gschwend, P. M. 1987. In *Aquatic Surface Chemistry*, Stumm, W., Ed.; J. Wiley & Sons, New York, NY, Chap. 15.
- Oliver, B. G. 1987. Biouptake of chlorinated hydrocarbons from laboratory spiked and field sediments by oligochaete worms. *Environ. Sci. Technol.*, 21, 785-790.
- Sangster, J. 1989. Octanol-water partition coefficients of simple organic compounds. *J. Phys. Chem. Ref. Data.*, 18, 1125.
- Schwarzenbach, R., Gschwend, P. M., Imboden, D. M. 1993. *Environmental Organic Chemistry*. John Wiley and Sons, Inc., New York, NY,, p. 262, p. 328.

Socha, S. B. and Carpenter, R. 1987. Factors affecting pore water hydrocarbon concentrations in Puget Sound sediments. *Geochim. Cosmochim. Acta.*, 51, 1273-1284.

Sugimura, Y. and Suzuki, Y. 1988. A high-temperature catalytic oxidation method for the determination of non-volatile dissolved organic carbon in seawater by direct injection of a liquid sample. *Mar.Chem.*, 24, 105-131.

Swackhamer, D. L., Skoglund, R. S. 1993. Bioaccumulation of PCBs by algae: Kinetics vs. Equilibrium. *Environ. Toxicol. & Chem.*, 12, 831-838.

Verado, D. J., Froelich, P. N., McIntyre, A. 1990. Determination of organic carbon and nitrogen in marine sediments using the Carlo Erba NA-1500 Analyzer. *Deep-Sea Research*, 37, 157-165.

Chapter 4. Polycyclic aromatic hydrocarbon deposition and geochemistry in Hudson River sediments

Abstract

Sediments and pore waters from the East River, New York and Newark Bay, New Jersey were sampled for polycyclic aromatic hydrocarbons (PAHs) and other geochemical variables including ^{210}Pb specific activities. Despite what appears to be similar sources of PAHs to East River and Newark Bay, as inferred by ratios of alkylated to non-alkylated PAHs and PAH isomer ratios, sediments and associated PAHs have undergone distinctly different depositional processes at each site. Sediments in the East River appear to have been subject to intense physically driven resuspension, resulting in selective depletion of low molecular weight PAHs from the sediment column due to processes such as from enhanced desorption and scouring of particle surfaces. Although sediment PAH concentrations were higher at the East River Site than the Newark Bay Site, pore waters were depleted of the majority of PAHs analyzed at the East River Site relative to the Newark Bay Site. Geochemical variables of sediments (e.g. C/N ratio, BET surface area, total lipid extract) were not related to PAH concentration profiles or organic carbon normalized PAH distribution coefficients (K'_{OCs}). At the Newark Bay site, K'_{OCs} were influenced by sediment mixing and pore water dissolved organic carbon (DOC). Our results indicate that the physical factors influencing time scales of sediment resuspension and deposition determine whether PAHs are able to equilibrate between estuarine sediments and pore waters.

4-1. Introduction

Pollutants in coastal marine environments easily become associated with a wide variety of particles (e.g. Olsen *et al.*, 1982). Because of thermodynamic forcing in aqueous systems, hydrophobic organic contaminants (HOCs) are particle reactive and tend to associate with organic matter in and on particles and other surfaces (Karickhoff *et al.*, 1979; Brown and Flagg, 1981). Hence, HOC accumulation, transport, and removal processes are often dictated by the same principles as those applied to fine particle dynamics (Olsen, *et al.*, 1993).

Estuaries are complicated depositional systems varying widely in spatial and temporal dynamics (Turekian *et al.*, 1980; Dyer 1989; Olsen *et al.*, 1993). As such, particle reactive HOC accumulation can vary tremendously from location to location within the same estuary due to variability in HOC sources, particle composition and reactivity, and short-term particle deposition/erosion processes (e.g. Bopp *et al.*, 1982; Schwarzenbach, *et al.*, 1993). Subsequent to deposition, HOC-organic matter associations are liable to change. For example, the extent to which this association is reversible is determined by the amount, composition, and availability of organic matter to which the contaminant is sorbed (Brownawell and Farrington, 1986; Schwarzenbach *et al.*, 1993). Thus, because sediments and sedimentary organic matter undergo transformation during burial and diagenesis (Berner, 1980; Westrich and Berner, 1984; Burdige, 1991; Henrichs, 1993), it is hypothesized that contaminant associations with sedimentary organic matter also change with depth.

Polycyclic aromatic hydrocarbons (PAHs) are one important group of particle reactive and ubiquitous contaminants in estuarine and coastal systems (Blumer, 1976; Neff, 1979; NRC, 1983). Many PAHs are known to be carcinogens (Gelboin, *et al.*, 1980; Denissenko, *et al.*,

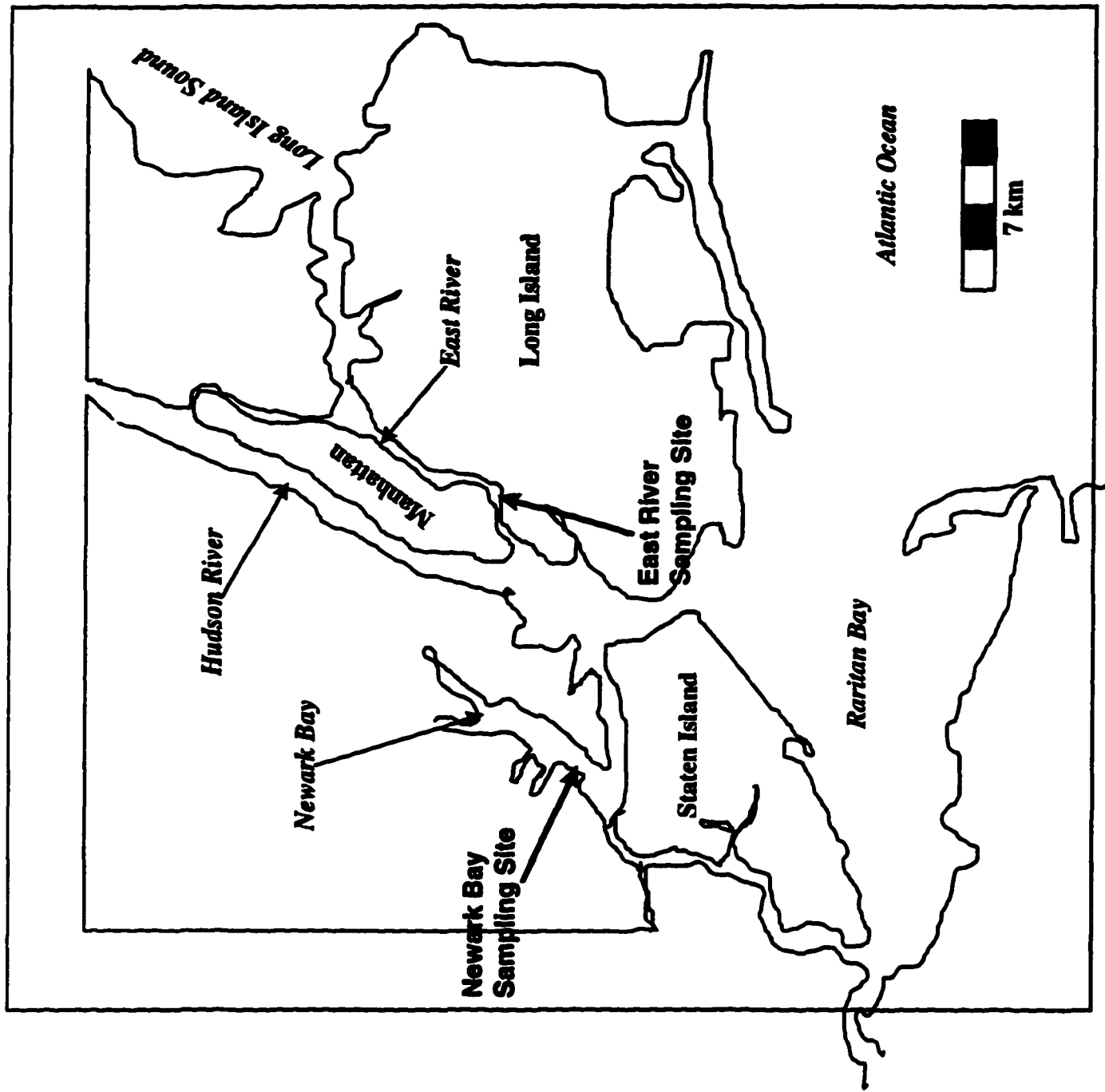
1996). PAHs can be formed by pyrolytic (high temperature) processes or by low temperature petrogenic processes (Wakeham and Farrington, 1980; Radke, 1987). As a result of elevated concentrations of PAHs and polychlorinated biphenyls (PCBs) in sediments, portions of the East River and Newark Bay are considered to be areas of environmental concern (Adams, 1996). In this study, sediments and pore waters from these two sites in the tidal region of the Hudson River watershed were sampled for PAHs as well as several geochemical markers. A previous study conducted in the urban Elizabeth River, Virginia demonstrated compositional variables of sediments were largely responsible for controlling sediment/pore water PAH distributions (see Chapters 2 & 3). Our objective in sampling the East River and Newark Bay, was to determine if similar factors were responsible for PAH deposition and distribution between sediments and pore waters in this watershed.

4-2. Methods

Sediment sampling.

Sediments from one site southeast of the Williamsburg Bridge in the East River, NY and one site immediately east of the main channel across from the Port Elizabeth Marine Terminal in Newark Bay, NJ (Figure 4-1) were collected in August 1996 using a box core (24 cm x 24 cm x 50 cm) and a kasten corer (12.7 cm x 12.7 cm x 3 m) (Kuehl *et al.*, 1985). Box cores were subsampled using (60 cm x 15.2 cm i.d. x 0.6 cm wall thickness) polyvinyl chloride tubing, which was sealed to maintain anoxic conditions. The East River Site (40°42.518' N, 73°58.250' W) was located in water ~ 2 m deep along the flanks outside the main channel of the river, whereas the Newark Bay Site (40°39.50' N, 74°08.43' W) was situated in ~ 4 m water approximately in the

Figure 4-1. Map of East River and Newark Bay sampling sites in the Hudson River. Sediment cores were collected from a location in Wallabout Cove in the East River and on the eastern side of the main channel across from Newark Airport in Newark Bay.



middle of the bay. At the time of sampling, salinity ranged ~20-22 psu in the East River and ~17-20 psu in Newark Bay.

Upon returning to the lab (within 48 h), box core sediments were extruded at 2 cm depth intervals and samples were collected for PAHs and other geochemical variables as described below. Due to a 35 % core compression and the pore water content, only 26 cm of sediment were available to be processed at this time. For each depth interval, the 0.5 cm outer edge was discarded to minimize cross-contamination. Sediments were placed in pre-ashed (400° C for 4 h) pint sized glass jars and homogenized before transferring approximately 15 ml to a plastic centrifuge tube for measurement of water content. Sediments for water content were dried at 60° C for several days until their weights stabilized for at least 48 h. Remaining sediment from each depth interval was centrifuged at 1250 rpm for 40 min. Overlying water was pipetted off and vacuum filtered through a 1µm nominal pore size Gelman Sciences (Ann Arbor, MI) Type A/E glass fiber filter (combusted 4h @ 450° C) to separate particulate and pore water fractions. Thus, the pore water filtrates contained both freely dissolved and dissolved organic carbon (DOC)-bound PAHs. The remainder of the sediment was frozen (-20 ° C) until analysis of PAHs and other geochemical variables.

Filtered pore water was collected in pre-ashed 20 ml glass scintillation vials. The majority of the filtered pore water from each depth interval was transferred to a 50 ml glass centrifuge tube, extracted with hexane (4 x 20 ml after addition of surrogate standards) and analyzed for PAHs as described below. Pore water remaining in the scintillation vials was immediately acidified with 1-2 drops 6N HCl and subsampled to analyze for DOC. The headspace of each vial with the remaining pore water was purged with N₂ prior to freezing (-80 ° C).

PAH Analyses: sediments and pore water

Sediment samples (~ 5 g wet wt) were transferred to pre-ashed 50 ml glass tubes, to which a surrogate standard mixture containing 5 deuterated PAHs in acetone (see Methods - Chapter 2) was added. Sediments were then extracted with acetone (1 x 10 ml) and methylene chloride (DCM) (4 x 20 ml) by sonicating 45 min and shaking for 2 min. All sample extracts (sediments and pore water) were then further purified by solid-liquid chromatography on silica to remove organic polymers, aliphatic, and polar compounds (Dickhut and Gustafson, 1995). Subsequently, the extracts were concentrated and an internal/recovery standard containing additional deuterated PAHs (see Methods - Chapter 2) was added. PAHs were quantified relative to deuterated surrogate PAHs by gas chromatography/mass spectrometry using selected ion monitoring. PAHs were quantified relative to deuterated surrogate PAHs by gas chromatography/mass spectrometry using selected ion monitoring. PAH recoveries for sediment and pore water samples are shown in Table 4-1. PAH concentrations were not quantified if deuterated standard recoveries were below 40%.

Radioisotope geochronology, x-radiographs, and grain size

Sediments for radioisotope analyses were taken from the kasten core at 5 cm depth intervals. Determination of ^{210}Pb content in sediments was made by measuring the concentration of its granddaughter ^{210}Po (Nittrouer *et al.*, 1979). Dried and ground sediments were spiked with

Table 4-1. PAH recoveries (%) in East River and Newark Bay sediment and pore water samples

					Deuterated PAH recoveries (%)				
					d_4 -naphthalene	d_{10} -anthracene	d_{12} -benz[a]anthracene	d_{12} -benzo[a]pyrene	
East River									
	Pore water	60.7 ± 9.6	89.4 ± 10	65.4 ± 8.2	63.6 ± 10				
	Sediment	46.7 ± 3.4	114 ± 9.2	83.3 ± 7.0	92.4 ± 9.2				
Newark Bay									
	Pore water	60.5 ± 13	81.9 ± 14	65.1 ± 6.1	60.9 ± 12				
	Sediment	50.0 ± 7.1	114 ± 6.5	90.0 ± 9.8	99.7 ± 8.3				

a ^{209}Po standard of known activity and acid leached (HNO_3 and HCl). The leachate was plated onto silver planchets and activity measured on an alpha detector. Sediments for analysis of ^{137}Cs and ^7Be were homogenized and packed into 70 ml plastic petri dishes, which were then sealed using electrical tape. Radioisotope activity was measured over 24 h using a semi-planar intrinsic Ge detector in conjunction with a multichannel analyzer. Net count rates were converted to activities using efficiency factors specific to each gamma-ray energy level. Sample geometry was identical for all petri dishes.

To assess fabric and faunal activity in sediments, a 6 cm x 2 cm x 40 cm acrylic liner was vertically imbedded into the box core from each site for X-radiography. Each acrylic liner was placed flush on Kodak (Rochester, NY) AA Industrex X-ray film and photographed using a Dinex 120-F X-ray unit set at 3 mA and 60 kV. Exposure time varied between 45-120 seconds depending on sediment density and grain size.

Grain size analysis was done on selected samples by wet sieving to separate coarse grains ($62.5\ \mu\text{m}$) from fine grains ($<62.5\ \mu\text{m}$), clays and silts. The 4ϕ and 8ϕ diameter fractions were quantified by pipette analysis.

Particulate organic carbon, nitrogen, and dissolved organic carbon

Particulate organic carbon (POC), and nitrogen were quantified using a CHNS-O (Fisons, EA 1108 - Beverly, MA) analyzer. Pre-weighed sediment was acidified with 6 N HCl and dried to remove inorganic carbon. The sample was then placed in the analyzer and flash heated to 1020°C to convert organic matter to CO_2 , NO_x , and H_2O (Verado *et al.*, 1990).

Dissolved organic carbon was measured using a Shimadzu TOC 5000 (Columbia, MD)

total organic carbon analyzer. Analysis was done by high temperature oxidation of pore water samples after acidification (Sugimura and Suzuki, 1988).

Particle surface area

Measurement of the volume of N₂ adsorbed onto a solid at various partial pressures of nitrogen are well correlated with intraparticle surface area (Gregg and Sing, 1982). Sediments were freeze-dried for 24 h and then gently separated for surface area analysis. Freeze-dried sediments were heated at 200°C under gentle N₂ flow for ~ 1 h to remove any residual water. Sediment surface area was determined by adsorbing N₂ at liquid nitrogen temperatures using a Micromeritics (Norcross, GA) Gemini III - 2375 Surface Area Analyzer.

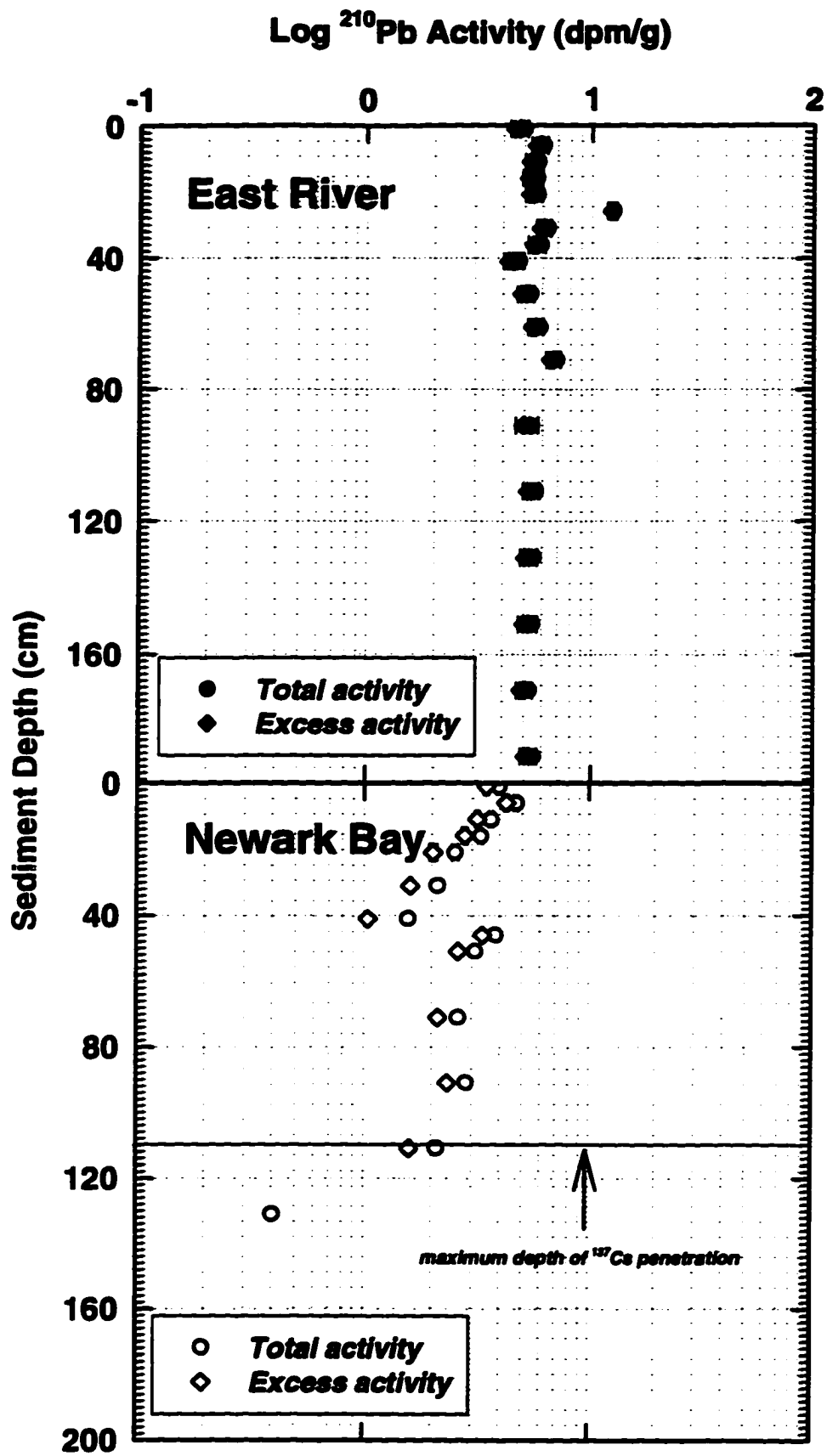
4-3. Results

Sediment Accumulation

Radioisotopes, grain size distributions, and x-radiographs

Sediment ²¹⁰Pb activity in the East River and Newark Bay show disparate profiles (Figure 4-2). In the East River kasten core, excess sediment ²¹⁰Pb activities range from ~ 4 dpm/g to ~ 6.5 dpm/g with anomalously high activity of 12 dpm/g at 26 cm depth. Further, ¹³⁷Cs was detected at the bottom of the core collected from the East River. Due to spatial heterogeneity, one core cannot delineate the geochronology of an entire estuary. Nonetheless, as ¹³⁷Cs does not occur naturally on earth and was first introduced globally in large quantities by atmospheric testing of nuclear devices in 1954 (Krishnaswami *et al.*, 1971), the entire 1.8 m sediment column sampled in the East River must have been deposited subsequent to that time. In contrast, ²¹⁰Pb

Figure 4-2. Depth profiles of ^{210}Pb activity (total and excess) from kasten cores collected in East River and Newark Bay sediments. ^{137}Cs was detected throughout the entire sediment column at the East River site whereas ^{137}Cs was found at a maximum depth of 110 cm at the Newark Bay Site.



activity decreases with depth in the upper 40 cm of Newark Bay sediments from 4.4 dpm/g to 1.0 dpm/g (Figure 4-2). Excess activity then increases sharply to 3.4 dpm/g and then subsequently drops to a mean activity of ~ 2 dpm/g down to 110 cm. The maximum depth of ^{137}Cs penetration was found to be 110-112 cm in the Newark Bay core.

Textural analysis of each kasten core indicates that sediments in the East River are comprised of relatively uniform down-core concentrations of sand, silt, and clay, with trace (< 5 %) amounts of gravel dispersed throughout the seabed (Figure 4-3). One exception to this trend is the sharp increase in clay content of the sediments observed at 30-32 cm depth. However, this increase in clay content does not correspond to the anomalously high ^{210}Pb activity observed in the East River core (Figure 4- 2).

X-radiographs of the top 30 cm of sediments from the East River (Figure 4-4) show fabric bereft of any physical structure with the exception of possibly methane and dense-non aqueous phase liquid (DNAPL) filled inclusions throughout the core. The surface of this core shows a dense assemblage of shells from the small bivalve *Mulinia lateralis* in living position with a few disarticulated *M. lateralis* shells distributed throughout the upper 15 cm of the core. Between 15-30 cm depth in sediments at this site, there are abundant and pervasive 0.5 mm diameter irregularly positioned worm burrows, probably the result of small polychaetes. These burrows may have been present in the upper 15 cm of the core but the spatial density of the DNAPL inclusions and the quality of the X-radiograph preclude their observations. The radiograph from 40-67 cm shows fewer gas and DNAPL inclusions and contains cm to mm scale laminations. Beginning at 47 cm, the sediment is finely laminated. Below this layer, at 62 cm, there is another layer of *M. lateralis* in living position. Although there is little evidence of larger diameter

Figure 4-3. Depth profiles of grain size distributions in kasten cores collected in East River and Newark Bay sediments. Highly variable grain size profiles with depth in Newark Bay sediments (including a rapid increase in sand with depth from 30-45 cm) and uniform grain size distributions in East River sediments, are coincident with the shape of ^{210}Pb profiles in figure 4-2 for each site respectively.

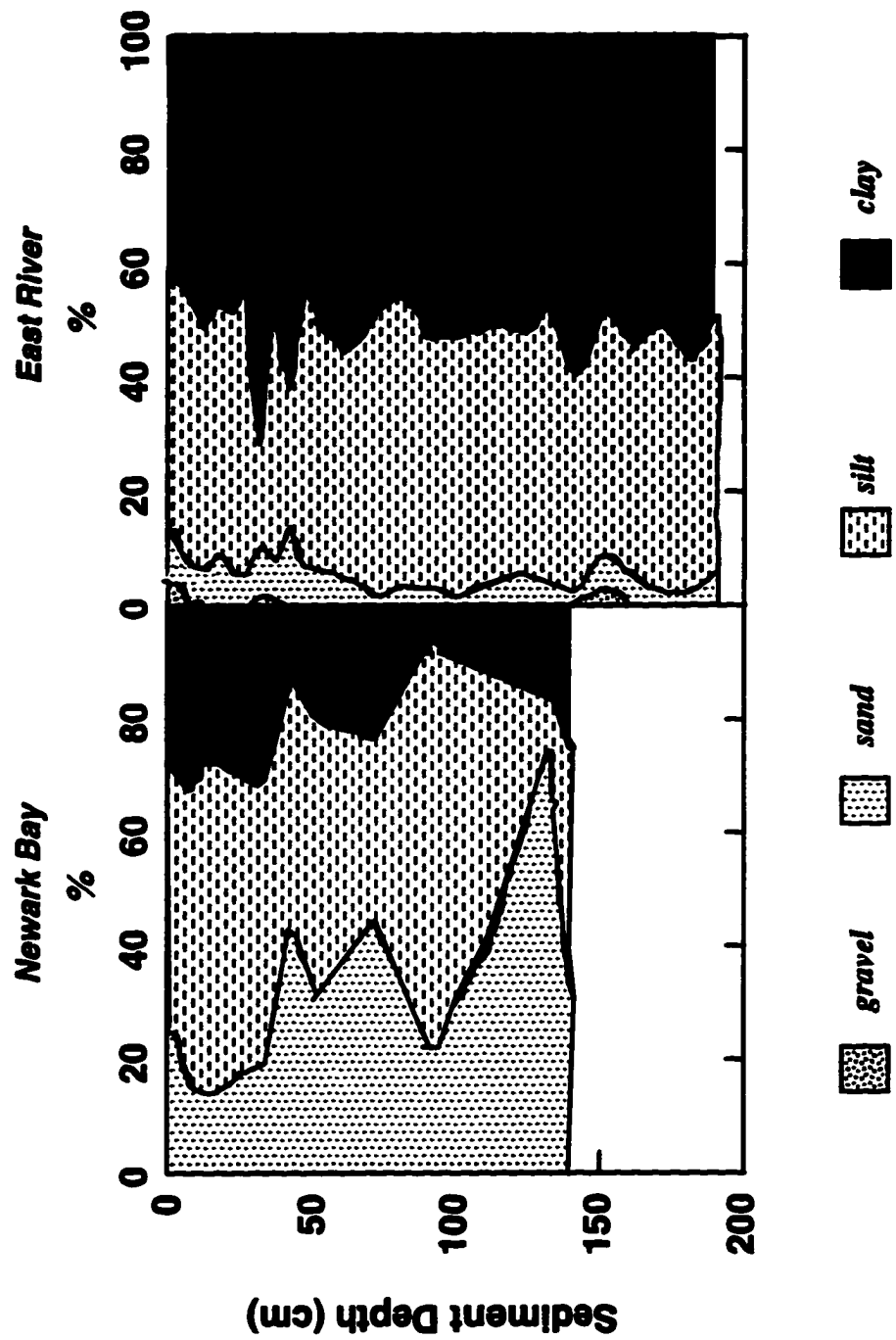
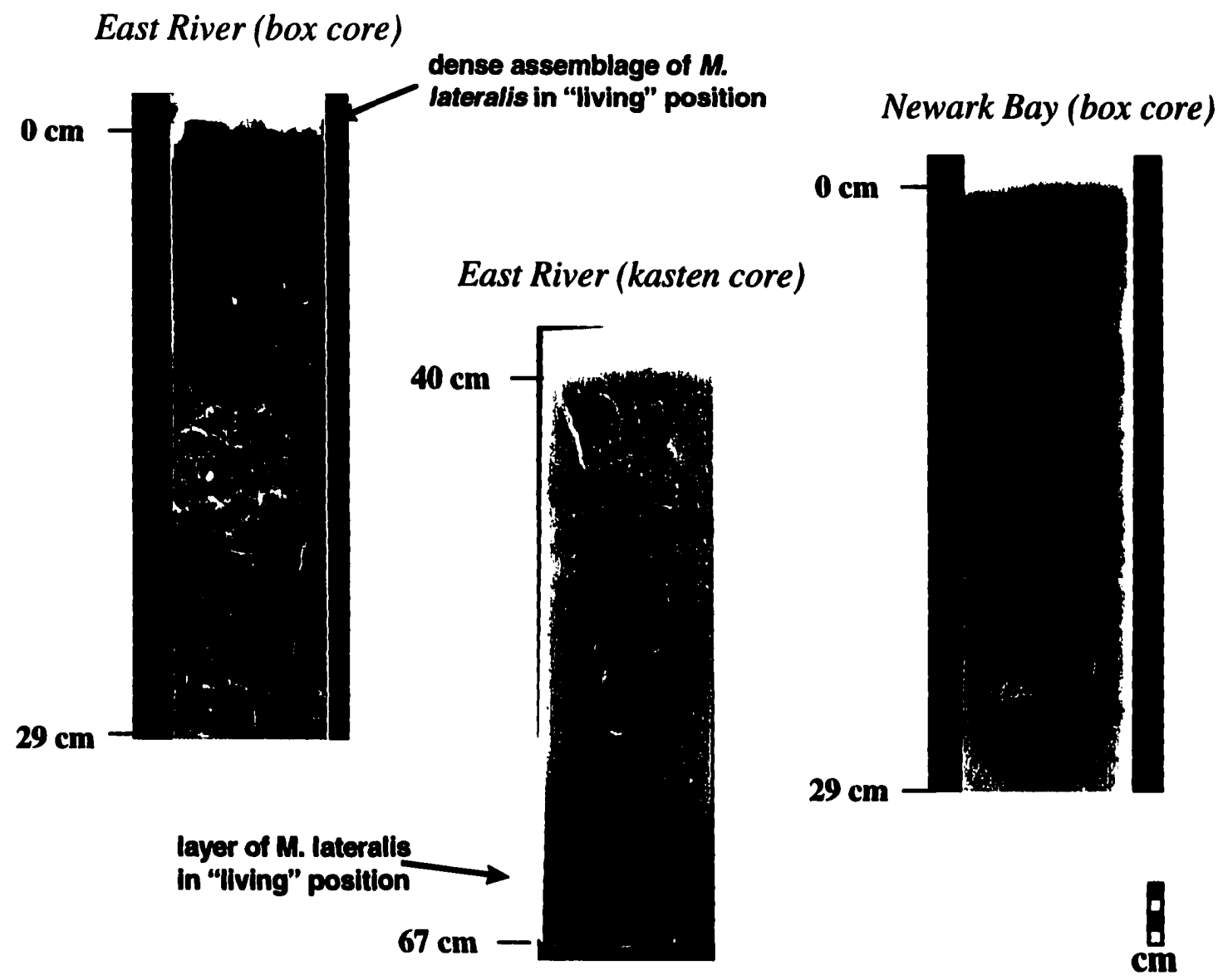


Figure 4-4. X-radiograph positives of sediment box cores and kasten cores. Very little preservation of sedimentary structure in East River sediments are representative of the high degree of anthropogenic disturbance at this site. In contrast, at the Newark Bay Site, sediments in the top 12 cm appear well mixed but seem to have undergone alternating cycles of scouring/deposition below this depth interval with evidence of periodic biological mixing.



burrows, 0.5 mm diameter burrows are present in sediment x-radiographs throughout the entire length of the core.

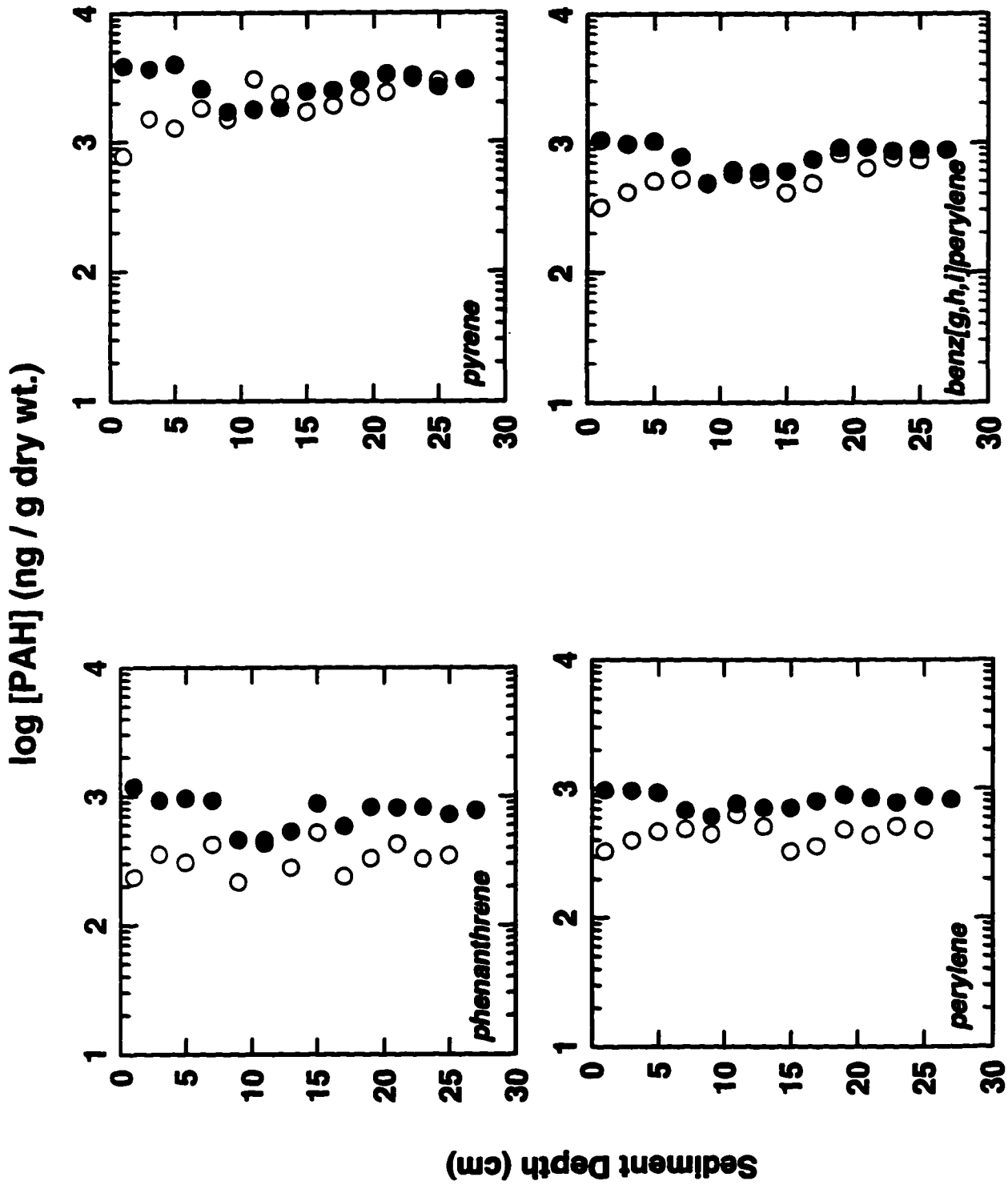
The sediment grain-size distribution in the Newark Bay core is highly variable (Figure 4-3). The most striking aspect of this grain size profile is the low sand content at 90 cm depth (22%) followed by a 72% sand content in the next depth interval (130-132 cm). In general, sediments are composed of sandy muds; however, in the upper 40 cm of the core, sand sized grains represent < 20% of the total mass of sediment, whereas from 40 to 70 cm, sand sized grains increase to 30 - 40%. Again, the excess ^{210}Pb minima measured in this core at 40 cm (Figure 4-2) corresponds to a decrease in clay content.

X-radiographs of a box core from the Newark Bay site (Figure 4-4) depict sediments from the surface to ~ 10 cm depth that have been intensely bioturbated and contain little evidence of physical laminations. From 10-17 cm, sediments are finely laminated with little evidence of bioturbation except the irregularities in the surface of this layer caused by worm burrows. The remainder of this entire column of sediment is comprised of similar packages of sediment alternating between finely laminated and moderate to intensely bioturbated layers, each being 3-7 cm thick.

PAH Profiles and Distribution in Seabed

Despite different sediment geochronologies at each site, the PAH profiles in sediments appear remarkably uniform with depth between sites (Figure 4-5). Additionally, except for the lightest PAHs (molecular weight (MW) < 166 amu), sediment PAH concentrations are all higher in the East River relative to Newark Bay (Figure 4-5). At both sites, sediment concentrations of

Figure 4-5. Depth profiles of box core sediment PAHs collected at the East River (closed symbols) and Newark Bay (open symbols). PAH concentrations are higher in the East River Site relative to the Newark Bay Site, but are uniform at both sites. Despite overall higher PAH concentrations at the East River Site, low molecular weight PAHs (naphthalene, 1-methylnaphthalene, acenaphthene, acenaphthylene) were not detected in the sediments at this site and PAHs were not detected in pore waters.



the lightest PAHs (naphthalene, acenaphthylene, fluorene and 1-methylfluorene) are one order of magnitude lower than the remainder of the PAHs detected (data not shown). In contrast to depth profiles of other PAHs, East River sediments are more depleted in these lower MW PAHs relative to Newark Bay sediments. Although overall PAH concentrations are significantly higher in East River sediments (Figure 4-5) and despite the fact that pore water is enriched in DOC at this site relative to the Newark Bay Site (Figure 4-6), PAHs in East River pore water were not detectable to any great extent. Rather, there was a greater abundance of detectable PAHs in pore water at the Newark Bay site.

Down-core profiles of organic carbon normalized PAH distribution coefficients between sediments and pore waters ($\log K'_{OCs}$) in Newark Bay (Figure 4-7) vary at most by ~ one order of magnitude for the range of PAHs shown. Thus, normalization of PAH distribution coefficients to the amount of sedimentary organic carbon does account for differences in K'_{OCs} at these sites to within a factor of two as suggested (Karickhoff, 1984; Schwarzenbach, *et al.*, 1993). K'_{OCs} for the various 4-6 ring PAHs are similar, a trend that is indicative of the influence of DOC binding on partition coefficients (Baker *et al.*, 1991). Using a three phase (sediment/pore water DOC/freely dissolved in pore water) model (Chapter 3), the role of pore water DOC concentration on PAH K'_{OCs} in the Newark Bay was calculated and found to range ± 0.5 log units (Figure 4-8).

PAH sources

Distinguishing among different sources of PAHs is of fundamental importance in assessing their transport and bioavailability. Ratios of total methylphenanthrenes to phenanthrene in

Figure 4-6. Depth profiles of pore water DOC in East River (closed symbols) and Newark Bay (open symbols) sediments indicate higher amounts of DOC in East River pore waters until a depth of ~14 cm. Note the onset of a rapid down-core increase in amounts of pore water DOC in the Newark Bay at 14 cm coincident with decreasing down-core PAH K'_{oc} s (see Figure 4-7).

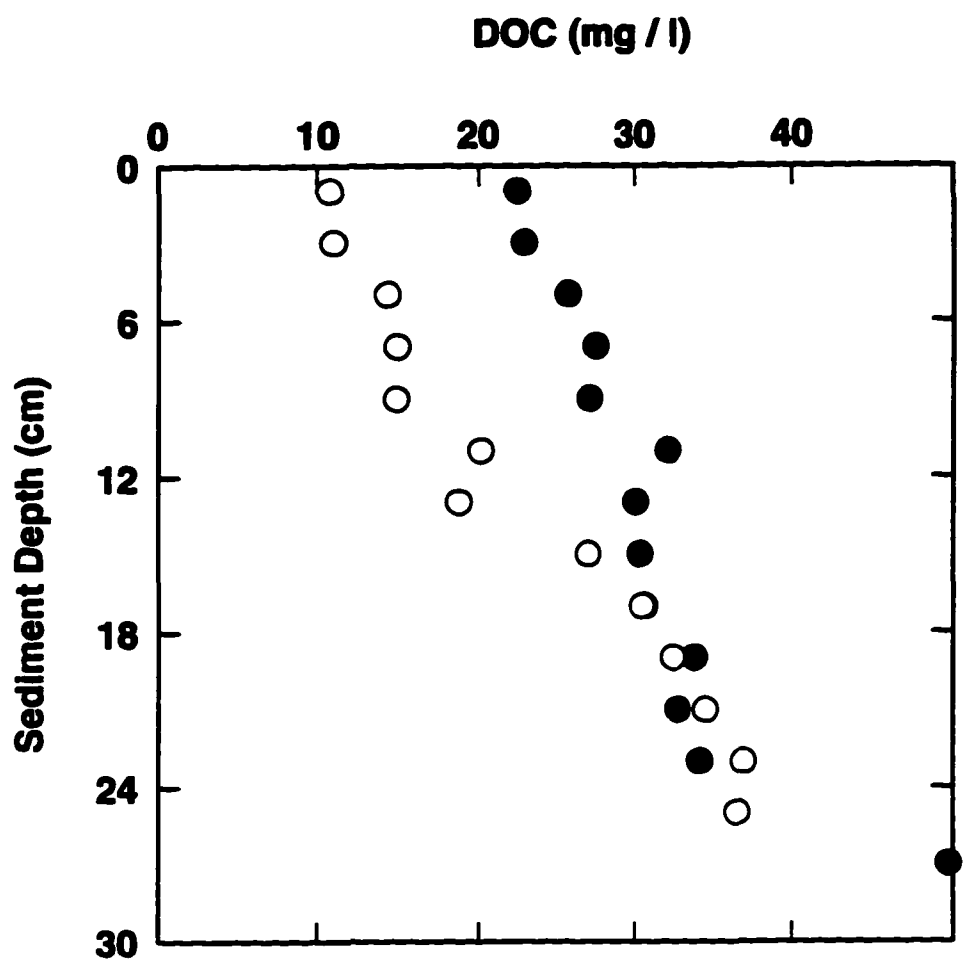


Figure 4-7. Depth profiles of organic carbon normalized sediment/pore water PAH distribution coefficients (K'_{OC} s) in Newark Bay sediments. Note the scattered K'_{OC} s for the top 14 cm of the sediment column followed by uniform decreasing down-core K'_{OC} profiles. K'_{OC} s from 0-14 cm in the seabed are proportional to the depth of the mixed layer (Figure 4-4) at this site. Below 14 cm K'_{OC} s decrease as pore water DOC increases (Figure 4-6).

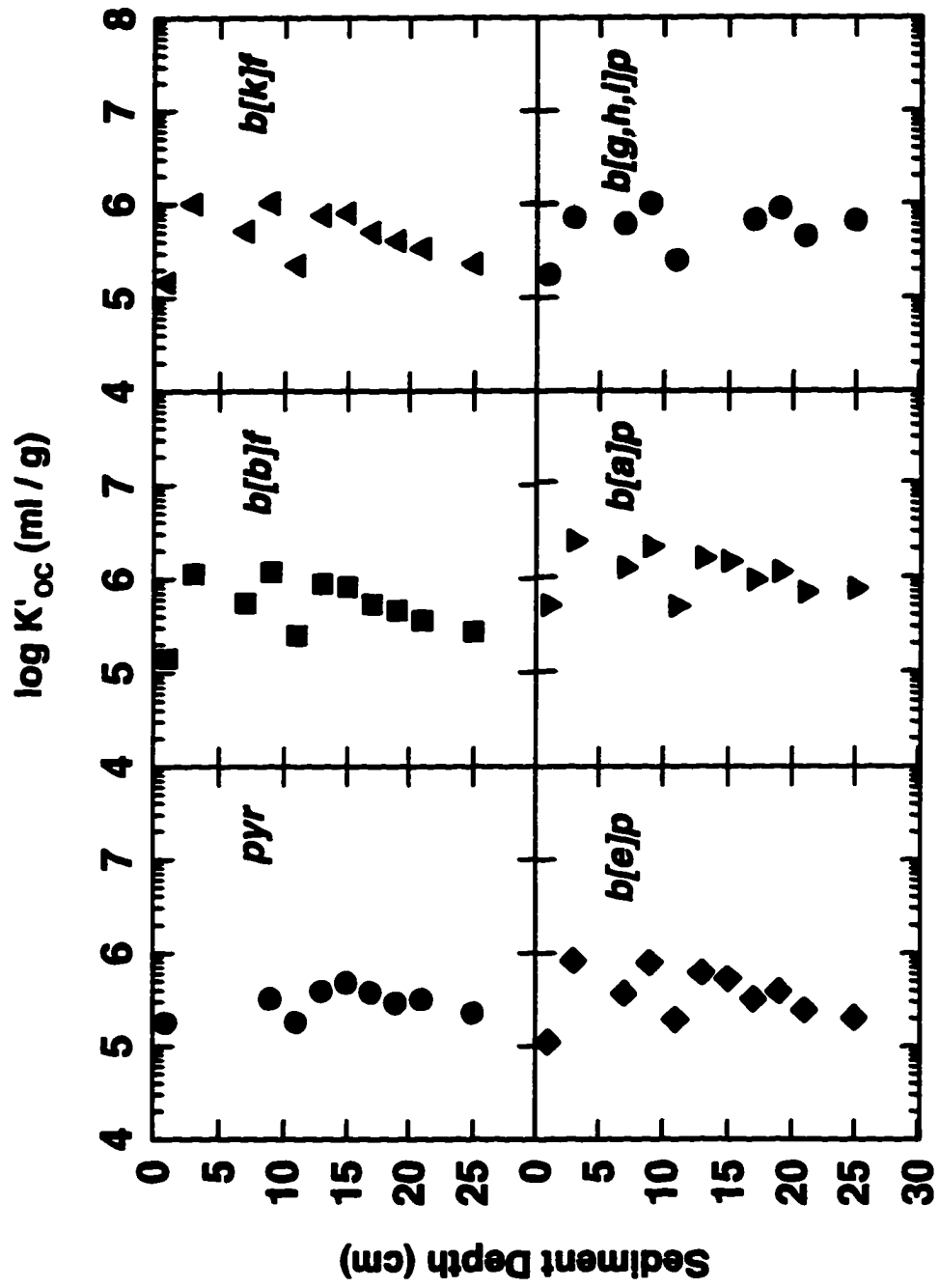
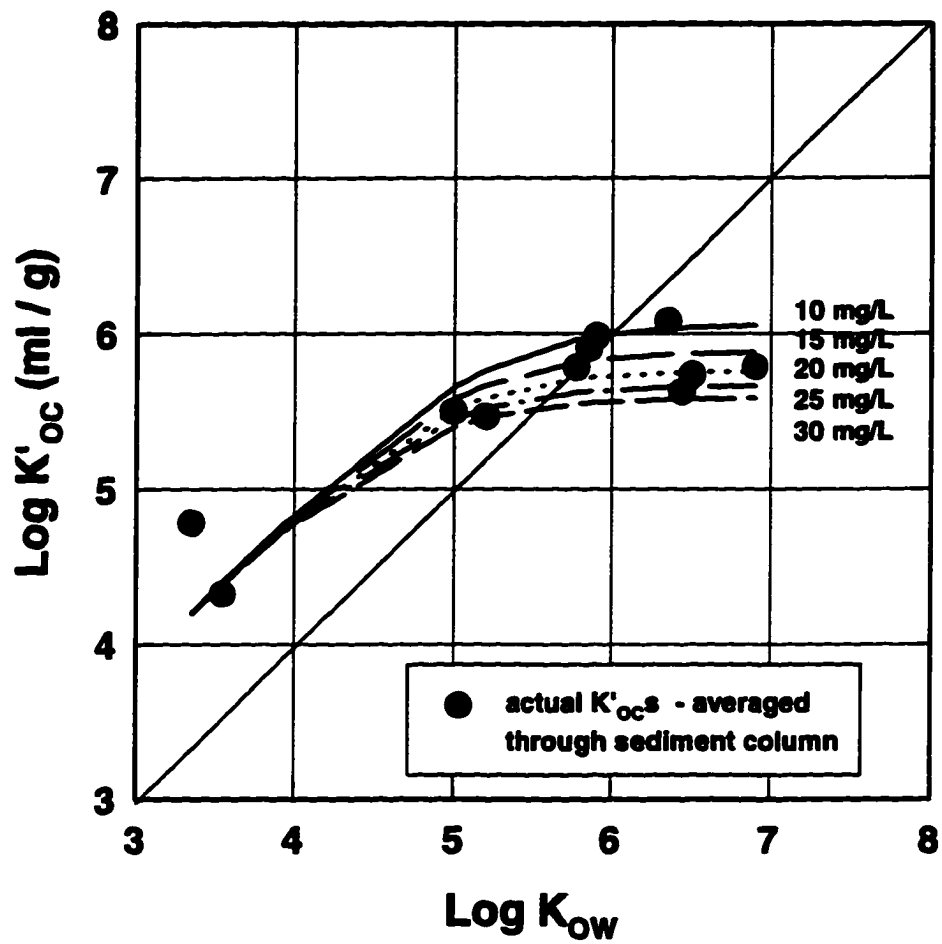


Figure 4-8. Actual PAH K'_{oc} s (symbols) averaged through the sediment column and modeled (lines) for various pore water DOC concentrations illustrating that the range in amount of DOC in the Newark Bay contributes to a maximum 0.5 log unit change in K'_{oc} .



samples can be used to infer sources of PAHs as being pyrolytic or petrogenic (Laflamme and Hites, 1978; Wakeham and Farrington, 1980; Prahl and Carpenter, 1983). For example, due to its low formation temperatures (< 150°C) a high amount of monomethyl PAH derivatives are preserved in petroleum relative to the parent PAH (Garrigues *et al.*, 1995). Likewise, variable ratios of PAH isomers can be a tracer of PAH transformation during transport from their origin to deposition and burial, or simply reflect differences in PAH sources between sites or with time (Sporstol *et al.*, 1983; Colombo *et al.*, 1989; Zeng and Vista, 1997). PAH isomer ratios such as: phenanthrene/anthracene, fluoranthene/pyrene, and benzo(e)pyrene/benzo(a)pyrene with the more reactive compound in the denominator have been indirectly used to infer differential transport mechanisms of particle-associated PAHs (see Chapter 2; Liu and Dickhut, 1997). Down-core ratios of PAH isomers and $(1\text{-methylphenanthrene} + 2\text{ methylphenanthrene}) / \text{phenanthrene}$ ($\sum\text{methylphenanthrene}/\text{phenanthrene}$) are similar between the Newark Bay and East River sites implying similar sources of PAHs to both areas (Figure 4-9).

Sediment Geochemistry and PAH Distribution

Total organic carbon concentrations were relatively uniform with depth at both the Newark Bay and East River sites but higher in East River sediments (Figure 4-10). Sedimentary soot carbon (Figure 4-10), as in the case of PAH concentrations (Figure 4-5), varies between sites in the top 10 cm of the seabed and then is similar in concentration below 10 cm sediment depth. C/N ratios, which are often used to distinguish between algal and plant origins of sedimentary organic matter (Meyers 1994 and references therein), increase with depth at the Newark Bay site, but remain constant in the East River core (Figure 4-10). Particle surface area of sediments is

Figure 4-9. Depth profiles of PAH source indicators (East River - solid symbols; Newark Bay - open symbols): 1-methylphenanthrene + 2-methylphenanthrene/phenanthrene; phenanthrene/anthracene; fluoranthene/pyrene; benzo[e]pyrene/benzo[a]pyrene. Values of (1+2) methylphenanthrene/phenanthrene < 1 at both sites imply sources are predominantly pyrogenic, whereas similar down-core ratios of phenanthrene/anthracene, fluoranthene/pyrene, benzo[e]pyrene/benzo[a]pyrene with depth at both sites imply PAHs have undergone similar modes of atmospheric transport prior to burial.

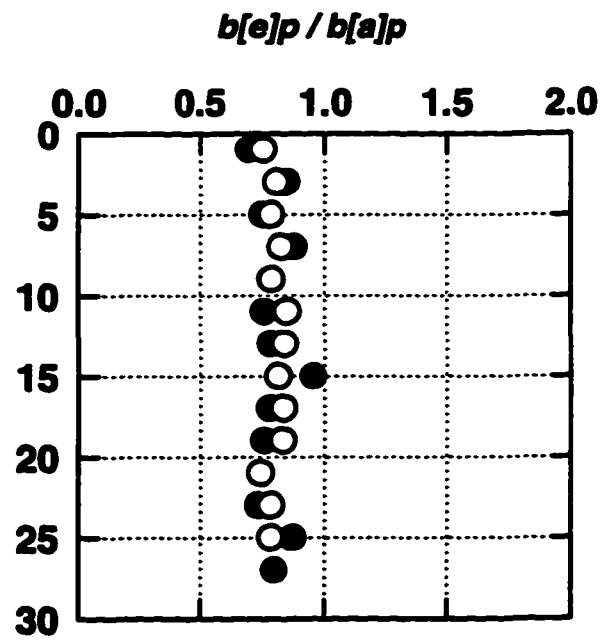
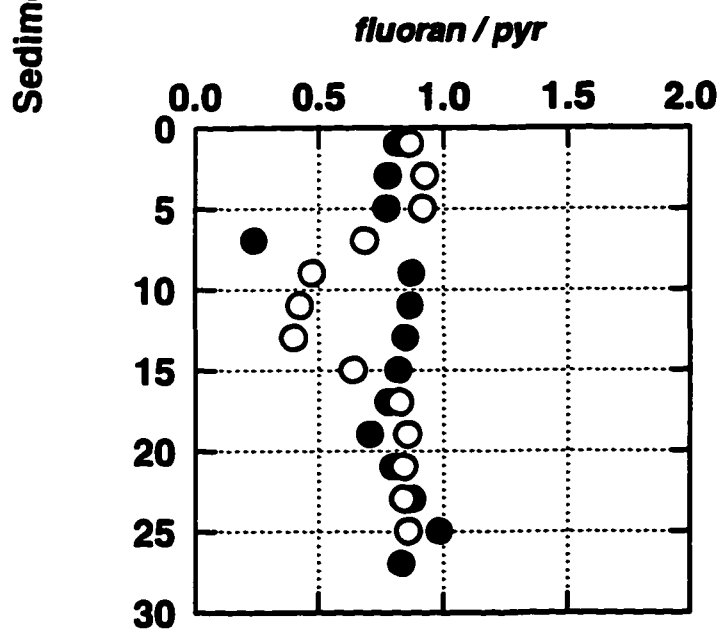
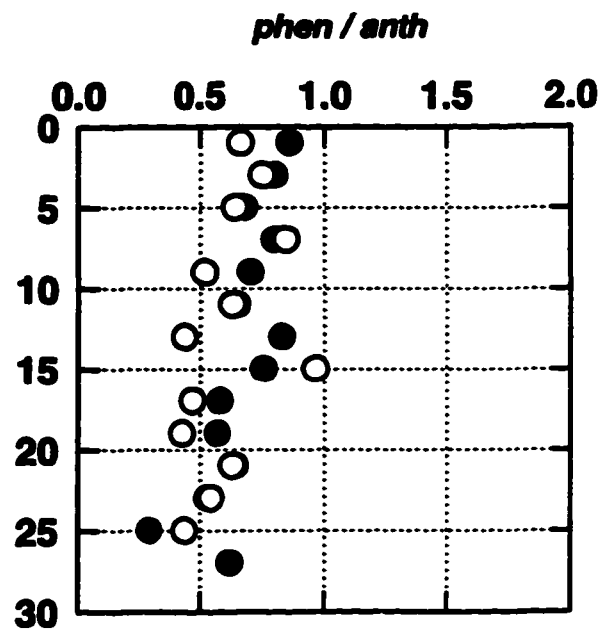
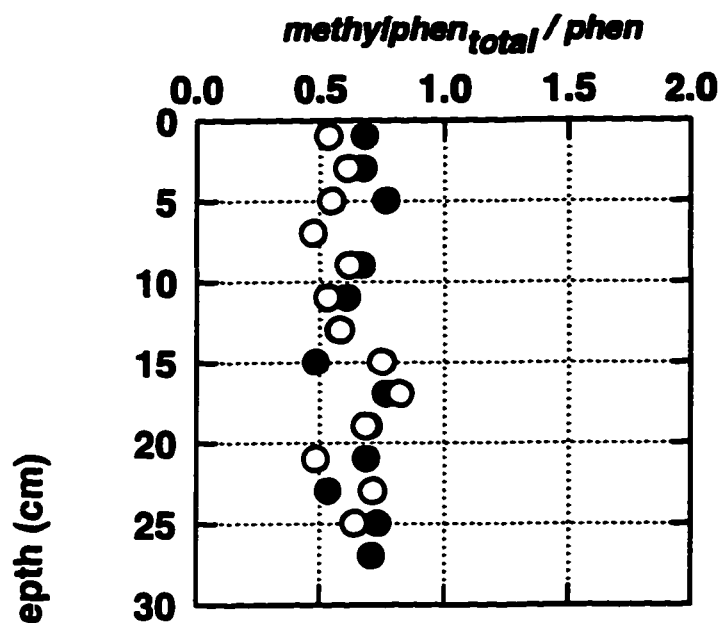
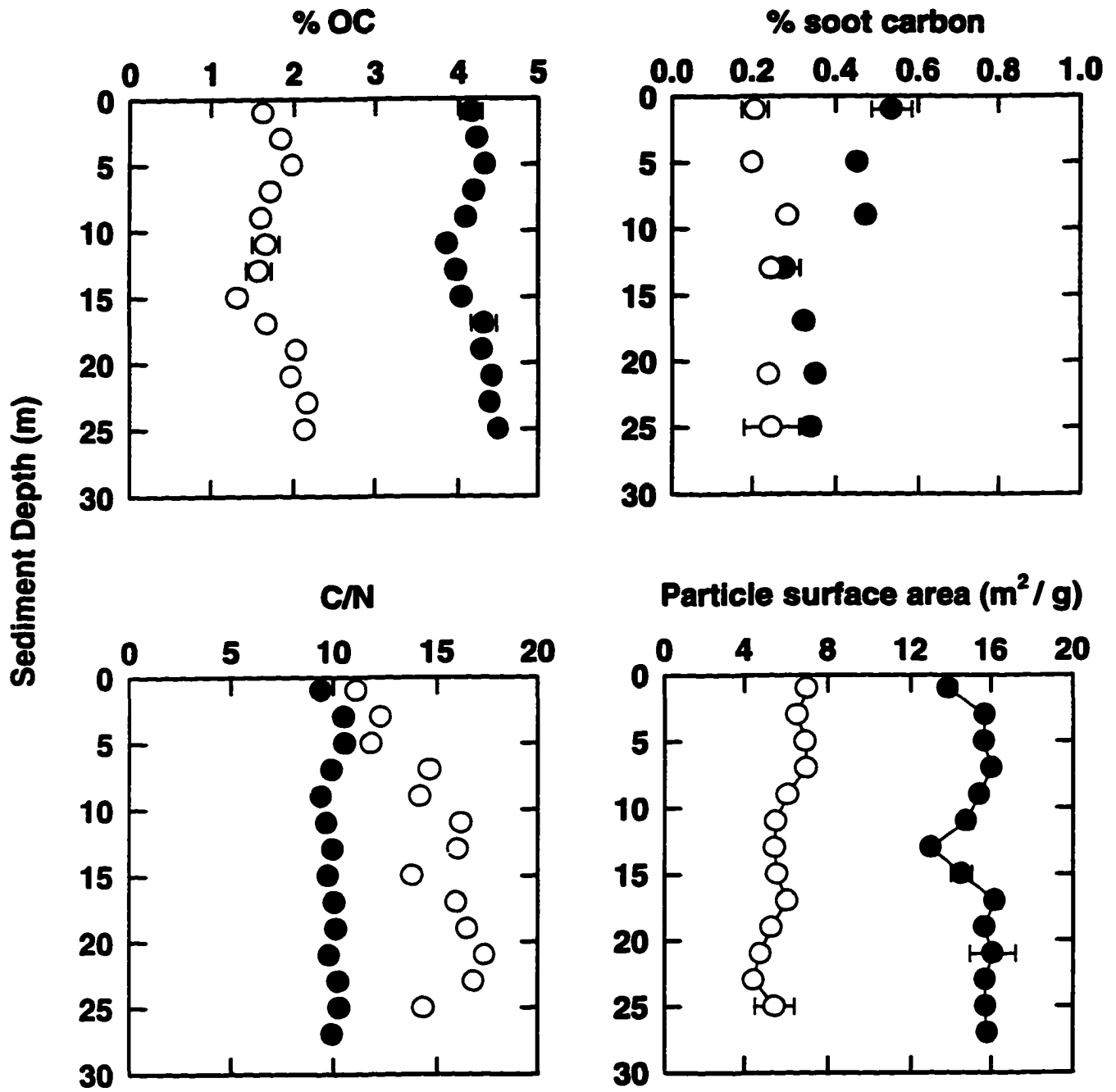


Figure 4-10. Depth profiles of % sediment organic carbon, % sedimentary soot carbon, carbon/nitrogen ratios, and particle surface area at the East River (solid symbols) and Newark Bay (open symbols) sites. Higher amounts of organic carbon and uniform C/N ratios at the East River site indicate that sediments at this site have not undergone any selective degradation of labile nitrogen-rich substances with depth; possibly the result of the frequent physical disturbances in this area. In contrast, increasing C/N ratios at the Newark Bay site imply that there has been down-core mineralization of labile nitrogenous substances relative to bulk carbon. Lower C/N ratios in the East River also indicate that sediments are more labile relative to Newark Bay sediments. Higher particle surface area in the East River relative to Newark Bay is not due to porous organic matter as digesting sediments with peroxide did not change surface areas at either site. Sedimentary soot carbon varies between East River and Newark Bay in the top 10 cm, below this soot carbon profiles are similar between sites. These profiles are similar to sediment [PAH] (Figure 4-5). Thus, soot carbon may explain higher PAH concentrations in East River sediments.



also higher in the East River compared to Newark Bay (Figure 4-10). However digesting the organic matter from these sediments did not appreciably change their surface areas (data not shown). Thus, sediment surface area seems largely a function of grain size.

4-4. Discussion

Sediment Deposition

Uniform and high excess ^{210}Pb activities in the sediments in the profile from the East River Site (Figure 4-2) and the presence of ^{137}Cs at the base of the core (~ 180 cm) suggest either deep physical mixing or rapid deposition. The absence of any apparent sedimentary structure including bioturbation signatures (Figure 4-4) and presence of undifferentiated silt and clay (Figure 4-3) throughout the sediment column agrees with the deposition scenarios suggested above.

Physical mixing occurs through cycles of erosion and deposition of varying intensity, with the net result being a high sediment deposition rate (Nittrouer and Sternberg, 1981; Dellapena, et al., 1998). The excess ^{210}Pb activity for the four samples in the top 20 cm in the East River core is 4.96 dpm/g while the mean ^{210}Pb activity in bottom 50 cm of the 1.9 m core is 4.99 dpm/g (Figure 4-2), suggesting that ^{210}Pb has not significantly decayed within the core. A minimum detectable change in ^{210}Pb specific activity of 1.0 dpm/g is proportional to ~7 y. The uniform ^{210}Pb activity profile in the East River core suggests that sediments at this site have been physically mixed and deposited within the last 7 y, and probably more recently. A minimum deposition rate for a 2 m sediment core that is at most 7 y old is 28.5 cm/y. Because we assume a conservative estimate for the age of the sediments for the bottom of the core and we do not know the maximum depth of homogenized excess ^{210}Pb , the actual deposition rate may be higher.

Mulinia lateralis are considered an invasive species of filter feeding bivalve (Schaffner et al., 1987). Their ability to survive at the sediment/water interface but not within the sediment bed renders their presence in sediments a useful "biochronometer." Based on their size, the *M. lateralis* at the surface of the East River core (Figure 4-4) appear 1-3 months old, suggesting that the sediment/water interface was stable for at least one month. The presence of *M. lateralis* in living position in the seabed below a 65 cm thick layer of sediment would suggest that sediment deposition at this site is episodic and has occurred in stages with extended periods of time (months to years) between disturbances. The proximity of the East River Site to a shipping channel, wharfs and other ship-loading facilities, the narrow width of the channel, and its shallow water depth can cause the seabed at this site to undergo rapid, intense physically-driven high energy resuspension events (e.g. ship and barge wakes, tidal energy).

The changes in excess ^{210}Pb activity throughout sediments at the Newark Bay Site (Figure 4-2) appear to result primarily from coincident changes in clay and silt/sand content. The surface area to volume ratio of fine grained sediments is much higher than for coarser sediments. Thus, sand and silt are not as efficient at scavenging ^{210}Pb as clay sized grains with greater porosity. To that end, the depressed excess ^{210}Pb activity at the bottom of these sediments (130 - 132 cm) results from an increased (72%) sand content rather than decay of excess activity to supported levels. Similarly, the excess ^{210}Pb minima in the Newark Bay core at 40 cm is coincident with both an increase in sand content and a decrease in clay content at this depth interval. Because of these grain size effects and the lack of a measurable decrease in ^{210}Pb activity, accumulation rates cannot be determined using ^{210}Pb geochronology. However, the elevated excess activities throughout the cores ($> 1\text{dpm/g}$) suggest deep mixing or recent episodic deposition has occurred

at both sites.

As stated above, the maximum depth of ^{137}Cs penetration in the Newark Bay core is 110 cm (Figure 4-2). Assuming sediments from the surface of the core to this horizon have been accumulating since 1954, the maximum long-term sediment accumulation rate is 2.6 cm/y. This is consistent with an approximate sedimentation rate of 2 cm/y estimated using ^{210}Pb for the top 25 cm of sediments in the Newark Bay core where no grain size effects are evident (Figure 4-3). Evidence of mixing from X-radiographs at this site and from the uniform excess ^{210}Pb activity profiles strictly between 45-110 cm of sediment suggest that this sediment accumulation rate is a gross underestimation. Note, laminations in X-radiographs (Figure 4-4) suggest that short-term *deposition* rates may be higher than 2.6 cm/y.

Although sedimentation rates cannot be estimated from the data available, a cyclic pattern of short-term deposition is revealed at the Newark Bay site via alternating physically laminated and moderately to intensely bioturbated layers. The finely laminated sediments from 10-17 cm (Figure 4-4) alternate between light and dark laminae, resulting from alternating fine-grained and coarse-grained sediments. This resembles tidalite deposits and may reflect either a slack versus flow or spring-neap signal, with coarse material being deposited during either flow/spring and fine material being deposited during either slack/neap tides. Similar alternating fine and coarse grained banding occurs throughout this core wherever physical laminations are preserved. Bioturbation intensity whenever present in these Newark Bay sediments, ranges from completely obliterating any physical laminations, to moderately obscuring them with macrofaunal burrows preserved in some layers. The alternating layers of physical laminated and bioturbated sediments suggests a depositional history of episodic disturbance, which may have involved erosion of the seabed,

followed by relatively rapid deposition of finely laminated sediments over the course of either numerous tidal cycles or spring-neap cycles. Finally, each sequence is stabilized for a duration of time such that settlement of benthic organisms could occur and biological mixing could become intense. Thus, this entire 1.5 m core contains depositional history that was developed over multiple seasons and probably represents a few decades of record.

PAH Sources and Deposition

The uniform down-core ratios of Σ methylphenanthrene/phenanthrene, phenanthrene/anthracene, fluoranthene/pyrene, and benzo[e]pyrene/benzo[a]pyrene (Figure 4-9) indicate historically similar PAH sources between the East River and Newark Bay sites. Likewise, the consistent down-core methylphenanthrene/phenanthrene ratio of 0.5-0.7 in the top 25 cm of sediments at both sites indicates mostly pyrogenic PAH source inputs (Garrigues *et al.*, 1995) to the East River and Newark Bay over the time course of deposition.

The uniform profiles in sediment PAHs at the East River site (Figure 4-5) in conjunction with the evidence of recent physical mixing and rapid deposition, and lack of pore water PAHs indicate that PAHs have not been able to attain true equilibrium distributions between the sediments and pore waters at this site. For example, sedimentary soot carbon may be responsible for limited PAH desorption from within the particle matrix. However, if porous soot carbon acts as a "sink" for PAHs, low molecular weight PAHs should still be detectable in these particles. If we apply the concept of an "equilibrium" surface for PAH deposition (Olsen *et al.*, 1993), the site in the East River can be classified as a "Type III" area: major fine-particle, organic carbon and contaminant sink subject to frequent anthropogenic disturbances. Sediment contaminant profiles

in such areas tend to be well homogenized. In addition, East River sediments were slightly more depleted in lower mass PAHs relative to Newark Bay sediments. This suggests greater removal (e.g. desorption) of these compounds, during sediment transport or deposition.

In contrast, although sediment accumulation at the Newark Bay site alternates between physical and biological mixing (Figure 4-4), uniform sediment PAH profiles (Figure 4-5), similar source(s) of PAHs as in the East River (Figure 4-9), and the presence of detectable quantities of PAHs in pore water, indicate that for at least some of the time sediments at this site were deposited in a "Type II" equilibrium area (Olsen *et al.*, 1993): particle and contaminant deposition in proportion to natural estuarine sedimentation processes. The time scale of this type of sediment accumulation would allow for PAHs desorbing from sediment to distribute into surrounding pore water as evidenced by the observed down-core profiles of PAH sediment/pore water distribution coefficients at this site (Figure 4-7).

PAH Distribution Coefficients

Sediment/pore water distribution coefficients of PAHs can be a function of their source, the compositional chemistry of the sediment associated carbon, and to a lesser extent, the amount and composition of pore water DOC (see previous chapters). Since sources of PAHs are similar throughout depth in the sediment column (Figure 4-9), variation in K'_{oc} profiles throughout the sediment column in Newark Bay (Figure 4-7) must be a function of particle geochemistry or binding of PAHs by pore water DOC. Variable $\log K'_{oc}$ s in Newark Bay sediments down to a depth of 12 cm (Figure 4-7) correspond to the depth of the mixed layer (Figure 4-4) suggesting the importance of deposition and mixing processes in establishing sediment/pore water equilibrium

distributions of PAHs. Interestingly, at 11 cm, a local maxima in pore water DOC (Figure 4-11) corresponds to a local minima in K'_{OC} , suggesting either less irrigation beginning at this depth or relatively higher rates of localized microbial activity. Below 12 cm in the seabed, PAH K'_{OC} s in Newark Bay decrease with depth in the core. Similarly, amounts of DOC in Newark Bay pore waters increase with depth especially below 12 cm (Figure 4-6). Thus, down-core profiles of PAH K'_{OC} s may be a function of increasing amounts of pore water DOC or decreased availability of particulate organic matter with depth (see Chapter 2 for elaboration). This latter explanation for decreasing PAH K'_{OC} s with depth is based on recent speculation that a great deal of sedimentary organic matter from a wide variety of marine depositional environments cannot be physically separated from its mineral matrix and hence is not bioavailable (Hedges and Kiel, 1995). Consequently, such an inaccessible sorbent, although consisting of natural organic matter, may be limited in its binding capacity for PAHs. The similarity between down-core pore water DOC concentrations profiles below 12 cm (Figure 4-6) and the results of our three phase model for PAH-DOC binding (Figure 4-8) indicate that increasing amounts of pore water DOC may be responsible for the 0.5 log unit decrease in PAH K'_{OC} s below 12 cm sediment depth in Figure 4-7.

4-5. Conclusions

On the basis of profiles of PAHs and other geochemical variables in sediments of the East River, New York and Newark Bay, New Jersey sediments, it would seem that each location undergoes different particle and associated PAH deposition patterns. Despite this fact, PAH sources and concentrations in sediments are reasonably uniform throughout depth at both sites. Pore water PAH concentrations are most notably influenced by the depositional environment at

each site. Although situated in areas of high amplitude physical disturbances, East River sediments are higher in particle-associated PAHs, as expected for sediments higher in amounts of organic carbon, sedimentary soot carbon, and particle surface area. Although the seabed at the East River Site may be a more effective sink of fine particles and organic matter (Olsen *et al.*, 1993), PAH distributions between sediments and pore waters do not seem to be able to attain equilibrium in such areas (i.e. pore water PAHs are depleted). In contrast, distributions of PAHs may be more likely to attain equilibrium between sediments and pore waters from environments in which physical disturbances are lower in energy (e.g. the Newark Bay Site). Down-core profiles of sediment/pore water PAH K'_{oc} s from Newark Bay sites seem to be controlled by pore water DOC concentrations rather than the amount of particulate organic carbon or the composition of the particle. These results coupled with results from other work (McGroddy and Farrington, 1995; Gustafsson *et al.*, 1997) indicate that any attempt at explaining equilibrium PAH distributions between sediments and pore water must not only take into account the geochemistry of the particle matrix (e.g. accessibility of PAHs to carbon within the particle matrix), but also the depositional environment of the particles.

4-6. References

- Adams, D. 1996. Comprehensive sediment quality of the NY/NJ Harbor Estuary. Poster abstract. Presented at the Society of Environmental Toxicology and Chemistry National Meeting, Washington, D.C.
- Baker, J. E., Eisenreich, S. J., Swackhamer, D. L. 1991. Field-Measured Associations between polychlorinated biphenyls and suspended solids in natural waters: an evaluation of the partitioning paradigm. In: R. A. Baker [ed.] Organic substances and sediments in water, v2. Lewis Publishers Inc., MI.

- Berner, R. A. 1980. Early Diagenesis: A theoretical approach. Princeton University Press, Princeton, NJ, 241 pp.
- Blumer, M. 1976. Polycyclic aromatic compounds in nature. *Scientific American*, 234, 34-45.
- Bopp, R. F., Simpson, H. J., Olsen, C. R., Trier, R. M., Kostyk, N. 1982. Chlorinated hydrocarbons and radionuclide chronologies in sediments of the Hudson River and estuary, New York. *Environ. Sci. Technol.*, 15, 210-218.
- Brown, D. S. and Flagg, E.W. 1981. Empirical prediction of organic pollutant sorption in natural sediments. *J. Environ. Qual.*, 10, 382.
- Brownawell, B., and Farrington, J. W. 1984. Biogeochemistry of PCBs in interstitial waters of a coastal marine sediment. *Geochim. Cosmochim. Acta*, 50, 157-169.
- Burdige, D. 1991. The kinetics of organic matter mineralization in anoxic marine sediments. *J. Mar. Res.*, 49, 727-761.
- Colombo, J. C., Pelletier, E., Brochu, C., Khalil, M. 1989. Determination of hydrocarbon sources using *n*-alkane and polyaromatic hydrocarbon distribution indexes. Case Study: Rio de La Plata Estuary, Argentina. *Environ. Sci. Technol.*, 23, 888-894.
- Dellapena, T. M., Kuehl, S. A., Schaffner, L. C. 1997. Seabed mixing and particle residence times in biologically and physically dominated estuarine systems: a comparison of lower Chesapeake Bay and the York River subestuary. *Estuarine Coastal Shelf Sci.* In press.
- Denisenko, M. F., Pao, A., Tang, M., Pfeifer, G. P. Preferential formation of benzo[a]pyrene adducts at lung cancer mutational hotspots in P53. *Science*, 274, 430-432.
- Dickhut, R.M and Gustafson, K. E. 1995. Atmospheric inputs of selected polycyclic aromatic hydrocarbons and polychlorinated biphenyls to southern Chesapeake Bay. *Mar. Pollut. Bull.*, 30, 385-396.
- Dukat, D. A., and Kuehl, S. A. 1995. Non-steady-state ²¹⁰Pb flux and the use of ²²⁸Ra/²²⁶Ra as a geochronometer on the Amazon continental shelf. *Marine Geology*, 125, 329-350.
- Dyer, K. R. 1989. Sediment processes in estuaries: Future research requirements. *J. Geophys. Res.*, C10, 14327-14340.
- Garrigues, P., Budzinski, H., Manitz, M. P., Wise, S. A. 1995. Pyrolytic and petrogenic inputs in recent sediments: A definitive signature through phenanthrene and chrysene compound distribution. *Polycyc. Arom. Compds.*, 7, 275-284.

- Gelboin, H. 1980. Benzo[a]pyrene metabolism, activation, and carcinogenesis: Role and regulation of mixed function oxidases and related enzymes. In Physiological Reviews - v. 60.
- Gregg, S. J. and Sing, K. S. W. 1982. Adsorption, surface area, and porosity. Academic Press.
- Gustafsson, O., Haghseta, F., Chan, C., MacFarlane, J., Gschwend, P. M. 1997a. Quantification of the dilute sedimentary "soot-phase": Implications for PAH speciation and bioavailability. *Environ. Sci. Technol.*, 31, 203-209.
- Hedges, J. I., and Kiel, R. G. 1995. Sedimentary organic matter preservation: an assessment and speculative synthesis. *Mar. Chem.*, 49, 81-115.
- Henrichs, S. M. 1993. Early diagenesis of organic matter: the dynamics (rates) of cycling of organic compounds. In: Engel, M.H. and Macko, S.A. [eds]. Organic geochemistry: principles and applications, pp. 101-114.
- Karickhoff, S. W. 1984. Organic pollutant sorption in aquatic systems. *J. Hydraul. Eng.*, 110, 707-735.
- Krishnaswami, S., Lal, D., Martin, J. M., and Meybeck, M. 1971. Geochronology of lake sediments. *Earth Planet. Sci. Lett.*, 11, 407-414.
- Kuehl, S. A., Nittrouer, C. A., DeMaster, D. J., Curtin, T. B. 1985. A long, square-barrel gravity corer for sedimentological and geochemical investigation of fine-grained sediments. *Mar. Geo.*, 62, 365-370.
- Laflamme R. E., and Hites, R. A. 1978. The global distribution of polycyclic aromatic hydrocarbons in recent sediments. *Geochim. Cosmochim. Acta*, 43, 1847-1854.
- Liu, K. 1996. Fate and transport processes for polycyclic aromatic hydrocarbons in the surface microlayer of southern Chesapeake Bay. PhD Dissertation. Virginia Institute of Marine Science
- Mackay, D., Shiu, W. Y., Ma, K.C. 1992. Illustrated handbook of physical-chemical properties and environmental fate for organic chemicals-v. 2: polynuclear aromatic hydrocarbons, polychlorinated dioxins, and dibenzofurans. Lewis Publishers, Ann Arbor, MI.
- Meyers, P. 1994. Preservation of elemental and isotopic source identification of sedimentary organic matter. *Chemical Geology*, 11, 289-302.
- McGroddy, S., and Farrington, J. 1995. Sediment porewater partitioning of PAHs in three cores from Boston Harbor, MA. *Environ. Sci. Technol.*, 29, 1542-1550.

National Research Council. 1983. Polycyclic Aromatic Hydrocarbons: Evaluation of Sources and Effects. National Academy Press, Washington DC.

Neff, J. M. 1979. Polycyclic aromatic hydrocarbons in the aquatic environment: sources, fates and biological effects. London, Applied science Publishers.

Nittrouer, C. A., and Sternberg, R. W. 1981. The formation of sedimentary strata in an allochthonous shelf environment: the Washington continental shelf. *Mar. Geo.*, 42, 201-232.

Nittrouer, C.A., Sternberg, R. W., Carpenter, R., Bennett, J. T. 1979. The use of ^{210}Pb geochronology as a sedimentological tool: application to the Washington Continental Shelf. *Mar. Geo.*, 31, 297-316.

Olsen, C. R., Larsen, I. L., Mulholland, P. J., VonDamm, K. L., Grebmeier, J. M., Schaffner, L. C., Diaz, R. J., Nichols, M. M. 1993. The concept of an equilibrium surface applied to particle sources and contaminant distributions in estuarine sediments. *Estuaries*, 16, 683-696.

Olsen, C. R., Larsen, I. L., Brewster, R. H., Cutshall, N. H., Bopp, R. F., and H. J. Simpson. 1984. A geochemical assessment of sedimentation and contaminant distributions in the Hudson-Raritan Estuary. National Oceanic and Atmospheric Administration Technical Report OMS NOS2, Rockville, Maryland. 106 pp.

Olsen, C. R., Cutshall, N. H., Larsen, I. L. 1982. Pollutant-particle associations and dynamics in coastal marine environments: A review. *Mar. Chem.*, 11, 501-533.

Prahl, F. G. and Carpenter, R. 1983. Polycyclic aromatic hydrocarbon (PAH)-phase associations in Washington Coastal Sediments. *Geochim. Cosmochim. Acta*, 47, 1013-1023.

Radke M., 1987. Organic geochemistry of aromatic hydrocarbons. Brooks, J and Welte, D. [eds.] Advances in petroleum geology. Hartcourt, Brace, and Jovanovich, Publishers. New York.

Schaffner, L. C., Diaz, R. J., Byrne, R. J. 1987. Processes affecting recent estuarine stratigraphy. Pp. 584-599 in Kraus, N. C. [ed.] Coastal Sediments '87. Proceedings fo a Specialty Conference on Advances in Understanding of Coastal Sediment Processes. vol I. American Society of Civil Engineers, New York, NY.

Schwarzenbach, R., Gschwend, P. M., Imboden, D. M. 1993. Environmental Organic Chemistry. John Wiley and Sons, Inc., New York, NY, p. 262-328.

Spies, R. B., Kruger, H., Ireland, R., Rice, D.W. 1989. Stable isotope ratios and contaminant concentrations in a sewage-distorted food web. *Marine Ecol. Prog. Ser.* 54, 157-170.

Sporstol, S., Gjøs, N., Lichtenthaler, R. G., Gustavsen, K. O., Urdal, K., Oreld, F., and Skel, J. 1983. Source identification of aromatic hydrocarbons in sediments using GC/MS. *Environ. Sci. Technol.*, 17, 282-286.

Sugimura, Y and Suzuki, Y. 1988. A high-temperature catalytic oxidation method for the determination of non-volatile dissolved organic carbon in seawater. *Mar. Chem.*, 24, 105-131.

Turekian, K. K., Cochran, J. K., Benninger, L. K., Aller, R. C. 1980. The sources and sinks of nuclides in Long Island Sound, p. 129-164. In B. Saltzman (ed.), Estuarine Physics and Chemistry: Studies in Long Island Sound, Advances in Geophysics, 22. Academic Press, New York.

Verado, D. J., Froelich, P. N., McIntyre, A. 1990. Determination of organic carbon and nitrogen in marine sediments using the Carlo Erba NA-1500 Analyzer. *Deep-Sea Research*, 37, 157-165.

Wakeham, S. G. and Farrington, J. W. 1980. Hydrocarbons in contemporary aquatic sediments. In Contaminants and Sediments - v. 1, Baker, R. A. [ed.] Ann Arbor Science.

Westrich, J. T. and Berner, R. A. 1984. The role of sedimentary organic matter in bacterial sulfate reduction: The G model tested. *Limnol. Oceanogr.*, 29, 236-249.

Zeng, E. Y., and Vista, C. L. 1997. Organic pollutants in the coastal environment off San Diego, California. 1. Source identification and assessment by compositional indices of polycyclic aromatic hydrocarbons. *Environ. Toxicol. Chem.*, 16, 179-188.

Chapter 5. Research Summary

Summary

Sediments and pore waters were sampled for polycyclic aromatic hydrocarbons (PAHs) and geochemical variables (e.g. C/N ratio, sedimentary soot carbon) in two urban estuaries. The central hypothesis being tested throughout these experiments was that changing down-core geochemical variables pertaining to sedimentary organic matter, are of primary importance in influencing observed trends in PAH distribution coefficients. The results presented in the previous chapters indicate that in addition to sediment geochemistry, sediment/pore water distributions of PAHs can also be significantly affected by physical energy regime and frequency of sediment mixing.

Sediments and pore waters were sampled from two locations in the Southern Branch of the Elizabeth River, Virginia. In the case of the Elizabeth River, sediments from both sites have been in a non-depositional zone for the past 70-80 y or consist of old dredge spoil. Sites are within 1 km of each other yet differ in their PAH distribution coefficients as well as sediment geochemistry. Down-core PAH distribution coefficients at Site 1 in the Elizabeth River decreased by several orders of magnitude, despite normalizing to amount of sedimentary organic carbon. Thus, at Site 1, it seems likely that the amount of organic carbon available for PAH binding varies between the top and deeper in the core. A greater portion of total sediment organic carbon may be available for PAH binding in sediments near the surface relative to deeper in the core; a finding consistent with the Weber *et al.* (1993) Distributed Reactivity Model discussed in Chapter 1. At Site 2, organic carbon normalized PAH distribution coefficients were higher than at Site 1 and fairly uniform with depth. PAHs seem to be entrapped within the particle matrix in sediments at this site. These results demonstrate the degree of spatial heterogeneity which can exist in

sediments from adjacent sites in the same watershed.

In sediments from a site in the Newark Bay, New Jersey x-radiograph profiles of the seabed showing alternating light and dark laminae (possibly due to tidal scouring) with periodic evidence of biological mixing (Chapter 4). Trends in down-core PAH distributions at this site were most closely related to amount of pore water dissolved organic carbon (DOC). In contrast, sediment x-radiographs, geochemistry, and geochronological information for a site in the East River, New York, indicate that sediments in this area are subject to frequent resuspensions. Although most sediment PAHs were higher in concentration at this site, pore water PAHs were depleted. Low molecular weight PAHs were also not detectable at this East River Site. Thus, PAH distributions at these sites in the Hudson River watershed seem representative of two alternating sediment mixing processes.

Pore water PAHs seem to remain in the seabed in sediments from inner harbor areas which are subject to low energy natural mixing processes or areas in which the seabed has been sedentary for extended periods of time. In areas subject to lower energy physical mixing processes, the potential for resident benthic organisms to bioaccumulate hydrophobic organic contaminants, may depend greatly on compositional aspects of particulate and dissolved organic carbon. In contrast, sediments in areas such as the site in the East River are subject to greater physical disturbances from passing ship traffic or current regime resulting in greater transport and mobility of pore water and colloidal-bound PAHs relative to "low energy" sites. Thus, sediments from such high energy mixing areas may have a greater capacity to act as potential secondary sources of contaminants throughout the watershed.

5. Appendices

Elizabeth River
Sedimentary Geochemical Variables
(wt. %)

Site 1

Sediment Depth Interval (cm)	% organic carbon	% peat carbon (mass)	% peat carbon (S.D.)	C/N ratio	% water	
0-1		1.83	0.51	0.61	14.02	46.20
1-2	NA	ND	ND	NA		33.04
2-3		1.63	ND	ND	14.66	47.86
3-4		1.29	ND	ND	10.87	45.89
4-5		1.37	ND	ND	13.51	48.32
5-6		1.58	2.49	2.40	12.82	48.17
6-7		1.61	ND	ND	14.37	48.73
7-8		1.22	ND	ND	14.84	50.82
8-9		1.58	ND	ND	14.23	43.00
9-10	NA	ND	ND	NA		46.18
10-11		1.38	0.06	0.01	12.75	47.25
11-12		1.75	ND	ND	15.88	45.82
12-13		2.06	ND	ND	13.97	47.09
13-14		1.98	ND	ND	8.78	46.88
14-15		1.98	ND	ND	4.74	51.24
15-16		1.92	0.23	0.29	14.80	48.99
16-17		1.87	ND	ND	14.73	52.18
17-18		2.19	ND	ND	8.66	53.40
18-19		1.98	ND	ND	11.70	52.56
19-20	NA	ND	ND	NA		54.92
20-21		2.40	0.11	0.02	14.36	54.95
21-22		2.23	ND	ND	14.14	54.38
22-23		2.31	ND	ND	12.58	55.98
23-24		2.18	ND	ND	12.07	57.37
24-25		2.20	ND	ND	11.58	55.98
25-26		2.27	0.21	0.02	14.07	57.41
26-27		2.38	ND	ND	14.36	56.70
27-28		2.22	ND	ND	14.33	54.16
28-29		2.26	ND	ND	6.71	57.52
29-30	NA	ND	ND	NA		55.40
30-31		2.11	0.15	0.05	11.88	55.84
31-32	NA	ND	ND	NA		55.57
32-33		2.36	ND	ND	5.98	55.95
33-34		2.35	ND	ND	11.88	55.81
34-35		2.25	ND	ND	14.58	53.80
35-36		2.39	0.13	0.05	11.10	52.88

Site 2

Sediment Depth Interval (cm)	% organic carbon	% peat carbon (mass)	% peat carbon (S.D.)	C/N ratio	% water	
0-1		4.03	0.51	0.03	41.55	57.93
1-2		3.41	ND	ND	31.84	50.91
2-3		2.57	ND	ND	27.98	52.34
3-4	NA	ND	ND	NA		46.21
4-5		3.55	ND	ND	32.58	45.75
5-6		1.83	2.49	0.12	28.61	40.03
6-7		2.37	ND	ND	34.71	36.60
7-8		1.53	ND	ND	28.90	42.38
8-9		1.36	ND	ND	29.37	41.08
9-10		3.70	ND	ND	45.42	39.52
10-11		1.87	0.06	0.37	22.82	42.90
11-12		2.42	ND	ND	31.58	42.13
12-13		4.61	ND	ND	47.38	41.50
13-14		2.67	ND	ND	22.46	40.48
14-15		1.67	ND	ND	21.88	38.41
15-16		3.27	0.23	0.15	28.58	45.71
16-17		1.82	ND	ND	35.14	43.58
17-18		2.21	ND	ND	27.25	43.63
18-19		6.84	ND	ND	48.34	44.72
19-20		3.11	ND	ND	29.18	45.83
20-21		3.64	0.11	0.10	41.33	47.80
21-22		2.41	ND	ND	21.71	48.34
22-23		2.94	ND	ND	35.84	52.88
23-24		2.32	ND	ND	23.47	46.70
24-25		1.79	ND	ND	17.33	50.23
25-26		1.65	0.21	0.04	18.73	46.78
26-27		1.65	ND	ND	12.24	48.64
27-28		1.44	ND	ND	5.77	50.94
28-29		1.87	ND	ND	18.38	51.58
29-30		1.84	ND	ND	21.43	45.91
30-31		1.80	0.15	0.01	15.05	48.28
31-32		1.98	ND	ND	8.52	38.98
32-33		1.80	0.13	0.02	4.97	53.27

Elizabeth River
Sediment Surface Area (m² / gram dry weight sediments)

Site 1	Sediment Depth Interval (cm)	Total Surface Area	Organic Free Surface Area
0-1		4.40	2.66
1-2		2.12 ND	
2-3		4.91 ND	
3-4		3.41 ND	
4-5		3.51 ND	
5-6		4.85	2.82
6-7		6.31 ND	
7-8		3.95 ND	
8-9		4.70 ND	
9-10		4.25 ND	
10-11		3.31	1.25
11-12		5.19 ND	
12-13		7.92 ND	
13-14		6.35 ND	
14-15		7.05 ND	
15-16		7.45	7.09
16-17		7.04 ND	
17-18		7.56 ND	
18-19		7.89 ND	
19-20		9.59 ND	
20-21		6.48	7.65
21-22		8.54 ND	
22-23		10.12 ND	
23-24		9.20 ND	
24-25		9.65 ND	
25-26		7.75	8.40
26-27		8.94 ND	
27-28		8.87 ND	
28-29		8.31 ND	
29-30		8.97 ND	
30-31		8.24	9.90
31-32		7.15 ND	
32-33		10.67 ND	
33-34		10.36 ND	
34-35		9.07 ND	
35-36		10.51	4.08

Site 2	Sediment Depth Interval (cm)	Total Surface Area	Organic Free Surface Area
0-1		2.45	1.53
1-2		2.82 ND	
2-3		3.66 ND	
3-4		ND	
4-5		1.30 ND	
5-6		1.35	1.31
6-7		1.16 ND	
7-8		0.28 ND	
8-9		1.82 ND	
9-10		4.14 ND	
10-11		2.74	2.15
11-12		3.58 ND	
12-13		3.21 ND	
13-14		2.76 ND	
14-15		4.97 ND	
15-16		6.51	2.57
16-17		4.59 ND	
17-18		6.37 ND	
18-19		6.22 ND	
19-20		7.06 ND	
20-21		10.10	2.71
21-22		11.48 ND	
22-23		8.34 ND	
23-24		9.01 ND	
24-25		6.00 ND	
25-26		9.99	2.99
26-27		10.57 ND	
27-28		9.86 ND	
28-29		10.86 ND	
29-30		10.78 ND	
30-31		9.70 ND	
31-32		14.27 ND	
32-33		ND	3.46

**East River and Newark Bay
Pb-210 activity (dpm/g dry wt. sed)**

East River

Sediment Depth Interval (cm)	Total activity	Excess Activity	% Error
0-2	4.9823	4.5131	0.1914
4-8	6.0671	5.6203	0.2347
10-12	5.7293	5.2756	0.2612
14-18	5.6571	5.2018	0.2931
20-22	5.7127	5.2585	0.2017
24-28	12.613	12.3006	0.4296
30-32	6.3215	5.8799	0.2266
34-38	5.9188	5.4689	0.264
40-42	4.7129	4.2383	0.1825
50-52	5.3112	4.8489	0.1884
60-62	5.8487	5.3974	0.2047
70-72	6.9431	6.5142	0.2565
90-92	5.3816	4.9207	0.3596
110-112	5.6042	5.1478	0.2264
130-132	5.5135	5.0553	0.2272
150-152	5.4535	4.9941	0.2612
170-172	5.299	4.8364	0.1869
190-192	5.5297	5.0719	0.2117

Newark Bay

Sediment Depth Interval (cm)	Total activity	Excess Activity	% Error
0-2	3.9518	3.4798	0.1402
4-8	4.7113	4.259	0.1576
10-12	3.6511	3.1713	0.1399
14-18	3.2855	2.7962	0.1273
20-22	2.5371	2.0284	0.1014
30-32	2.1261	1.6067	0.0903
40-42	1.5747	1.041	0.0709
44-48	3.8323	3.3572	0.1447
50-52	3.114	2.6203	0.1116
70-72	2.6292	2.1229	0.1016
90-92	2.844	2.3433	0.1094
110-112	2.1143	1.5946	0.0853
130-132	0.4034	-0.1607	0.036

**East River and Newark Bay
Sediment Grain Size Distributions
(% by weight)**

East River

Sediment Depth Interval (cm)	% gravel	% sand	% silt	% clay
0-2	3.72	9.23	44.21	42.83
5-7	0.00	7.69	47.38	44.93
10-12	0.42	5.76	42.49	51.33
15-17	0.00	9.45	44.59	45.96
20-22	0.00	5.23	46.35	48.42
25-27	0.00	6.13	50.20	43.68
30-32	1.26	10.06	16.98	71.70
35-37	1.00	7.13	46.96	44.90
40-42	0.00	14.59	23.26	62.16
45-47	0.22	6.95	49.36	43.47
50-52	0.00	6.78	43.56	49.67
60-62	0.00	5.21	39.89	54.90
70-72	0.00	2.12	49.59	48.28
80-82	0.00	3.40	51.99	44.61
90-92	0.00	2.68	44.62	52.70
100-102	0.00	2.01	45.98	52.01
110-112	0.00	3.85	45.87	50.28
120-122	0.00	5.40	42.98	51.63
130-132	0.00	4.60	47.85	47.55
140-142	0.00	2.96	37.37	59.67
150-152	3.20	5.92	43.35	47.52
160-162	0.00	4.91	41.03	54.06
170-172	0.00	2.75	47.03	50.22
180-182	0.00	2.14	40.53	57.33
190-192	0.00	8.19	42.55	49.26

Newark Bay

Sediment Depth Interval (cm)	% gravel	% sand	% silt	% clay
0-2	0.00	25.25	46.17	28.58
5-7	0.00	14.64	52.92	32.44
10-12	0.00	15.23	58.31	26.47
20-22	0.00	16.26	54.93	28.81
30-32	0.00	20.10	48.71	31.19
40-42	0.00	43.62	44.56	11.82
50-52	0.00	32.28	47.27	20.45
70-72	0.00	45.07	31.46	23.47
90-92	0.00	22.34	71.96	5.70
110-112	0.00	39.85	48.94	11.22
130-132	2.02	71.96	9.56	16.45
140-142	0	30.5797	44.2029	25.2174

East River
Sediment PAH Concentrations (ng/g dry wt. sed)

Sediment Depth Interval (cm)	Acenaphthene	Fluorene	Anthracene	Phenanthrene	Fluoranthene	Pyrene	Benzo[a]fluoranthene	Benzo[a]anthracene	Benzo[b]fluoranthene	Benzo[k]fluoranthene	Benzo[e]pyrene	Benzo[a]pyrene	Indeno[1,2,3-cd]perylene	Benzo[ghi]perylene
0-2	ND	ND	ND	ND	182.54	182.54	182.54	1168.62						
2-4	ND	ND	ND	ND	182.54	182.54	212.22	682.82						
4-6	ND	ND	ND	ND	182.54	182.54	141.82	682.71						
6-8	ND	ND	ND	ND	131.72	117.82	117.82	687.84						
8-10	ND	ND	ND	ND	92.22	78.82	482.82							
10-12	275.19	885.82	147.16	111.72	82.22	78.82	482.82							
12-14	ND	ND	ND	ND	91.82	78.82	534.82							
14-16	382.82	387.72	182.77	391.24	184.74	184.74	682.11							
16-18	ND	ND	ND	ND	122.22	182.42	682.81							
18-20	478.87	684.22	382.82	184.84	137.87	137.87	682.82							
20-22	ND	ND	ND	ND	182.87	138.42	612.82							
22-24	ND	ND	ND	ND	182.72	114.22	682.82							
24-26	445.31	682.22	281.82	182.22	182.22	118.27	728.82							
26-28	ND	ND	ND	ND	182.72	145.82	781.22							

Sediment Depth Interval (cm)	Acenaphthene	Fluorene	Anthracene	Phenanthrene	Fluoranthene	Pyrene	Benzo[a]fluoranthene	Benzo[a]anthracene	Benzo[b]fluoranthene	Benzo[k]fluoranthene	Benzo[e]pyrene	Benzo[a]pyrene	Indeno[1,2,3-cd]perylene	Benzo[ghi]perylene
0-2	357.22	482.22	1372.82	721.84	482.22	ND								
2-4	382.42	384.82	1182.82	882.17	382.22	ND								
4-6	381.22	482.72	1478.72	714.82	482.82	ND								
6-8	215.81	382.24	1151.87	648.42	222.82	ND								
8-10	128.82	182.87	682.16	278.72	178.42	ND								
10-12	121.72	228.12	782.82	342.51	182.42	ND								
12-14	148.82	182.57	841.74	321.47	187.22	ND								
14-16	182.82	281.72	1182.72	422.72	282.82	ND								
16-18	182.19	347.42	1082.21	422.42	278.22	ND								
18-20	218.47	487.24	1482.82	582.82	382.22	ND								
20-22	212.24	482.22	1282.71	522.82	342.72	ND								
22-24	182.22	441.82	1582.22	482.82	251.47	ND								
24-26	182.81	482.42	2512.24	522.82	328.87	ND								
26-28	212.21	487.22	1282.82	522.42	327.72	ND								

Sediment Depth Interval (cm)	Acenaphthene	Fluorene	Anthracene	Phenanthrene	Fluoranthene	Pyrene	Benzo[a]fluoranthene	Benzo[a]anthracene	Benzo[b]fluoranthene	Benzo[k]fluoranthene	Benzo[e]pyrene	Benzo[a]pyrene	Indeno[1,2,3-cd]perylene	Benzo[ghi]perylene
0-2	3121.82	3842.81	2182.82	1782.42	1784.24	672.17	1222.22	1782.82	1782.82	1782.82	1782.82	1782.82	1782.82	1782.82
2-4	3822.22	3822.82	1882.21	1814.16	1942.41	682.17	1222.22	1782.82	1782.82	1782.82	1782.82	1782.82	1782.82	1782.82
4-6	3882.51	3872.42	2141.57	1878.82	1722.82	682.22	1247.77	1822.82	1822.82	1822.82	1822.82	1822.82	1822.82	1822.82
6-8	618.14	2582.22	1084.82	1084.82	1278.82	482.82	882.42	882.42	882.42	882.42	882.42	882.42	882.42	882.42
8-10	1472.18	1882.77	882.82	727.22	842.82	282.44	882.42	882.42	882.42	882.42	882.42	882.42	882.42	882.42
10-12	1822.22	1771.82	1182.19	821.11	1011.47	322.24	722.74	722.74	722.74	722.74	722.74	722.74	722.74	722.74
12-14	1522.82	1882.22	1122.54	882.82	887.22	382.84	782.81	782.81	782.81	782.81	782.81	782.81	782.81	782.81
14-16	1882.82	2422.42	1217.42	1082.42	1242.82	382.22	882.82	882.82	882.82	882.82	882.82	882.82	882.82	882.82
16-18	1822.82	2482.27	1512.82	1122.82	1272.31	484.77	917.24	917.24	917.24	917.24	917.24	917.24	917.24	917.24
18-20	2882.12	2872.21	1867.81	148.82	1551.12	474.18	1122.82	1122.82	1122.82	1122.82	1122.82	1122.82	1122.82	1122.82
20-22	2882.42	2342.12	1872.12	1511.84	1582.71	881.22	1122.82	1122.82	1122.82	1122.82	1122.82	1122.82	1122.82	1122.82
22-24	2782.24	2882.82	1784.82	1387.82	1421.31	881.82	872.82	872.82	872.82	872.82	872.82	872.82	872.82	872.82
24-26	2882.82	2841.17	1741.82	1812.22	1887.51	482.82	1182.82	1182.82	1182.82	1182.82	1182.82	1182.82	1182.82	1182.82
26-28	2511.24	3821.47	1882.82	1382.24	1522.82	482.82	1082.81	1082.81	1082.81	1082.81	1082.81	1082.81	1082.81	1082.81

Sediment Depth Interval (cm)	Acenaphthene	Fluorene	Anthracene	Phenanthrene	Fluoranthene	Pyrene	Benzo[a]fluoranthene	Benzo[a]anthracene	Benzo[b]fluoranthene	Benzo[k]fluoranthene	Benzo[e]pyrene	Benzo[a]pyrene	Indeno[1,2,3-cd]perylene	Benzo[ghi]perylene
0-2	27.87	872.42	1222.22	1054.82	324.81									
2-4	21.81	887.22	1222.84	884.11	311.82									
4-6	27.82	822.54	1182.12	1082.22	382.87									
6-8	28.22	882.72	842.81	772.21	282.19									
8-10	18.47	618.87	582.22	482.37	182.82									
10-12	13.77	772.18	742.82	612.87	184.77									
12-14	15.82	712.82	717.42	582.82	177.22									
14-16	12.24	712.24	781.16	682.82	172.17									
16-18	18.82	884.22	872.19	742.42	222.84									
18-20	27.84	882.82	1087.82	882.22	282.42									
20-22	22.42	882.22	1074.42	817.72	284.82									
22-24	18.82	781.81	1082.22	882.82	282.87									
24-26	21.22	872.42	1042.42	872.82	282.82									
26-28	18.12	882.87	1082.87	872.81	212.82									

Newark Bay
Sediment PAH Concentrations (ng/g dry wt. sed)

Sediment Depth Interval (cm)	anthracene	acenaphthylene	acenaphthene	fluorene	1-methylfluorene	phenanthrene
0-2	NQ	NQ	NQ	35.78	28.53	234.83
2-4		188.82	219.72	63.88	60.23	74.42
4-6		210.27	185.99	67.08	68.72	45.84
6-8		193.77	182.74	43.05	70.28	47.82
8-10		191.06	304.32	51.87	55.83	35.88
10-12		271.08	201.51	68.43	77.10	55.74
12-14		238.88	282.77	51.24	67.98	48.34
14-16		244.78	151.14	57.09	65.82	44.85
16-18		208.18	235.55	44.58	48.71	78.13
18-20	NQ	NQ	NQ	70.70	58.88	333.07
20-22		587.05	191.48	65.20	80.28	48.71
22-24	NQ	NQ	NQ	54.89	48.83	328.10
24-26	NQ	NQ	NQ	52.73	55.41	352.20

Sediment Depth Interval (cm)	2-methylphenanthrene	3-methylphenanthrene	anthracene	5-methylphenanthrene	1-methylphenanthrene	6-methylphenanthrene
0-2		84.09	88.82	351.50	122.58	61.88
2-4		97.31	188.80	473.73	243.89	121.88
4-6		87.31	140.10	478.48	180.15	81.70
6-8		104.75	118.14	500.22	185.28	98.88
8-10		63.48	123.54	415.57	137.84	71.48
10-12		98.71	158.91	684.41	204.77	131.37
12-14		74.80	148.84	638.01	171.20	88.71
14-16		188.51	128.58	541.38	298.02	203.23
16-18		88.08	148.16	511.37	188.84	108.32
18-20		84.77	180.78	777.21	207.78	133.28
20-22		95.08	185.52	675.85	177.43	113.83
22-24		108.83	172.85	588.48	188.85	127.44
24-26		111.80	263.88	802.83	278.54	114.05

Sediment Depth Interval (cm)	fluoranthene	pyrene	benz[a]anthracene	chrysene	benz[b]fluoranthene	benz[k]fluoranthene	benz[e]pyrene	benz[a]pyrene
0-2		672.48	778.48	571.03	447.18	532.85	177.95	384.83
2-4		1380.88	1504.85	844.58	812.48	816.51	270.87	570.42
4-6		1187.02	1273.75	737.83	603.51	848.11	282.15	578.18
6-8		1237.73	1808.10	788.72	601.51	988.72	313.41	688.08
8-10		700.88	1478.84	616.28	473.48	803.88	250.13	587.48
10-12		1280.58	3036.21	745.28	657.78	1080.32	347.03	788.71
12-14		834.83	2335.98	588.88	478.28	904.91	287.84	685.71
14-16		1081.25	1708.88	618.44	304.17	840.72	211.47	432.08
16-18		1558.84	1880.72	788.01	585.48	888.90	220.28	481.84
18-20		1878.25	2188.73	987.70	745.88	884.38	283.75	783.40
20-22		2028.03	2422.29	1078.27	861.88	914.88	305.51	632.48
22-24		2748.85	3272.79	1208.88	888.54	1118.33	388.42	758.00
24-26		2543.88	2985.38	1150.82	614.15	970.31	274.88	707.38

Sediment Depth Interval (cm)	7-methylhop	perylene	indeno(1,2,3-cd)perylene	benz[ghi]perylene	benz[ghi]perylene
0-2	NQ		330.23	374.58	318.87
2-4	NQ		400.83	478.88	416.84
4-6		7.74	488.88	805.43	504.94
6-8		7.85	481.94	805.35	523.77
8-10		8.88	453.12	551.25	481.38
10-12		9.58	633.01	682.28	578.08
12-14		15.07	514.85	581.57	528.45
14-16		6.84	330.85	477.05	414.34
16-18		8.53	380.80	542.91	488.08
18-20		22.45	488.53	878.84	825.70
20-22		9.83	441.47	733.78	635.38
22-24		14.13	514.88	805.44	758.45
24-26		18.80	483.47	842.53	731.88

East River
Pore Water PAH Concentrations (ng/g pore water)

Sediment Depth Interval (cm)	acridanthrene	fluoranthene	pyrene	benzo(a)anthracene	benzo(b)fluoranthene	benzo(k)fluoranthene
1-0	NO	NO	NO	NO	NO	NO
0-2	NO	NO	NO	NO	NO	NO
2-4	NO	NO	NO	NO	NO	NO
4-6	NO	NO	0.045	NO	NO	NO
6-8	NO	NO	NO	NO	NO	NO
8-10	0.214	0.100	0.182	NO	0.128	NO
10-12	NO	NO	NO	NO	NO	NO
12-14	NO	NO	NO	NO	NO	NO
14-16	0.281	0.220	0.078	NO	NO	NO
16-18	NO	NO	NO	NO	NO	NO
18-20	NO	NO	NO	NO	NO	NO
20-22	0.191	0.080	0.078	NO	NO	NO
22-24	NO	NO	0.088	NO	NO	NO
24-26	0.981	1.461	0.203	NO	NO	NO
26-28	0.182	NO	0.163	NO	NO	NO

Sediment Depth Interval (cm)	fluoranthene	pyrene	benzo(a)anthracene	chrysene	benzo(g,h)perylene	benzo(i)perylene
1-0	NO	NO	NO	NO	NO	NO
0-2	NO	NO	NO	NO	NO	NO
2-4	NO	NO	NO	NO	NO	NO
4-6	0.167	0.297	NO	NO	NO	0.011
6-8	NO	NO	NO	NO	NO	NO
8-10	NO	NO	NO	NO	NO	NO
10-12	NO	NO	NO	NO	0.040	0.012
12-14	NO	NO	NO	NO	NO	NO
14-16	NO	NO	NO	NO	NO	NO
16-18	NO	NO	NO	NO	NO	NO
18-20	NO	NO	NO	NO	NO	NO
20-22	NO	NO	NO	NO	NO	NO
22-24	NO	NO	NO	NO	NO	NO
24-26	NO	NO	NO	NO	NO	NO
26-28	0.179	NO	NO	NO	NO	NO

Sediment Depth Interval (cm)	benzo(e)pyrene	benzo(a)pyrene	perylene	indeno(1,2,3-cd)pyrene	benz(ghi)perylene	benz(ghi)perylene
1-0	NO	NO	NO	NO	0.031	NO
0-2	NO	NO	NO	NO	NO	NO
2-4	NO	NO	NO	NO	NO	NO
4-6	0.041	0.026	NO	0.032	0.056	NO
6-8	NO	NO	NO	NO	NO	NO
8-10	NO	NO	NO	NO	NO	NO
10-12	0.039	NO	NO	NO	NO	NO
12-14	NO	NO	NO	NO	NO	NO
14-16	NO	NO	NO	NO	NO	NO
16-18	NO	NO	NO	NO	NO	NO
18-20	NO	NO	NO	NO	NO	NO
20-22	NO	NO	NO	NO	NO	NO
22-24	NO	NO	NO	NO	NO	NO
24-26	NO	NO	NO	NO	NO	NO
26-28	0.028	NO	NO	NO	NO	NO

Newark Bay
 Pore Water PAH Concentrations (ng/g pore water)

Sediment Depth Interval (cm)	naphthalene	acenaphthylene	acenaphthene	fluorene	phenanthrene	anthracene
1-0	NQ	NQ	NQ	0.086	NQ	NQ
0-2	NQ	NQ	NQ	NQ	NQ	NQ
2-4	NQ	NQ	NQ	NQ	NQ	NQ
4-6	0.203	0.446	NQ	NQ	NQ	NQ
6-8	NQ	NQ	NQ	NQ	NQ	NQ
8-10	NQ	NQ	NQ	NQ	NQ	NQ
10-12	NQ	NQ	NQ	NQ	NQ	NQ
12-14	NQ	NQ	NQ	NQ	NQ	NQ
14-16	0.275	NQ	NQ	NQ	NQ	NQ
16-18	NQ	NQ	NQ	NQ	NQ	NQ
18-20	NQ	NQ	NQ	NQ	NQ	NQ
20-22	NQ	NQ	NQ	NQ	NQ	NQ
22-24	NQ	NQ	NQ	NQ	NQ	NQ
24-26	0.466	0.411	0.042	NQ	NQ	NQ

Sediment Depth Interval (cm)	fluoranthene	pyrene	benz(a)anthracene	chrysene	benz(b)fluoranthene	benz(k)fluoranthene
1-0	NQ	NQ	NQ	NQ	NQ	NQ
0-2	0.174	0.267	0.051	0.047	0.233	0.075
2-4	NQ	NQ	NQ	NQ	0.039	0.015
4-6	NQ	NQ	NQ	NQ	NQ	NQ
6-8	NQ	NQ	NQ	NQ	0.104	0.035
8-10	NQ	0.280	NQ	NQ	0.042	0.015
10-12	NQ	1.007	0.048	0.040	0.258	0.084
12-14	NQ	0.378	NQ	NQ	0.065	0.024
14-16	NQ	0.263	NQ	NQ	0.059	0.020
16-18	0.257	0.297	NQ	NQ	0.075	0.026
18-20	0.324	0.366	NQ	NQ	0.095	0.035
20-22	0.292	0.363	0.043	NQ	0.129	0.046
22-24	NQ	NQ	NQ	NQ	NQ	NQ
24-26	0.584	0.804	NQ	NQ	0.167	0.056

Sediment Depth Interval (cm)	benzo(e)pyrene	benzo(a)pyrene	benz(a)pyrene	indeno(1,2,3-cd)pyrene	benz(ghi)perylene	dibenz(ah)anthracene
1-0	NQ	NQ	NQ	NQ	NQ	NQ
0-2	0.202	0.059	NQ	0.111	0.111	NQ
2-4	0.037	0.016	NQ	NQ	0.032	NQ
4-6	NQ	NQ	NQ	NQ	NQ	NQ
6-8	0.106	0.039	NQ	0.037	0.049	NQ
8-10	0.045	0.022	NQ	NQ	0.030	NQ
10-12	0.246	0.115	NQ	0.105	0.140	NQ
12-14	0.071	0.033	NQ	NQ	NQ	NQ
14-16	0.062	0.028	NQ	NQ	NQ	NQ
16-18	0.090	0.037	NQ	NQ	0.043	NQ
18-20	0.097	0.040	NQ	NQ	0.046	NQ
20-22	0.132	0.063	NQ	0.050	0.071	NQ
22-24	NQ	NQ	NQ	NQ	NQ	NQ
24-26	0.163	0.056	NQ	0.035	0.051	NQ

**East River and Newark Bay Sites
Sedimentary Geochemical Variables**

East River

<i>Sediment Depth Interval (cm)</i>	<i>% OC (mean)</i>	<i>% OC (S. D.)</i>	<i>% soot C (mean)</i>	<i>% soot C (SD)</i>	<i>C/N ratio</i>	<i>Surface Area (m²/g)</i>	<i>Surface Area (SD)</i>	<i>DOC (mg/L)</i>
0-2	4.16	0.13	0.54	0.05	9.37	13.85	0.01	22.47
2-4	4.22	ND	ND	ND	10.50	15.70	0.15	22.87
4-6	4.33	0.01	0.45	ND	10.57	15.65	0.07	25.67
6-8	4.19	0.08	ND	ND	9.92	16.03	0.04	27.47
8-10	4.09	0.02	0.47	ND	9.38	15.42	0.09	27.07
10-12	3.86	ND	ND	ND	9.65	14.76	0.34	32.17
12-14	3.97	0.08	0.28	0.04	9.95	13.01	0.19	30.07
14-16	4.04	0.07	ND	ND	9.73	14.51	0.53	30.37
16-18	4.31	0.16	0.33	ND	10.04	16.20	0.32	30.67
18-20	4.29	0.05	ND	ND	10.13	15.67	0.22	33.87
20-22	4.42	ND	0.35	ND	9.79	16.09	1.13	32.77
22-24	4.39	0.01	ND	ND	10.23	15.72	0.12	34.17
24-26	4.50	0.04	0.34	0.02	10.27	15.73	0.00	ND
26-28	4.58	ND	ND	ND	9.95	15.81	0.28	49.67

Newark Bay

<i>Sediment Depth Interval (cm)</i>	<i>% OC (mean)</i>	<i>% OC (S. D.)</i>	<i>% soot C (mean)</i>	<i>% soot C (SD)</i>	<i>C/N ratio</i>	<i>Surface Area (m²/g)</i>	<i>Surface Area (SD)</i>	<i>DOC (mg/L)</i>
0-2	1.62	0.01	0.21	0.03	11.12	7.01	0.20	10.79
2-4	1.84	0.06	ND	ND	12.27	6.51	0.06	10.99
4-6	1.98	0.00	0.20	ND	11.84	6.91	0.17	14.29
6-8	1.71	0.08	ND	ND	14.62	6.95	0.10	14.92
8-10	1.60	0.00	0.29	ND	14.18	6.08	0.04	14.69
10-12	1.65	0.16	ND	ND	16.14	5.54	0.18	20.19
12-14	1.57	0.15	0.25	0.00	16.00	5.47	0.03	18.79
14-16	1.32	0.08	ND	ND	13.81	5.58	0.07	26.99
16-18	1.66	0.06	1.60	ND	15.92	6.05	0.02	30.49
18-20	2.03	0.08	ND	ND	16.44	5.31	0.01	32.49
20-22	1.96	0.01	0.24	ND	17.30	4.78	0.01	34.59
22-24	2.17	0.00	ND	ND	16.77	4.46	0.05	36.99
24-26	2.14	0.00	0.25	0.07	14.34	5.48	0.94	36.59